EFFICIENCY ANALYSIS OF VARYING EGR UNDER PCI MODE OF COMBUSTION IN A LIGHT DUTY DIESEL ENGINE

A Thesis

by

RAHUL RADHAKRISHNA PILLAI

Submitted to the Office of Graduate Studies of
Texas A&M University
in partial fulfillment of the requirements for the degree of

MASTER OF SCIENCE

August 2008

Major Subject: Mechanical Engineering

EFFICIENCY ANALYSIS OF VARYING EGR UNDER PCI MODE OF COMBUSTION IN A LIGHT DUTY DIESEL ENGINE

A Thesis

by

RAHUL RADHAKRISHNA PILLAI

Submitted to the Office of Graduate Studies of
Texas A&M University
in partial fulfillment of the requirements for the degree of

MASTER OF SCIENCE

Approved by:

Chair of Committee,	Timothy Jacobs
Committee Members,	Jerald Caton
	Jorge Alvarado
Head of Department,	Dennis O'Neal

August 2008

Major Subject: Mechanical Engineering

ABSTRACT

Efficiency Analysis of Varying EGR Under PCI Mode of Combustion in a Light Duty Diesel Engine. (August 2008)

Rahul Radhakrishna Pillai, B.Tech., Mar Athanasius College of Engineering

Chair of Advisory Committee: Dr. Timothy Jacobs

The recent pollution norms have brought a strong emphasis on the reduction of diesel engine emissions. Low temperature combustion technology such as premixed compression ignition (PCI) has the capability to significantly and simultaneously reduce nitric oxides (NO_x) and particulate matter (PM), thus meeting these specific pollution norms. There has been, however, observed loss in fuel conversion efficiency in some cases. This study analyzes how energy transfer and brake fuel conversion efficiency alter with (or are affected by) injection timings and exhaust gas recirculation (EGR) rate. The study is conducted for PCI combustion for four injection timings of 9°, 12°, 15° and 18° before top dead center (BTDC) and for four exhaust gas recirculation (EGR) rates of 39%, 40%, 41% and 42%. The data is collected from the experimental apparatus located in General Motors Collaborative Research Laboratory at the University of Michigan. The heat release is calculated to obtain various in-cylinder energy transfers.

The brake fuel conversion efficiency decreases with an increase in EGR. The decrease in the brake fuel conversion efficiency is due to the decrease in work output. This decrease is due to an increase in the pumping work and an increase in friction and decrease in gross indicated work. The decrease in the combustion efficiency is because of the increased formation of unburnt products due to increased ignition delay caused by the application of EGR and decreasing air-fuel (A/F) ratio. A definite trend is not obtained for the contribution of heat transfer to the total energy distribution. However the total heat transfer decreases with retardation of injection timing because of decreasing combustion temperature.

As the injection timing is retarded, the brake fuel conversion efficiency is found to decrease. This decrease is because of a decrease in net work output. This is because the time available for utilization of the energy released is less because of late combustion. The total heat transfer decreases with retardation of injection timing because of decreasing combustion temperature. The contribution of heat transfer to the total energy distribution decreases with increase in EGR.

DEDICATION

To My Dearest Parents

ACKNOWLEDGMENTS

First I would like to thank my thesis chair, Dr. Timothy Jacobs, for his continued support and guidance. He has motivated me a lot during this entire period of thesis. He serves as an excellent role model to all students. I am honored that he was able to serve as my chair. My thesis committee members –Professor Jerald Caton, and Dr. Jorge Alvarado– are thanked for their involvement in the successful completion and scientific validity of this thesis. Each committee member has provided helpful comments and suggestions which I greatly appreciate.

My loved ones have supported me completely along the way. For this, I wish to thank my family. My mom and dad have always encouraged and supported my pursuit of high education. They have influenced me a lot in my life. Finally, I would like to thank all my friends for their continued motivation and support during the entire period of my masters.

NOMENCLATURE

Abbreviations

A/F	Air-Fuel
A_s	Heat transfer surface area
ASME	American Society of Mechanical Engineers
ATDC-°c	After Top Dead Center-Compression
atm	Atmosphere
BMEP	Brake Mean Effective Pressure
BSFC	Brake Specific Fuel Consumption
BTDC	Before Top Dead Center
BTDC-°c	Before Top Dead Center-Compression
C	Celsius
cc	Cubic Centimeters
cm	Centimeter
CO	Carbon Monoxide
CO_2	Carbon Dioxide
deg	Degree
DI	Direct Injection
DOC	Diesel Oxidation Catalyst
DPF	Diesel Particulate Filter
EGR	Exhaust Gas Recirculation

FMEP	Friction Mean Effective Pressure
g	Gram
GMIDEL	GM Isuzu Diesel Engine Limited
GUI	Graphical User Interface
HC	Hydrocarbon
HCCI	Homogenous Charge Compression Ignition
HiMICS	Homogenous Charge Intelligent Multiple Injection Combustion System
IC	Internal Combustion
IDI	Indirect Injection
IMEP	Indicative Mean Effective Pressure
ISPOL	Isuzu Poland
J	Joule
K	Kelvin
kg	Kilogram
kJ	Kilo Joule
kW	Kilo Watt
L	Liter
LHV	Lower Heating Value
LNT	Lean NO_x Trap
LTC	Low Temperature Combustion
min	Minute

MJ	Mega Joule
MK	Modulated Kinetics
N	Newton
NDIR	Non-Dispersive Infra Red
NO	Nitric Monoxide
NO_x	Nitrous Oxides
PAH	Polycyclic Aromatic Hydrocarbon
PCI	Premixed Compression Ignition
PREDIC	Premixed Diesel Combustion
PM	Particulate Matter
PMEP	Pumping Mean Effective Pressure
ppm	Parts Per Million
rpm	Revolutions per minute
s	Second
SI	Spark Ignition
SOF	Soluble Organic Fraction
TDC	Top Dead Center
TWC	Three-Way Catalyst
UM	University of Michigan
UMHR	University of Michigan Heat Release
UNIBUS	Uniform Bulky Combustion Systems
VGT	Variable Geometry Turbocharger

Greek Letters and Other Symbols

γ	Ratio of specific heats
η_c	Combustion efficiency
η_f	Brake fuel conversion efficiency
η_m	Mechanical efficiency
η_{th}	Net indicated thermal efficiency
θ	Total engine crank shaft angle
µm	micrometer

Mathematical Variables

B	Cylinder Bore
C_p	Specific heat at constant pressure
C_v	Specific heat at constant volume
F	Fuel air ratio
h_c	Convective heat transfer coefficient
h_{out}	Specific enthalpy of species exiting the control volume
h_T	Radiative heat transfer coefficient
m	Meter
m	Mass of cylinder mixture
m_f	Fuel mass flow rate
m_{out}	Mass exiting the cylinder
MW_f	Molecular Weight of the fuel per carbon atom
n	Polytropic Index

n_R	Crank revolutions for each power stroke per cylinder
P	Pressure of contents inside the cylinder
$\dot{P}$	Brake power output
Q_{ch}	Apparent fuel heat released
Q_{HT}	Total Heat Transfer from Control Volume
Q_{LHV}	Lower heating value of the fuel
R	Mixture gas constant
R^*	Gas constant for un-dissociated products
S	Cylinder stroke
$\overline{S_p}$	Mean piston speed
T	Temperature of contents inside the cylinder
T_w	Cylinder wall temperature
U_{cv}	Internal energy of control volume
V	Volume of the control volume
V_d	Displaced volume of piston inside the cylinder
W_{cv}	Work from the control volume
W_{gross}	Gross indicated work
W_{net}	Net indicated work
W_p	Pumping work
W_{total}	Total engine output work

TABLE OF CONTENTS

Page

LIST OF FIGURES

FIGURE Page

FIGURE Page

FIGURE Page

FIGURE Page

FIGURE Page

FIGURE Page

FIGURE Page

LIST OF TABLES

1. INTRODUCTION: THE IMPORTANCE OF RESEARCH

1.1 Motivation

The motivation of this research study is to conserve natural resources (reduced fuel consumption) and reduction of air pollution. The effort here in is to analyze the various reasons for decrease in the fuel conversion efficiency. With depleting crude oil reserves across the globe, this problem needs a greater attention.

Conventional diesel engines are more efficient than gasoline engines for the same power, resulting in lower fuel consumption. For an efficient turbo diesel, the common margin of fuel consumption is about 35% less for a diesel engine when compared to its gasoline counterpart [1]. This increase in efficiency of a diesel engine is partly due to higher compression ratio and lean fuel operation. The high compression ratio results in high temperature within the cylinder that is required to achieve auto ignition. The high compression ratio also results in a higher expansion ratio there by enabling maximum utilization of energy released during the expansion stroke.

However the operation of diesel engine results in the emission of various products such as nitric oxides (NO_x), particulate matter (PM), carbon monoxide (CO) and hydrocarbon (HC) [1, 2]. Most of these products are harmful for the health and wellness of human beings. Stringent pollution norms call for the reduction in emission of these harmful species. This has resulted in research and development of new technology

---

This thesis follows the style of ASME Journal of Engineering for Gas Turbine and Power.

to achieve lower emissions to match these pollution norms. One such technology developed is premixed compression ignition (PCI) combustion mode. Previous researchers [2-18] suggest that this novel mode of combustion greatly reduces the emission of NO_x and PM. But, this technology sometimes results in a loss of fuel efficiency [2]. In the case of diesel homogenous combustion cycles, the combustion of fuel will take place before the compression stroke [4]. This leads to excessive efficiency reduction and combustion roughness. The low fuel conversion efficiency is partly due to the decreased combustion efficiency, which results in a large emission of CO and HC. Hence, any attempt to satisfy the strict pollution norms results in a loss of fuel conversion efficiency [3-4, 10, 16-19]. It is important to analyze how the energy released inside the cylinder during combustion is distributed. This analysis also gives a picture on how the efficiency of the engine can be improved. With an improvement in efficiency, there will be a decrease in fuel consumption, hence saving the crude oil reserves around the world and a decrease the air pollution.

1.2 Background

1.2.1 Soot-NO_x Trade off

There are three primary nitric monoxide (NO) formation mechanisms: thermal NO formation, prompt NO formation and fuel NO formation. In a typical combustion system, the thermal NO formation dominates. Thermal NO formation is the result of dissociation of oxygen, nitrogen and hydroxyl radical which occurs at high temperature. Prompt NO is the result of interaction of HC fuel molecules with molecular nitrogen to ultimately generate NO. Prompt NO formation occurs even before the attainment of high

temperature. Fuel NO is the result of oxidation of the nitrogen in the fuel. Hence, it can be seen that NO formation is a strong function of temperature. Higher the temperature, higher is the NO formation.

The soot formation is a characteristic of HC diffusion flames. The net soot release is the difference between the soot formation and soot oxidation. The soot formation is a strong function of the air-fuel (A/F) ratio as well as temperature, while the soot oxidation is a function of temperature (assuming a lean equivalence ratio). The soot formation and oxidation depends on the formation of precursor species, polycyclic aromatic hydrocarbons or PAH, particle oxidation, particle inception, and surface growth and agglomeration [20]. Dec [21] observed that the formation of PAH occurs within a premixed reaction zone which supplies fragmented and radical species to a diffusion reaction zone. Thus a rich premixed mixture generates high levels of soot precursors thus increasing the soot formation.

Conventionally any attempt to reduce NO_x formation increases soot, and vice versa. For example, an advance in injection timing generally results in a lower net soot release, as it assures a premixed burn and combusts at higher temperatures (thus increasing soot oxidation). As this action increases NO formation also increases. This relationship is known as the diesel soot-NO_x tradeoff.

The soot-NO_x trade off relationship also exists with the application of exhaust gas recirculation (EGR). Addition of EGR reduces the local equivalence ratio by increasing the ignition delay. The ignition delay depends on the degree of fuel dispersion and the temperature inside the cylinder of the engine [20]. This increased ignition delay

provides sufficient time for mixing of air and fuel. Both the physical and chemical components of ignition delay are increased by EGR. The physical part of the ignition delay is increased by acting as a barrier for the mixing of air and fuel. EGR increases the chemical part of ignition delay by introducing components such as carbon dioxide and water that have higher specific heats than oxygen and nitrogen at the pre-combustion temperatures [5]. Thus the incoming EGR takes up a part of energy generated inside the engine thus delaying the combustion. Also, EGR reduces the rate of burn inside the cylinder. EGR reduces the reaction temperature which reduces the NO_x formation [6-8]. However the addition of EGR reduces the concentration of oxygen inside the cylinder. This reduction of oxygen concentration tends to raise the local equivalence ratios resulting in lower fuel conversion efficiency [6]. Thus even though there is an increase in injection delay, overly rich premixed burn pattern exist, resulting in a higher soot formation. Also, lower reaction temperatures also decrease soot oxidation, so net soot release increases. Thus the addition of EGR reduces NO_x but increases the soot.

1.2.2 Defeating Soot-NO_x Trade off

Recent research has focused on how to defeat soot-NO_x trade off. Two main methods have been developed to defeat this soot-NO_x trade off. One method is the after treatment of exhaust gas. Within the realm of gasoline engines the development of exhaust oxygen sensors, fuel injectors and closed loop electronic control modules encouraged the development and use of three-way-catalyst (TWC). The TWC is a combination of platinum, palladium and rhodium that reduce and oxidize the exhaust mixtures NO, CO and HC. The TWC catalyst has an efficiency of more than 80% [22].

Even thought the TWC catalyst successfully reduces the emissions, the successful working of TWC requires the engine to operate consistently at an equivalence ratio that provides the best mixture of the exhaust species. In case of a conventional diesel engine, the after treatment method include the use of a diesel oxidation catalyst (DOC). DOC can reduce the emission of CO and HC. DOC is very efficient when used with a lean NO_x trap (LNT). In some cases diesel particulate filters (DPF) are used to remove the PM. The second method of defeating the soot-NO_x trade off is to prevent the formation of regulated species. This is achieved by proper mixing of fuel and lowering of flame temperature. This lead to the development of low temperature combustion (LTC). But the new LTC methods, results in an increase in HC and CO formation [2]. Two main methods have been developed to achieve the low temperature combustion. They are homogenous charge compression ignition (HCCI) and premixed compression ignition (PCI).

1.2.3 HCCI and Its Development

HCCI combustion combines two famous modes of combustion used in internal combustion (IC) engines: homogenous charge spark ignition (conventional gasoline engines) and heterogeneous charge compression ignition (conventional diesel engines). HCCI attempts to burn a perfectly homogenous mixture of air and fuel by auto ignition induced by compression. A nearly homogenous mixture reduces locally rich zones. Coupled with dilution by addition of EGR, HCCI can reduce the soot and NO_x formation [23]. Diesel fuel has poor volatility and high ignitability thus making it is difficult to

vaporize the fuel. Once it is vaporized, it results in a rapid combustion, thus making it difficult to control [24].

Various methods have been developed to achieve diesel HCCI. Gray et al. [25] uses manifold injection of diesel to create HCCI combustion. It involves the use of an air heating device to vaporize the fuel which mixes uniformly with the air.

Several researchers have worked on the possibility of early direct injection to achieve diesel HCCI. Toyota's uniform bulky combustion system (UNIBUS) [26] uses direct injection of the fuel in the early compression stroke. A low injection pressure is created by a low bore injector nozzle and a spray obstacle placed at the end of the nozzle minimizes the spray penetration. More spray penetration leads to a higher soot production. This strategy reduces the rate of air-fuel mixing and produces a uniform distribution of equally mixed air-fuel particles. The authors also employed EGR to reduce the combustion temperature. Thus the reduced combustion temperature along with an improved air-fuel distribution resulted in a reduction of NO and soot formation. The level of NO_x obtained was 1:100 that of a conventional direct injection (DI) diesel engine. The DI may cause high soot production if wall penetration issues exist.

New ACE institute developed a new method known as premixed diesel combustion (PREDIC) [9]. The term "Premixed Diesel Combustion" was used because the authors could not achieve a true HCCI combustion. This technology used two fuel injectors where the two injectors spray and collide in the center bowl region, thus minimizing the fuel penetration there by reducing soot formation. A considerable reduction in NO_x was also observed due to better air-fuel mixing. ACE institute

improved the performance of the engine by developing a pintle-type of fuel injector nozzle [10]. This type of injector had lower penetration, wider dispersion, and better uniformity of air-fuel ratio. ACE institute tried to investigate a new concept of a second injection near top dead center (TDC). The first injection, which is referred to as early injection, initializes the cool flame reactions. The second injection ignites the high temperature diffusion reactions. This resulted in the oxidation of the HC that were produced by the first stage combustion which in turn reduced the soot formation.

1.2.4 PCI and Its Development

Both manifold injection and early injection strategies have their own limitations. The use of the former is limited due to low power density at low compression ratios. And the latter creates a very high HC and CO, often accompanied by high smoke if wall wetting issues exist. A possible alternative is the injection of fuel more close to the TDC; say 25° before top dead center (BTDC), single injection strategy combined with a high level of EGR. The ignition delay caused by the EGR results in proper mixing of the A/F mixture. This is followed in PCI combustion strategy. Various methods of achieving PCI combustion are described below.

One method is late injection premixed compression ignition combustion. Toyota developed this new strategy by using a heavy EGR and late injection timings [11]. The use of heavy EGR reduced the combustion temperature significantly. This reduction in the temperature resulted in the freezing of the production of PAH which are the precursors of soot formation. The other soot precursors such as benzene, acetylene and acepyrene form at low temperatures. But the temperature inside the cylinder is too low to

initiate the reactions that lead to their formation. The low temperature strategy reduced the formation of NO as well.

Nissan's modulated kinetics (MK) method [12] also involves the use of late injection timing and heavy use of EGR. But this method includes a reduced compression ratio, high EGR cooling and high injection pressure. A lower compression ratio creates a longer ignition delay. This is because, the lower pressure as a result of the lower compression ratio reduces the atomization of the fuel and delays premixing of air and fuel. The lower compression ratio also decreases the temperature inside the cylinder at the point of injection, thus increasing the ignition delay. The higher injection pressure also increases the ignition delay. The incoming fuel particles act as a heat sink by absorbing heat from the surroundings and getting vaporized. Hence faster the introduction of the fuel droplets (due to higher injection pressure), larger will be the heat absorption and slower will be the rise in temperature during compression. Also the high injection pressure provides more atomization of the fuel which results in quick vaporization of fuel thus decreasing the mixing time. However, this phenomenon accelerates the possibility of incidence of readily ignitable parcel of A/F, thus decreasing the ignition delay. Thus there is a competing trade off for increase in rail pressure.

In their research Shimazaki et al. [13] provided an insight on the benefits of using a late injection strategy. The cylinder pressure, the gas temperature and the swirl will be maximum as the piston reaches TDC. Hence if the fuel injection occurs near the TDC, it results in a better mixing (high swirl), better vaporization (high temperature) and reduced spray penetration (high pressure). But this strategy tends to create or produce

diffusive burning as the normal diesel fuel is having a high Cetane number. Hence this problem could be overcome by using diesel with lower Cetane number. This was the method followed in Isuzu's dual mode combustion concept [13]. They used diesel with lower Cetane number with zero EGR supply and normal injection timing.

Yokota et al [14] developed a concept known as homogenous charge intelligent multiple injection combustion system (HiMICS). This concept used a premixed compression ignition combined with multiple injections. The pre-mixture is formed by early injection performed during early stage of the intake stroke to the middle stage of the compression stroke. The authors proved that the trade-off between NO_x emission and fuel consumption, NO_x emission and smoke emission can be improved when the injection timing is excessively retarded. There is a reduction in NO_x emission because of the pilot injection that shortens the ignition delay of the main ignition. Pieroont et al. [27] also investigated the multiple fuel injection combined with EGR. There was a substantial reduction in NO_x and particulate matter emissions. NO_x emission was reduced by the use of EGR and the reduction in particulate matter was obtained by the use of multiple injections.

1.2.5 Problems of PCI Combustion

PCI is definitely an answer to the strict pollution regulations. However there are lots of problems associated with PCI. One factor is the operational region for a stable combustion is very limited in the case of PCI combustion because of knocking at high load condition and misfiring of the engine at low load condition. Because at high load conditions, more amount of air-fuel mixture will be present inside the cylinder of the

engine, and the time for air-fuel mixing is less. Thus parts of A/F mixture that have a stoichiometric A/F ratio results in a rapid heat release, which ends up in knocking. If low load condition persists, then the mixture will become excessively lean, leading to unstable self-ignition and misfiring.

Second factor is high production of CO and HC in PCI combustion. HC and CO are formed as a result of incomplete combustion. The main reasons for the formation of HC and CO are over lean A/F reactions or over rich A/F reactions [20]. When the mixture is over lean, then the excess oxygen surrounds the diffusion flame sheath, lowering the mixture's equivalence ratio below the lean flammability limit. In the case of over rich A/F ratio reactions, incomplete combustion occurs. As the EGR is increased, the mixture becomes leaner. This results in a higher production of HC and CO. Another factor affecting the formation of CO is the ignition delay. As EGR increases, the ignition delay lengthens that creates a chance of lean A/F reactions. Another reason for the production of incomplete combustion products is A/F ratio. Decreasing A/F ratio increases the products of incomplete combustion. In PCI combustion, the aim is to increase the ignition delay. This results in lower combustion duration. As a result, incomplete oxidation of the fuel can occur that increases the CO formation. Iwabuchi et al. [15] in his research says that during early part of compression stroke, the fuel gets impinged and adhere to the cylinder wall causing an in sufficiency heat release. This problem of impingement and surface adhering of the fuel is overcome by the design of an impinged spray nozzle that results in a higher dispersion of the fuel inside the cylinder and also significant reduction in fuel consumption.

The third problem associated with PCI is a generally observed decrease in efficiency. The following section describes the normally observed trend in the change in efficiency for PCI combustion.

1.2.6 Efficiency Trade off for PCI Combustion

Jacobs et al. [3] performed an analysis on the impact of EGR on the performance and emissions of a heavy-duty diesel engine. It was found that the fuel conversion efficiency decreases with an increase in the EGR rate. The decrease in the fuel conversion efficiency was attributed to the decreased combustion work and increased pumping work. The decrease in combustion work was due to the decrease in combustion efficiency and decrease in combustion temperature. EGR reduces the concentration of oxygen in the air. The increase in the pumping work was due to the effect of variable geometry turbocharger (VGT) used in the experimental set up to force the flow of EGR by increasing the exhaust manifold pressure. The change in the A/F ratio also causes a decrease in the heat release inside the cylinder, as the EGR is increased [19].

Ogawa et al. [16] worked on the modulated kinetics (MK) to reduce the NO_x and smoke by combining low temperature combustion and premixed combustion. They observed that there is a decrease in heat flux to the piston head as the injection timing is retarded. This was due to the reduction in combustion temperature and difference in combustion rates inside and outside the cavities due to the reduction in heat flux at the piston head than the cavity wall. A high swirl ratio was used to decrease the HC and soluble organic fraction (SOF) which is included in the PM emission. The authors tried to increase the efficiency of premixed combustion by decreasing the heat rejected to the

chamber wall. This was achieved by a higher swirl ratio. Higher swirl ratio decreases the heat flux near combustion chamber wall, which contributes to a decrease in heat flow rate during MK combustion. Ogawa et al. also investigated the effect of the injection amount and injection pressure in MK combustion method and a comparison was made to a combustion process that included a pilot injection. The results showed that the increase in heat flux with higher load and injection pressure was suppressed under a low oxygen concentration. The indicated efficiency decreased in the case of pilot injection due to vigorous combustion inside the combustion chamber.

Akagawa et al. [10] discusses the problems of using PREDIC. The author states the reason for higher fuel consumption and hence less efficiency for PREDIC as premature ignition. The factors affecting ignition are temperature, ignitability, mixture concentration and mixture distribution. The prevention of premature ignition was accomplished by the application of low EGR and compression ratio, addition of low ignitability oxygenated fuel component and decrease in mixture heterogeneity.

Tsurushima et al. [17] observed the decrease in thermal efficiency in PCI combustion. The inefficiencies of the PCI combustion were studied by heat balance estimation. Authors suggested the improvement in the thermal efficiency of PCI combustion under light load by controlling the fuel concentration with injection timing control. In addition, the unburnt fuel during the combustion process can be reduced by injection retardation. The heat loss was suppressed by controlling the speed of combustion reaction by the effect of EGR. The increase in efficiency by controlling the fuelling rate was also suggested by Zheng et al. [19].

Alriksson et al. [28**]** studied the emission characteristics in LTC of a heavy duty diesel engine using high levels of EGR. The authors were able to reduce the soot and the NO_x production, but they observed a rise in the brake specific fuel consumption (BSFC) and emission of CO and HC. A solution for this problem was described in the same article. Authors advanced the injection timing thus reducing the emissions. Soot emissions were also found to be decreasing for every level of advanced injection timing. But the NO_x level was found to increase for all the injection levels other than for EGR levels greater than 50%. There is a reduction in BSFC because of earlier and faster combustion inside the cylinder. However a higher level of EGR resulted in a higher CO production that in turn leads to an increase in BSFC.

Kumar et al. [4] discuss the reasons for a loss in efficiency in low temperature combustion. The expense of the efficiency was attributed to an increase in the production of CO and HC. Other factors that decrease the efficiency of diesel LTC are the presence of split combustion event, the fuel condensation leading to oil dilution and the off phasing of combustion event. In their article Kumar et al. also have provided the reasons for higher HC and CO emissions. This was mainly due to the low volatility of the diesel fuels, low combustion efficiency caused by the dilution of the in-cylinder mixture by EGR, fuel condensation and flame quenching on the surface of the combustion chamber and the flame-out of the locally excessive lean mixture caused by the non-homogeneity of the cylinder charge. Authors also made an attempt to increase the burning efficiency. The first method is the use of HCCI-plus-late-main injection that resulted in a better CO oxidation. The second solution is the selection of an appropriate

injection strategy equivalent with the boost, and EGR offered a possibility of avoiding fuel condensation and wall impingement of fuel injected early during the compression stroke. This method has shown in an improvement in HC emissions.

Lechner et al. [18] analyzes the effect of spray cone angle and advanced injection timing strategy to achieve partially PCI combustion in a diesel engine. The authors proved that low flow rate of the fuel, 60 degree spray cone angle injector strategy, optimized EGR and split injection strategy could reduce the engine NO_x emission by 82% and particular matter by 39%. This resulted in a slight loss of efficiency or a higher fuel consumption because of the lower oxygen concentration and lower combustion chamber temperature due to the circulation of cooled EGR.

A thermodynamically based approach to analyze the potential loss in efficiency of low temperature modes of diesel combustion lacks extensive presence in PCI combustion literature. To fill this need, this research study investigates total energy release, heat transfer, work done and corresponding efficiencies of various regimes of LTC.

1.3 Objective

The objectives of this research study are to evaluate how energy transfer and brake fuel conversion efficiency alter with (or are affected by) injection timings and EGR rate.

The first task in order to achieve the above objective is to study the effect of EGR and injection timings on pressure and heat transfer characteristics inside the cylinder. The second task is to study the energy distribution during the combustion

process and find the contribution of the heat transfer in it. The third task is to study the variation of the efficiency with injection timing and EGR.

The data is collected from an experimental apparatus located in General Motors Collaborative Research Laboratory at the University of Michigan as a part of previous study [2]. High levels of EGR along with late injection timing are used to achieve PCI Combustion. This method is used because of its capability to reduce NO_x and soot formation by using high injection pressure (1000bar) and low compression ratio (16:1). The data is obtained for four injection timings of 9°, 12°, 15°, and 18° BTDC and for four EGR rates of 39%, 40%, 41% and 42%. The pressure data obtained from the data acquisition system is used in the heat release calculation. Heat release is calculated using a method prescribed by Depcik et al. [29]. The in-cylinder properties obtained as a result of the heat release calculations are then used to calculate the net indicated thermal efficiency and brake fuel conversion efficiency. This thesis highlights major results and conclusions discovered while performing the named tasks to satisfy the study's objective.

2. METHODOLOGY

2.1 Engine Specifications

The test engine is located in the Engine Systems Research of the General Motors Collaborative Research Laboratory at the WE Lay Automotive Laboratory of the University of Michigan (UM). The engine was designed by Isuzu Advanced Engineering Center in Japan and manufactured by ISPOL / GMIDEL (Isuzu Poland / GM Isuzu Diesel Engine Limited) for use in Opel Vehicles.

The test engine is a four cylinder inline type. The total displaced volume is 1.7 liters. The engine uses common rail direct injection system designed and developed by Robert Bosch Corporation. The rail pressure in the common rail system can be varied between 100 and 2000 bar. The compression ratio of the prototype was 19:1. But with this high compression ratio, it was difficult to obtain a PCI combustion mode. So the compression ratio was reduced to 16:1 by modifying the bowl-in piston crown [30], thus increasing the clearance volume and hence a decrease in the compression ratio. But the other features of the engine remain unchanged.

The test engine is attached with a VGT. The turbocharger provides more control on the EGR rate and also on the boost pressures at various speeds and loads. The turbocharger is manufactured by Garret Turbo charging Systems. The EGR flow occurs when there is a favorable pressure difference between the exhaust and intake manifold. The VGT present in the exhaust tends to increase the pressure in the exhaust manifold. This is accomplished by the vanes inside the VGT. The vanes alter the exhaust gas flow

across the turbine blades thus providing a resistance of flow. This resistance of flow increases the pressure in the exhaust manifold.

A poppet style control valve is present to control the rate of flow of EGR. This is necessary because at times the pressure difference between exhaust and intake manifolds becomes favorable that EGR flow occurs automatically. But since this study requires a high precision and control in the flow of EGR rate, the poppet style EGR valve is kept fully open and the EGR flow rate is controlled by adjusting the vanes of VGT.

In addition to the poppet style control valve, a flapper style intake throttle is provided at the downstream of the compressor stage. This throttle provides a favorable pressure difference between the exhaust and intake manifolds.

The study is conducted for four injection timings of 9°, 12°, 15° and 18° BTDC at four EGR rates of 39%, 40%, 41% and 42%. A summary of the test engine specifications are given in Table 2.1.

2.2 Test Fuel

The fuel used in this study is the ultra low sulfur (<15 ppm) Swedish diesel fuel. But the current fuel used in the US is referred to as Diesel # 2. There is a large difference in the properties of ultra low sulfur Swedish diesel fuel and Diesel # 2. Table 2.2 indicates the difference in the properties between these two fuels. Paragon laboratories in Livonia, Michigan conducted the fuel analysis provided in the table [2].

Table 2.1 Test engine specifications

Designer / manufacturer	ISUZU / Opel
Number of Cylinders	4
Displaced Volume (L)	1.7
Bore (m)	0.079
Stroke (m)	0.086
Connecting Rod Length (m)	0.1335
Wrist Pin Offset (m)	0.0006
Compression Ratio	16:1
Piston Geometry	Bowl – in
Number of Valves / Cylinder	4
Number of Cams	2
Cam Location	Overhead with hydraulic lash adjusters
Fuel System	Common rail Direct-Injection
Injection Location	Centrally Mounted
Intake Valve Opening (°BTDC-c)	366
Intake Valve Closing (°BTDC-c)	136
Exhaust Valve Opening (°ATDC-c)	122
Exhaust Valve Closing (°ATDC-c)	366
Injector Nozzles Number of Holes	6
Injector Nozzle Spray Angle (deg)	150
Injector Nozzle Flow Rate (cc/30-s)	320
Intake throttle	Flapper style downstream of compressor
Turbocharger	Variable Geometry Turbocharger
Exhaust Gas Recirculation Valve	Poppet-style control valve

Table 2.2 Comparison of the properties of Swedish Diesel and Diesel # 2

Properties	**Ultra low sulfur Swedish Diesel**	**Diesel # 2**
Cetane Number	51.6	49.6
Sulfur Concentration (ppm)	12	500
A/F Stoichiometric ratio	14.74	14.46
Density (kg/m^3)	810	840
T_{50} (K)	530	498
Lower Heating Value(MJ/kg)	43.481	42.91

As observed from the table, the key differences between the two fuels are in the Cetane number, lower heating value, density and 50% distillation temperature. All these factors except density affect the combustion process in this study.

Cetane number is a measure of the quality of the diesel fuel. It is defined as the percentage of normal-Cetane in a mixture of normal-Cetane and alpha-Methyl Naphthalene which has the same ignition delay as that of the test fuel when combustion is carried out under prescribed operating conditions. Hence Cetane number is the measure of the ignition delay. Larger the Cetane number indicates shorter ignition delay. The challenge faced in using the low sulfur Swedish diesel fuel is to develop a PCI combustion mode. To obtain PCI combustion, the fuel must be mixed fully before ignition begins. A higher Cetane number means that the time available for the pre-mixing of the fuel is less.

Lower heating value (LHV) is defined as the amount of energy released by the combustion of a unit mass of fuel with gaseous air, at constant volume and producing gaseous products (including water vapor). The lower heating value of the fuel is measured using a fully insulated bomb calorimeter [31]. The brake fuel conversion efficiency is dependent on the lower heating value of the fuel thus making thus parameter significant in this research.

50% distillation temperature refers to the temperature at which 50% of the fuel gets converted to its vapor state and is ready for ignition. The fuel is distilled in a distillation apparatus and the variation of temperature with distillation is observed to obtain the distillation curve [32]. Swedish diesel fuel is having a higher 50% distillation

temperature than Diesel # 2. This means that at any instant of time before ignition, lesser amount of the Swedish diesel fuel has vaporized when compared to Diesel # 2. This factor makes it difficult to obtain PCI combustion because complete vaporization of the fuel has to be achieved before the ignition. The experimental apparatus is fitted with a diesel oxidation catalyst (DOC) to remove higher quantities of HC and CO emissions. Presence of sulfur in the fuel impacts the performance of the catalyst. Hence the use of Swedish diesel fuel is preferred because of its low sulfur content and hence a lower sulfur contamination.

2.3 Data Collection

The following section describes various instrumentations and data collection methodologies involved in this research.

2.3.1 Instrumentation

To collect data from the test engine various types of measuring instruments are used.

2.3.1.1 Piezo Electric Pressure Transducer

Kistler 6041A, water cooled piezo electric pressure transducer is used to measure the in-cylinder pressure. These transducers have a high response time. This makes this instrument suitable as there are fast rates of pressure changes inside the cylinder of the test engine. The calibration of the sensor is done using a dead weight tester. Piezo electric sensor is a dynamic sensor.

2.3.1.2 Max Machinery Flow Meter

Max Machinery model 213 positive displacement flow meter is used to measure the engine fuel flow. Precise measurement of the fuel flow is required as it is used in the calculation of heat release, net indicated thermal efficiency and brake fuel conversion efficiency. The flow meter can measure the flow from 1 cm^3/min to $7.57x10^3$ cm^3/min. The typical fuel flow rate in this research is approximately 0.55 g/s or 40.7 cm^3/min.

2.3.1.3 Laminar Flow Element

Air flow measurement is achieved using two instruments. The first instrument used is the Meriam Instrument Laminar Flow Element model 50MC2-4F. The flow element uses a honey comb structure to stabilize the flow of air for accurate flow measurement using pressure-differential method. A pressure drop is created in the air flow because of the presence of an orifice in the middle of the laminar flow element. This pressure drop is then measured using the second instrument, OMEGA differential pressure sensor model; PX653-10D5V. The typical air flow rate in this research is approximately 11 g/s. Precise measurement of the air flow is required as it is used in the calculation of temperature using the ideal gas law and hence the computation of heat release.

2.3.1.4 Dyno-Loc Controller

The speed and torque produced by the engine is measured by the dynamometer and it is processed by Dyn-Loc Controller (Dynamometer Controller). To one end of the dynamometer's drive shaft, on a gear, an eddy current speed sensor is fixed. This sensor measures the speed. The output from the sensor is a frequency signal, which is fed to the

Dyn-Loc Controller for processing. This frequency signal is converted to engine speed (in revolutions per minute). Corresponding to the speed frequency, the Dyn-Loc Controller produces an analog voltage. This analog voltage is recorded by low speed data acquisition system. This analog voltage signal is also fed into a high speed data acquisition system, but the system is not resolved enough to observe engine speed fluctuations in a cycle.

A standard load cell transducer is used to measure the engine torque. It measures the applied force exerted by the dynamometer housing. The output from the load cell transducer is voltage that is fed into the Dyn-Loc Controller. The Dyn-Loc Controller outputs the torque. The torque is then used to calculate the brake power.

2.3.1.5 AVL CEB Π Emission Analyzers

Non-Dispersive Infra Red (NDIR) AVL CEB Π Emission Analyzer is used to measure EGR flow rate. EGR flow rate is calculated from the measurement of CO_2 in the intake and exhaust manifolds. The NDIR emission analyzer is also used to measure the exhaust CO. Flame ionization detector type AVL CEB Π Emission Analyzer is used to measure the total exhaust HC measurement.

2.3.2 Collection Methodology

The engine is started and is warmed up. After the engine warm up, engine torque and speed are set to the required values. Other engine parameters such as injection pressure, injection timing, boost pressure, EGR rates are adjusted to the required values. The test is conducted at 1500 rpm for lean PCI combustion strategy at four different

injection timings of 9°, 12°, 15° and 18° BTDC with varying EGR of 39%, 40%, 41% and 42%.

After the parameters are set, the engine is allowed to get stabilized (until the temperature gets stabilized). This process might take around 20 minutes. After the engine stability is attained, a time based data log is recorded. This data log records 200 points every 2 or 3 seconds. All the data summarized in Table 2.3 is recorded. Similarly a crank angle based data log records the data at a crank angle resolution of 0.25 degrees. 20 continuous cycles of crank angle based data are recorded. Two output files are generated by crank angle based data acquisition system. First one is the individual cycle data file (pressure data for each of 20 cycles) and the second one is an averaged data file (20 cycle average pressure data). After data logging, the stability of the engine during log is analyzed. If any instability found, the log is repeated.

Table 2.3 Summary of the description of the instruments used in the study

Designation	Description	Instrument Used
Torque	Engine brake torque (N-m)	Load Cell Transducer
Speed	Engine rotational speed (rpm)	Eddy Current Sensor
Fuel Flow	Engine fuel flow rate (g/s)	Max Machinery Flow Meter
Air Flow	Engine air flow rate (g/s)	Laminar Flow Element
EGR	Engine EGR rate (%)	NDIR AVL CEB II Emission Analyzer
CO, CO_2, HC	Emissions (ppm)	AVL CEB II Emission Analyzer

The in cylinder pressure is collected for each cylinder for each test. The pressure data obtained is the averaged pressure data over 20 cycles. This data is then used for the calculation of heat release. Other parameters required for the heat release analysis are EGR rates and air and fuel flow rates. First law of thermodynamics is used to analyze the heat release. Detailed explanation of the heat release is explained in section 2.4.3.

By knowing the cylinder bore, stroke, compression ratio and connecting rod wrist pin offset, the cylinder volume is calculated.

2.4 Data Manipulation and Analysis

This section describes the method of computation of the heat release using the University of Michigan heat release (UMHR) software, calculation of various parameters such as net indicated fuel conversion efficiency, brake thermal efficiency, pumping mean effective pressure etc.

2.4.1 UMHR Analysis

The UMHR program consists of two components. The graphical user interface (GUI) and heat release code. The GUI is written in Visual C++ and the heat release code is written in FORTRAN. The GUI serves as a means by which a user inputs the data, selects the parameters and views the results. Once user has input the data, the GUI calls for FORTRAN part of the program, which calculates the results. The final results are then sent to the GUI to be reported to the user.

The UMHR software calculates the energy released by the fuel during the combustion stroke of the engine cycle on a crank angle basis. This is achieved by analyzing the measured in-cylinder pressure. The measurement of the in cylinder

pressure is explained in section 2.3.2. The heat release is calculated during the closed part of the engine cycle, that is, from intake valve closing to the exhaust valve opening.

The heat release is calculated using the first law of thermodynamics. The first law states that energy can neither be created nor be destroyed, but it can be transformed from one form to another. This means that the total energy released (Q_{ch}) by the reacted fuel in the cylinder must be balanced by (1) the piston output work (W_{CV}), (2) the change in internal energy (ΔU_{CV}), (3) the heat transfer losses through the cylinder walls (Q_{HT}), and (4) the lost mass exiting the cylinder due to blow-by or crevice flow losses and any unreacted fuel exits as such and results in a combustion inefficiency. In mathematical terms this can be explained by the following equation:

$$\frac{\delta Q_{ch}}{d\theta} = \frac{dU_{CV}}{d\theta} + \frac{\delta W_{CV}}{d\theta} + \frac{\delta Q_{HT}}{d\theta} + \sum h_{out} \frac{dm_{out}}{d\theta} \qquad (1)$$

The equation above is written on a crank angle basis. This is because the in cylinder pressure is measured on a crank angle basis. The solution for the above equation theoretically should be exactly equal to the energy liberated by the combustion of the fuel. Each term is calculated by appropriate numerical methods and models of physical processes which are explained later in this section.

The first term in the equation indicates a change in internal energy on a crank angle basis. The pressure and temperature inside an engine cylinder are constantly changing. This means that there will be a change in internal energy also. The equation used in the calculation of change in internal energy is

$$\frac{dU_{cv}}{d\theta} = m\, C_v \frac{dT}{d\theta} \tag{2}$$

Where, *m* indicates the mass of the cylinder mixture. In the calculation of change in internal energy it is assumed that the cylinder mixture is an ideal gas (*PV= mRT*). The constant volume specific heat (C_v) is determined by knowing the ratio of the specific heats, γ as

$$C_v = \frac{R}{\gamma - 1} \tag{3}$$

This method is applied as it is possible to fix a value for *R* and find relationship between the ratio of the specific heats depending on the composition and/or temperature. The initial value of γ is taken as 1.25. Later Brunt and Platts correlation [33, 34] is used to iterate the value of γ changes with temperature inside the cylinder as combustion progress.

The mass of the cylinder mixture is calculated by adding the measured mass of fuel, the measured mass of air flowing, and the calculated mass of EGR into the cylinder. The heat release analysis is done for a single cylinder inside the engine. Thus the amount of fuel and air to each cylinder must be known. Thus for a multi-cylinder engine, this is approximated by dividing the total mass of air and fuel flowing into the engine by the number of cylinders. The temperature in the cylinder is calculated from the ideal gas law using the experimentally measured pressure.

The mixture gas constant used in the ideal gas law, *R*, is related to the specific heat values ($R= C_p - C_v$). The two specific heat constants have same dependence on

temperature and pressure. Hence the difference between the two is always the same. That is, *R* is not a function of temperature and pressure. But *R* will change if there is a change in A/F ratio or if dissociation occurs. An assumption is made that the A/F mixture is mixed perfectly and instantaneously as the A/F ratio is changed. This assumption is known as single-zone model. The initial value of *R* is assumed to be 300 J/kg/K. As combustion progress inside the engine, there will be dissociation and change in A/F ratio. This results in a change of *R* inside the cylinder. Thus the changed value of *R* is determined by the Krieger and Borman correlation [35]. Once the value for *R* and γ is determined, value for specific heat constants are found out.

The second term on the right hand side of first law analysis is the work output on a crank angle basis. The indicated work per cycle is obtained by calculating the area bound by the P-V diagram. The work produced by the engine is calculated by the relation:

$$\frac{\delta W_{cv}}{d\theta} = P\frac{dV}{d\theta} \tag{4}$$

The above equation is numerically equivalent to the true work term, which is the integral of *PdV*. The pressure and volume of the cylinder can be calculated on a crank angle basis as explained in section 2.3.2.

The third term on the right hand side of the first law analysis is the heat transfer term. Generically, the heat transfer is calculated by

$$\frac{\delta Q_{HT}}{d\theta} = h_c A_s (T - T_w) + h_T A_s (T^4 - T_W{}^4) \tag{5}$$

Where A_s is the area of convective heat transfer which can be calculated analytically, T_W is the cylinder wall temperature. The first term on the right side of equation 5 is the heat transfer due to convection and the second term represents the radiative heat transfer. However this calculation used a linear relation for the heat transfer. The temperature used is the bulk gas temperature.

Spark Ignition (SI) heat transfer correlation involves only convective heat transfer, while compression ignition correlation involves both convective and radiative heat transfer effects. Various correlations are provided in the software for the calculation of the heat transfer coefficients. In this particular study, Hohenberg correlation [36] is used to determine the value of the in-cylinder heat transfer coefficient (h). Hohenberg modified Woschni's correlation for the heat transfer coefficient for a diesel engine. He has included the effect of combustion swirl, effect of pipe diameter on mass flow rate inside the cylinder, effect of radiation etc. for the calculation of the total heat transfer.

The fourth term on the right hand side of the first law analysis is the blow-by and/or crevice flow effects in the engine. Due to the imperfect sealing of the piston rings inside the cylinder, gases flow into the crevice region (crevice flow) and possibly past the rings (blow-by). For a homogenous charge engine, this will result in a loss of fuel mass. But for a heterogeneous charge engine, usually air mass is the only loss mass. Although the fuel mass is not lost, the loss of air leads to a decrease in the trapped mass, which will affect the heat release calculation. This program does not account for the blow-by or crevice flow. It is also assumed that the EGR and residual fraction inside the cylinder do not alter the composition in the cylinder. Table 2.4 indicates the various

correlations used in the current study. In Krieger and Borman correlation, R^* is the gas constant for undissociated products.

For more details on the heat release computation of the UMHR software, refer [29].

Table 2.4 Summary of correlations used in the UMHR software for the current study

Parameter	Source	Correlation
R	Krieger and Borman [30]	$R = R^* + \frac{[11.98 - 45.796(\frac{1000}{T}) - .4354\ln(P)]F + 0.2977\ln(F)}{1000}$
γ	Brunt and Platts [18, 29]	$1.350 - 6.0\times10^{-5}T + 1.0\times10^{-8}T^2$
h	Hohenberg [31]	$3.26.V^{-0.06}.P^{0.8}.T^{-0.4}.(\overline{S_P} + 1.40)^{0.8}$

2.4.2 Use of UMHR

As described in section 2.4.1 various inputs have to be given to the UMHR software for heat release analysis. The program is run for 15 sets of data, as listed in table 2.5.

Table 2.5 Combinations of injection timings and EGR rates under study

Injection Timing (° BTDC)	EGR rates (%)
9	39, 40, 41, 42
12	39, 40, 41, 42
15	39, 40, 41, 42
18	40, 41, 42

2.4.2.1 Constant Parameters

All the cases are studied at 1500 rpm. The wall temperature is assumed constant at 500° C with a "best guess" estimate. In an actual engine, there are several mechanisms that cause variations in wall temperature; for example, heterogeneity in the combustion process and differences in cooling passages [29]. Table 2.6 indicates the various parameters that are held constant throughout the study.

Table 2.6 Summary of the constant parameters in the study

Compression Ratio	16
Engine Speed	1500
Top Dead Center Adj (deg)	0
Inlet Valve Closing (deg)	-136
Exhaust Valve Opening (deg)	122
Initial Gas Constant (J/kg/K)	300
Initial Gamma	1.25
Stoichiometric A/F ratio	14.74
Lower Heating Value (kJ/kg)	43481
Cylinder head surface area (m^2)	0.0049017
Piston crown surface area (m^2)	0.007353

2.4.2.2 Mass of Fuel

The fuel measurement to the test engine is done by a Max Machinery flow meter as explained in section 2.3.1.2. The fuel flow into a single cylinder is approximated by dividing the total mass of fuel flowing into the engine by the number of cylinders. The fuel flow is different for each injection timing and for each EGR rate. Table 2.7 indicates the fuel mass flow into Cylinder 1 in the test engine set up for various cases of study. Total mass of air and fuel is used for heat release calculation, which is used in the calculation of brake thermal efficiency.

Table 2.7 Fuel flow rate (g/s-cylinder) for different combinations of injection timings and EGR

	Injection Timing 9° BTDC	Injection Timing 12° BTDC	Injection Timing 15° BTDC	Injection Timing 18° BTDC
EGR=39%	0.135704	0.136929	0.135283	-
EGR=40%	0.136929	0.134244	0.136592	0.135323
EGR=41%	0.136072	0.133363	0.134399	0.134791
EGR=42%	0.134592	0.134279	0.134898	0.140422

2.4.2.3 Mass of Air

The air flow measurement into the test engine is done using a laminar flow element described in section 2.3.1.3. The air flow calculation is done using the same principle as that of fuel flow. Table 2.8 indicates the air flow into a Cylinder 1 in the test engine set up for various cases of study. Total mass of air and fuel is used for heat

release calculation, which is used in the calculation of brake thermal efficiency. The fuel flow rate and the air flow rate into Cylinders 2, 3 and 4 will be the same as that of Cylinder 1.

Table 2.8 Air flow rate (g/s-cylinder) for different combinations of injection timing and EGR

	Injection Timing 9° BTDC	Injection Timing 12° BTDC	Injection Timing 15° BTDC	Injection Timing 18° BTDC
EGR=39%	2.60024	2.605888	2.544795	-
EGR=40%	2.540562	2.494494	2.490556	2.461599
EGR=41%	2.423473	2.410886	2.401001	2.389053
EGR=42%	2.354299	2.31257	2.229433	2.281455

2.4.2.4 Brake Power

The brake power is calculated from the torque and speed measured by the dynamometer as explained in section 2.3.1.4. The brake power is used for the calculation of brake fuel conversion efficiency which is explained later in this section. Table 2.9 indicates the total brake power generated by the test engine for various cases of study.

Table 2.9 Brake power (kW) generated by the engine for the different combinations of injection timing and EGR

	Injection Timing 9° BTDC	Injection Timing 12° BTDC	Injection Timing 15° BTDC	Injection Timing 18° BTDC
EGR=39%	8.08	8.10	7.96	-
EGR=40%	7.99	7.95	7.99	7.90
EGR=41%	7.74	7.74	7.73	7.72
EGR=42%	7.36	7.74	7.89	8.30

2.4.3 Correction of Pressure Data

Influence of external disturbance is observed for certain pressure crank angle data obtained from the data acquisition system. The presence of external influence can widely affect the heat release calculation performed by the UMHR software. To rectify this error, smoothing is done at those points where the "spike" is observed in the pressure crank angle diagram for the respective case. The spike is observed for the following cases: cylinder 1 injection timing 15° BTDC EGR= 40%, cylinder 2 injection timing 15° BTDC EGR= 39%, cylinder 2 injection timing 15° BTDC EGR= 40%, and cylinder 3 injection timing 15° BTDC EGR= 40%.

Pressure crank angle diagram for cylinder 1 injection timing 15° BTDC EGR=40% is shown in Figure 2.1. Influence of an external disturbance can be observed for crank angles -109° to -107.75° BTDC.

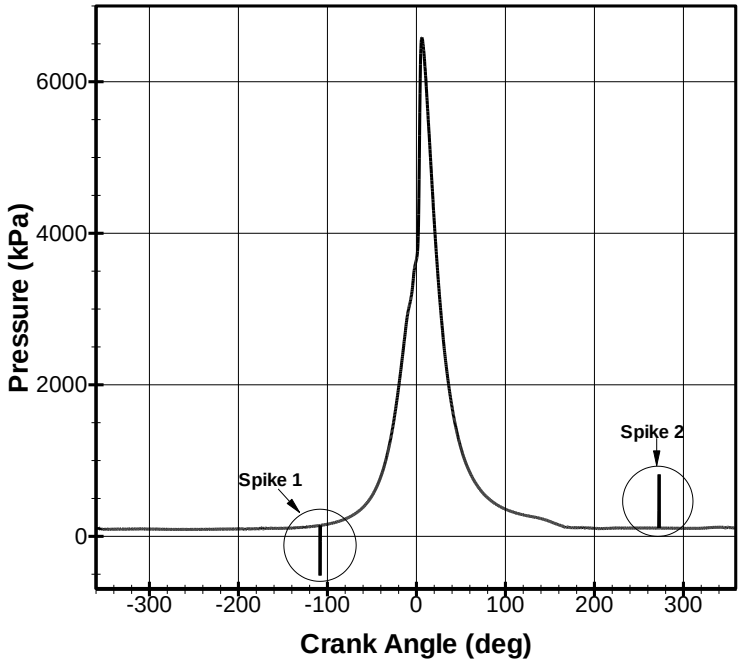

Fig. 2.1 Pressure versus crank angle for cylinder 1 for an injection timing of 15° BTDC and EGR= 40% before pressure data correction.

If the spike occurs during compression, or expansion stroke the smoothing process is done by assuming that the process is polytropic. Figure 2.2 indicates the calculation involved in this process. Table 2.10 shows the corrected pressure values. If the spike is seen during the intake or exhaust stroke, then pressure is assumed to be constant. In this case discussed the constant pressure is 108 kPa.

$$PV^n = Const$$

$$\therefore P_{109.75}V_{109.75}{}^n = P_{107}V_{107}{}^n$$

$$(1.42\times10^5)(3.39\times10^{-4})^n = (1.45\times10^5)(3.33\times10^{-4})^n$$

$$\therefore n = 1.165$$

$$P_{109}V_{109}{}^n = P_{109}V_{109}{}^n$$

$$(1.42\times10^5)(3.39\times10^{-4})^{1.165} = P_{109}(3.38\times10^{-4})^{1.165}$$

$$\boxed{P_{109} = 1.43\times10^5\,Pa}$$

Fig. 2.2 Calculation involved in the pressure correction for cylinder 1 at an injection timing of 15° BTDC and EGR= 40%.

Table 2.10 Corrected pressure values for cylinder 1 at an injection timing of 15° BTDC and EGR= 40% after pressure data correction

Crank Angle (° BTDC)	Pressure (kPa)
108.75	143
108.5	143
108.25	144
108	144
107.75	145

Figure 2.3 indicates the pressure versus crank angle diagram for cylinder 1 for an injection timing of 15° BTDC, at an EGR= 40% after the smoothing operation.

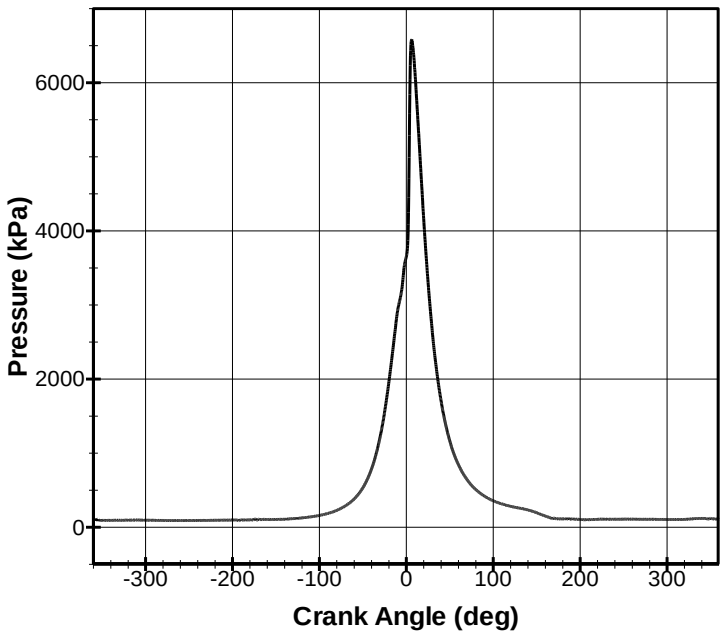

Fig. 2.3 Pressure versus crank angle plot for cylinder 1 at an injection timing of 15° BTDC and EGR= 40% after pressure data correction.

2.4.4 Processing of UMHR Data

The output data obtained from the heat release analysis is used for the calculation of the different parameters needed for the study. The following section describes the methodology used for the calculation of these parameters.

2.4.4.1 Indicated Work

The indicated work data is required for the calculation of net indicated thermal efficiency and pumping mean effective pressure. The heat release analysis gives change in indicated work (ΔW) per 0.25 degrees of crank angle revolution ($\Delta\theta$). ΔW is calculated as $P\Delta V$. Thus,

$$\text{Total indicated work} = \frac{\Delta W}{\Delta \theta} \cdot \Delta \theta \qquad (6)$$

There are two common definitions of indicated work in use. They are the gross indicated work per cycle (W_{gross}) and net indicated work per cycle (W_{net}). Gross indicated work per cycle is defined as the sum of the work delivered by the piston during compression and expansion strokes. Net indicated work per cycle is defined as total work delivered by the piston over the entire four stroke cycle. It is known that the area bound within the *P*-*V* curve gives the indicated work.

Figure 2.4 indicates the *P*-*V* diagram for a four-stoke cycle compression ignition at part load condition. W_{gross} is area A and W_{net} is area A– area B. Area B is known as the pumping work (W_p). It is defined as the work transfer between the piston and the exhaust gases during the intake and exhaust strokes. If the pressure during the exhaust stroke is greater than the pressure during the intake stroke, then the work transfer will be *to* the cylinder gas. This is commonly observed in all the naturally aspirated engines. If the intake stroke pressure is greater than the exhaust stroke pressure, then the work transfer will be *from* the cylinder gases to the piston. This is commonly observed in highly loaded turbocharged engines.

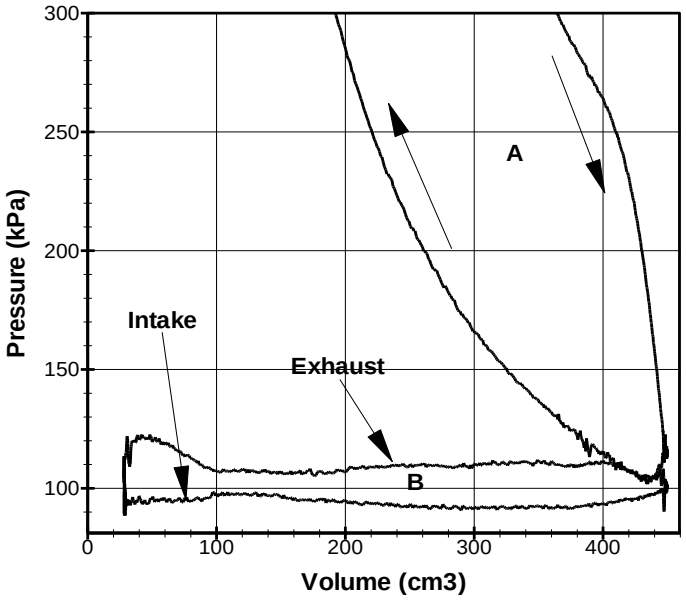

Fig. 2.4 P-V diagram for a four-stoke cycle compression ignition engine at part load.

Thus net indicated work per cycle is calculated as

$$W_{net} = \sum_{\theta=-360}^{360} \frac{\Delta W}{\Delta \theta} \cdot \Delta \theta \tag{7}$$

And the gross indicated work per cycle is calculated as

$$W_{gross} = \sum_{\theta=-180}^{180} \frac{\Delta W}{\Delta \theta} \cdot \Delta \theta \tag{8}$$

It is assumed that the crank angle at the start of the intake stroke is -360°

2.4.4.2 Pumping Mean Effective Pressure

The usable work that is delivered to the drive shaft is expended for many secondary purposes. One of the purposes is to draw fresh mixture to the intake system

and to drive out the burnt gases through the exhaust system. This is known as pumping work (W_p). Hence pumping work is defined as the work transfer between the piston and the exhaust gases during the intake and exhaust strokes. The pumping mean effective pressure (PMEP), as defined here is a positive quantity. It is defined as, the difference between gross indicated mean effective pressure ($IMEP_{gross}$) and net indicated mean effective pressure ($IMEP_{net}$). $IMEP_{gross}$ is the ratio of gross indicated work per cycle and the total displaced volume. $IMEP_{net}$ is the ratio of net indicated work per cycle and the total displaced volume (V_d). Hence mathematically,

$$PMEP = \frac{\sum_{\theta=-180}^{180} \frac{\Delta W_{gross}}{\Delta\theta} \cdot \Delta\theta}{V_d} - \frac{\sum_{\theta=-360}^{360} \frac{\Delta W_{net}}{\Delta\theta} \cdot \Delta\theta}{V_d} \tag{9}$$

$$V_d = \frac{\Pi}{4} \times B^2 \times S \tag{10}$$

Where B is the bore and S is the stroke of the cylinder.

2.4.4.3 Brake Mean Effective Pressure

Brake mean effective pressure (BMEP) is calculated using the relation

$$BMEP = \frac{\dot{P} \cdot n_R \cdot 60}{V_d \cdot N} \tag{11}$$

Where n_R is the crank revolutions for each power stroke per cylinder. In this case n_R=2.

2.4.4.4 Friction Mean Effective Pressure

Friction mean effective pressure (FMEP) is calculated using the relation

$$FMEP = IMEP_{net} - BMEP \tag{12}$$

FMEP gives an indication of the role of friction in combustion.

2.4.4.5 Total Heat Transfer

The total heat transfer to the walls (Q_{HT}) is obtained directly from the output of the heat release program. The method of calculation of heat transfer is explained in section 2.4.1. The total heat transfer is vital for this study as it is needed in the analysis if the energy distribution.

2.4.4.6 Total Heat Release

The total heat release (Q_{ch}) is required for the calculation of net indicated thermal efficiency. The total heat release is directly obtained from the output of UMHR program. As described in section 2.4.1, the total heat release is calculated based on the first law of thermodynamics. But it should be noted that this heat release won't be the actual heat release inside the cylinder of the engine due several assumptions that are made during the calculation of the heat release. These assumptions include uniform and homogenous properties (single-zone model), negligible crevice flow and blow-down, constant wall temperature, negligible change in the composition of the cylinder mixture as a result of EGR and residual fraction after exhaust.

2.4.4.7 Combustion Efficiency

In practice, a fraction of fuel's chemical energy is not released inside the cylinder of the engine during the combustion process. A part of it will be expelled through the exhaust in the form of incomplete combustion products. Combustion efficiency (η_c) is 100%, if all the chemical energy of the fuel is converted to heat. More unburnt products

in the exhaust imply lesser combustion efficiency. The combustion efficiency is calculated using the formula [37]:

$$\eta_c = 100.0 - \frac{100.0}{[CO]+[CO_2]+3\cdot[C_3H_{3Y}]}\cdot\left[\frac{254.0\cdot[CO]+217.1\cdot[H_2]}{MW_f}+3\cdot[C_3H_{3Y}]\right] \quad (13)$$

Where MW_f is the molecular weight of fuel per carbon atom. [CO], [CO_2] and [C_3H_{3Y}] are measured using AVL CEB Π Emission Analyzer (section 2.3.1.5).

2.4.4.8 Brake Fuel Conversion Efficiency

Brake fuel conversion efficiency (η_f) is the ratio of the brake power output ($\dot{P}$) of the engine to the rate of energy delivered to the engine by the fuel. Mathematically it can expressed as

$$\eta_f = \frac{\dot{P}}{\dot{m}_f \cdot Q_{LHV}} \quad (14)$$

$\dot{m}_f$ is the mass of fuel (g/s**)**

Q_{LHV} is the lower heating value of the fuel (kJ/kg) and

$\dot{P}$ is the power (kW).

The denominator of the equation indicates the total amount of energy released by complete combustion of the fuel. Brake fuel conversion efficiency is a product of net indicated thermal efficiency, combustion efficiency and mechanical efficiency. That is,

$$\eta_f = \eta_{th,net}.\eta_c.\eta_m \quad (15)$$

Where, η_m is the mechanical efficiency.

The net indicated thermal efficiency consists of pumping work.

2.4.5 Uncertainty Analysis

For all the experimental study, there are several sources of uncertainties. For this study, experimental error is defined as the difference between the true value and experimentally measured value.

2.4.5.1 Uncertainty Analysis of Net Indicated Thermal Efficiency

It is assumed that the uncertainty in net indicated thermal efficiency is largely due to cycle to cycle variations in pressure data. As explained in section 2.3.2, the pressure data obtained is the averaged pressure data over 20 cycles. This data is then used for the calculation of heat release. Given below is the procedure followed for the uncertainty analysis of brake thermal efficiency. The pressure data used in this calculation is at the operating point of injection timing 9° BTDC and EGR= 41%.

a) Total work done and total heat released is found out for all the 20 set of pressure crank angle data.
b) Calculate the net indicated thermal efficiencies for these two cycles using the respective work and heat release as explained in section 2.4.4.5.
c) Calculate the differences in efficiencies between the maximum efficiency and the average efficiency and the minimum efficiency and the average efficiency.

Table 2.11 indicates the work done, heat release and the net indicated thermal efficiency for 20 cycles of pressure data. The average efficiency is 45. 385%. Hence the upper uncertainty is 0.615% and lower uncertainty is 0.985%. These uncertainties are assumed for other operating points.

Table 2.11 Work done, heat release and the net indicated thermal efficiency for 20 cycles of pressure data

Case #	Work Done (J)	Heat Supplied (J)	Brake Thermal Efficiency (%)
1	181	399	45.2
2	178	390	45.6
3	178	390	45.6
4	182	403	45.2
5	179	399	44.8
6	182	397	45.8
7	179	392	45.7
8	184	404	45.6
9	180	406	44.4
10	181	398	45.4
11	181	404	44.8
12	178	393	45.2
13	184	407	45.2
14	181	400	45.2
15	185	407	45.5
16	185	403	46.0
17	181	401	45.2
18	179	394	45.3
19	181	394	46.0
20	181	393	46.0

2.4.5.2 Uncertainty Analysis of Brake Fuel Conversion Efficiency

Calculation of brake fuel conversion efficiency is explained in section 2.4.4.7. Uncertainty in brake fuel conversion efficiency can occur due to uncertainties in torque, speed of the engine, and mass of fuel. The ultimate torque uncertainty in the experiment is 2.48Nm. The experimental error associated with the measurement of engine speed is

± 5 RPM. Based on the accuracy stated by the manufacturer, the measurement of the flow rate of fuel is 2.7×10^{-6} kg/s of the true value. Injection timing of 9° BTDC and EGR= 41% is taken to determine the uncertainty. The average brake fuel conversion efficiency at this point is calculated to be 32.7%. The maximum brake fuel conversion efficiency is calculated by taking the maximum errors of torque, engine speed and mass of fuel. It is calculated to be 33.80%. Similarly, the minimum brake fuel conversion efficiency is calculated by taking the minimum values of the three parameters mentioned above and it comes out to be 30.37%. Hence the upper uncertainty is 1.1% and lower uncertainty is 2.33%.

3. DIESEL ENGINE COMBUSTION

3.1 Introduction

3.1.1 History of Diesel Engine

The diesel engine was invented by German engineer Rudolph Christian Karl Diesel in the year 1892. The initial motivation for the development of the diesel engine was the low efficiency of the steam engine. Diesel initially tried to change the working fluid in the steam engine from steam to ammonia vapor. However, the toxicity and its difficult management lead to the discontinuity of this research. Frustrated at his inability to improve the efficiency of steam engine, he realized from his research experience of using air as working fluid, that the high temperature and pressure created by compressing the air is enough to ignite a fuel introduced into the chamber [38]. Thus in 1892 Diesel conceptualized that fuel when injected into a high pressure compressed air would ignite, thus avoiding the external heat addition (as in a steam engine).

Diesel proposed four conditions for successful execution of his design [38]. The first condition is that the ignition temperature is created by compression of air. Second condition indicates a deviation from standard operating cycle (Carnot cycle) is necessary. This is because Carnot cycle would create a high pressure that is untenable by any mechanical device. The third condition states that the combustion should occur isothermally. Fourth condition is that the engine should run lean.

Rudolf Diesel designed the diesel engine to replace steam engine in industries. Early set of diesel engines used the same set of layout as that of steam engines of the

time with long cylinder bore, external valve gear, cross head bearings and open crank shaft connected to a large flywheel. During early twentieth century, double acting four stroke diesel engines were constructed to increase the power output. Here the combustion took place on both sides of the piston. But the main problem with this engine was the absence of a good seal at the bottom of the cylinder where the piston rod pass through to the cross head bearing. In 1923, Robert Bosch developed a number of designs for fuel injection pumps [39]. By 1930s the use of turbochargers was introduced [40]. In 1936, Mercedes came out with Mercedes 260D fitted with a diesel engine [41]. This is the first volume production car to be fitted with diesel engines. Later part of the 20^{th} century saw the stringent pollution norms along with the demand for higher efficiency leading to a lot of improvements in the design of the conventional diesel engine, such as electronic diesel engine controllers.

3.1.2 Engine Terminologies

In this section, some common terms associated with engine and its operation is defined.

- Displaced volume: It is also known as swept volume. Displaced volume is defined as the volume swept by the piston of the cylinder when it moves from TDC to bottom dead center (BDC).
- Clearance volume: It is the volume inside the cylinder of the engine between the TDC and cylinder head.
- Compression ratio: It is the ratio of maximum cylinder volume to minimum cylinder volume. The minimum volume refers to the clearance volume.

- Ignition delay: The time period between the injection of fuel into the combustion chamber to the start of combustion.
- Brake power: The power that is available at the crankshaft of the engine that is readily available for work.
- Indicated work: The indicated work per cycle is obtained by integrating around the pressure volume data curve for a cycle, to obtain the area under the curve. There are two common definitions of indicated work in use. They are the gross indicated work per cycle (W_{gross}) and net indicated work per cycle (W_{net}). Gross indicated work per cycle is defined as the sum of the work delivered by the piston during compression and expansion strokes. Net indicated work per cycle is defined as total work delivered by the piston over the entire four stroke cycle.
- Pumping work (W_P): It is defined as the work transfer between the piston and the exhaust gases during the intake and exhaust strokes. If the pressure during the exhaust stroke is greater than the pressure during the intake stroke, then the work transfer will be *to* the cylinder gas. This is commonly observed in all the naturally aspirated engines. If the intake stroke pressure is greater than the exhaust stroke pressure, then the work transfer will be *from* the cylinder gases to the piston. This is commonly observed in highly loaded turbocharged engines.
- Mechanical Efficiency: It is the ratio of brake power to the net indicated power. The difference between the net indicated power and brake power gives the friction power.

- Combustion efficiency: In practice, a fraction of fuel's chemical energy is not released inside the cylinder of the engine during the combustion process. A part of it will be expelled through the exhaust in the form of incomplete combustion products. Combustion efficiency is 100%, if all the chemical energy of the fuel is converted to heat energy. More unburnt products in the exhaust imply lesser combustion efficiency.
- Fuel conversion efficiency: It is the ratio of the brake power output of the engine to the rate of energy delivered to the engine by the fuel.

3.1.3 Ideal Diesel Cycle

The ideal diesel cycle is a thermodynamic cycle that assumes heat addition occurs while the piston expands the volume, maintaining constant pressure. Figure 3.1 indicates the P-V diagram for the four process diesel ideal cycle (with open intake and exhaust process also shown).

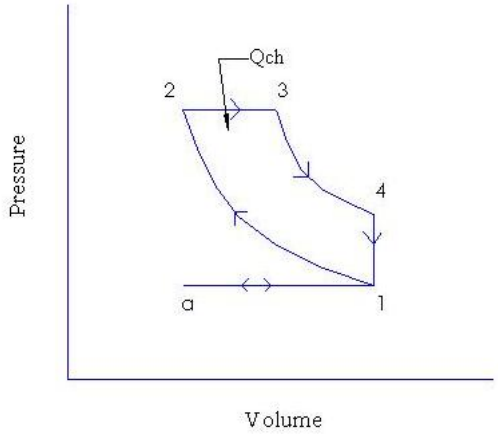

Fig. 3.1 P-V diagram for a standard diesel cycle.

- Process a-1 indicates the intake process
- Process 1-2 indicates isentropic compression process
- Process 2-3 shows the heat addition at constant pressure
- Process 3-4 shows the isentropic expansion process
- Process 4-1 indicates reversible constant volume heat rejection
- Process 1-a indicates exhaust process

Point “a” denotes the start of intake process. Air enters the cylinder and it reaches point 1. Point 1 indicates the start of compression process. The air is compressed isentropically to point 2. This adiabatic compression results in a high temperature inside the combustion chamber. When the piston reaches the end of compression stroke, heat addition occurs while the piston moves away from TDC, expanding the volume. This heat addition is shown from 2-3 (constant pressure). The high temperature gas inside the cylinder expands inside the cylinder thus pushing the piston downwards. This results in a power stroke. Process 4-1 indicates a reversible constant volume heat rejection process. Process 1-a indicates exhaust process, where the working fluid is expelled out of the engine.

3.1.4 Actual Combustion Process

The actual combustion process taking place inside a diesel engine can be summarized as follows. The fuel is injected into the combustion chamber towards the end of compression stroke, just before the desired start of combustion. The liquid fuel is usually injected as a jet, through a nozzle or orifice into the combustion chamber, at high velocity. The tip of the injector atomizes the fuel into small droplets which penetrates

into the combustion chamber. The fuel vaporizes and mixes with the high temperature and pressure cylinder air. The in-cylinder air temperature and pressure is above the fuel's ignition point which results in a spontaneous combustion of A/F mixture after a delay of a few crank angle degrees. This increase in temperature and pressure inside the cylinder due to the above mentioned combustion reduces the delay and evaporation time before the ignition for remaining liquid fuel. The injection process will continue till the desired amount of fuel enters the cylinder. Almost all the fuel injected inside the cylinder undergoes the processes- atomization, vaporization, mixing of A/F, and combustion. Also, the mixing of already burned gases and air remaining in the cylinder will continue throughout the combustion and expansion process.

Hence it is clear from the above discussion that the diesel engine combustion is extremely complex. An actual diesel engine combustion is "unsteady, heterogeneous, and three-dimensional" in nature. Some of the consequences of this mode of combustion are mentioned below:

- There is no knock limit in a diesel engine because the start of injection is just before start of combustion. This result in the feasibility of a higher compression ratio for a diesel engine, thus improving its fuel conversion efficiency compared to SI engine.
- Diesel engine is "quantity" governed. This means that the output torque is controlled by controlling the "quantity" of the fuel injected into the cylinder. The amount of intake air is uncontrolled and generally constant for naturally aspirated engines. This allows the engine to be operated without throttling. This lowers the

pumping work, again improving the fuel conversion efficiency relative to SI engine.

- Diesel engine generally operates with lean A/F ratio. This increases the effective value of ratio of specific heats over the expansion process which results in a higher fuel conversion efficiency when compared to SI engine.
- As the fuel injected per cycle increases, problems with fuel vaporization and mixing with causes increase in net soot release.

3.2 Direct-Injection Diesel Engines

There are two categories of diesel engines depending on the design of combustion chamber: (1) indirect-injection (IDI) engines (2) direct-injection (DI) engines. In an IDI engine, the chamber is divided into two chambers and the fuel is injected into a “prechamber” which is connected to the main chamber through a nozzle. These types of engines are becoming obsolete as fuel system technology improves.

In a DI engine, the fuel is injected into a single open combustion chamber. In a large diesel engine, the momentum and energy of the injected fuel is enough to achieve adequate fuel distribution and mixing with air. A center multihole injector is normally used. The shape of the combustion chamber is shallow bowl in the crown of the piston. As the size of the engine reduces, the proper mixing of A/F is achieved by increasing the swirl. The swirl is created by suitable design of inlet port. It is amplified by the compression process inside the cylinder, by forcing the air towards the cylinder axis into deep bowl-in piston combustion chamber.

3.3 Fuel Injection

The fuel is injected into the cylinder towards the end of compression stroke. The cylinder pressure during fuel injection is around 50-100 atm. The fuel at 200-1700 atm is injected into the combustion chamber through a nozzle. Large pressure difference across the nozzle is advised because the fuel will get injected into the combustion chamber at high velocity. This is important to (1) allow proper atomization of fuel in the chamber and (2) allow the fuel to traverse combustion chamber during the time available and thus enable its utilization of the air charge.

The start and end of time of injection is very vital. It should start and end cleanly. The main task of a fuel injection system is to meter adequate fuel for any particular load and speed to each cylinder at proper time in the cycle, at desired rate with spray configuration required for particular combustion chamber.

3.3.1 Spray Structure

The fuel at 200-1700 atm is injected into the combustion chamber through a nozzle, with a large pressure differential between the cylinder and fuel line pressure. There are different types of fuel injectors: single orifice, multi orifice, pintle, throttle etc. The selection of the injector depends on the need of the combustion system.

The fuel is injected into the cylinder at a velocity of 10^2 m/s. As the fuel is injected, the liquid jet of fuel becomes turbulent, and mixes with the surrounding air. The fuel at the outer surface of the spray disintegrates into droplets of $10\mu m$. Figure 3.2 indicates a schematic of diesel fuel spray [1]. Break up length is defined as the finite length along the axis of the cylinder over which the liquid fuel leaving the nozzle

disintegrates. As the distance from the spray increases, the mass of mixture increases, spray diverges, its width increases, and velocity reduces. The fuel continues to evaporate with mixing of air. As the injection continues the penetration of the fuel into the combustion chamber proceeds. But the rate decreases.

The fuel at the outer periphery evaporates first. This creates a sheath of air-fuel around the spray. The velocity of the spray is maximum at the center line. The equivalence ratio is also maximum at the center line. It decreases to zero at the spray boundary. There will be fuel-wall interaction, once the fuel is penetrated to the outer region of the combustion chamber. This forces the fuel to flow tangentially along the wall.

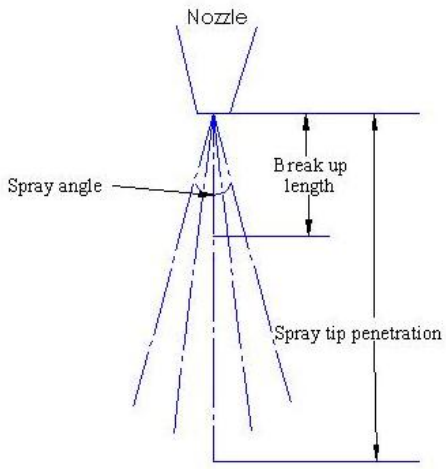

Fig. 3.2 Schematic of a diesel fuel spray defining major parameters.

3.3.2 Atomization

Spray of fuel when injected into the cylinder at high velocity, causes it to form a cone shape at the exit of the nozzle. This type of behavior is known as the atomization break up regime. This process generates droplets whose diameter is less than the nozzle exit diameter. Small fuel droplets are desired as it increases the surface area across which liquid fuel can evaporate.

At low velocity, in the Rayleigh regime, the breakup of the fuel droplets is caused by the force of surface tension that results in droplets larger than the jet diameter. This is called first wind induced break up regime. As the velocity increases further, there will be an increase in the surface tension force. A further increase in velocity causes the divergence of the fuel from its usual intact or undisturbed length downstream of the nozzle. This is known as the second wind induced break up regime. During this regime, the relative velocity of the fuel with the air causes an unstable growth of short-wavelength length forces. This results in the formation of fuel droplets with diameter less than the nozzle exit diameter. Further increase in jet velocity results in the breakup of the atomization regime causing it to breakup before or at the nozzle exit plane resulting in a an average droplet diameter lesser than the nozzle diameter. Main factors affecting the atomization process are the density and viscosity of the fuel, density of the gas, and nozzle geometry [42].

3.3.3. Spray Penetration

The rate and extend of spray penetration has a lot of effect on the air utilization and fuel mixing rates inside the combustion chamber. In the case of some hot diesel

engines where there is limited swirl, the impingement of spray on the wall is desired. But for latest multi spray DI diesel combustion systems, over penetration results in lowering the mixing rates, and hence incomplete combustion of the fuel. But if the penetration is less, then the air at the periphery of the combustion chamber do not contact the fuel. Hence the penetration of fuel into the combustion chamber is a critical parameter.

3.3.4 Spray Evaporation

The liquid fuel droplet injected into the cylinder must evaporate fully before it mixes with air and burn. The structure of a fuel spray consists of a dark core region which consists of dense liquid fuel, surrounded by a sheath of vapor. The temperature of the fuel at the start of injection is approximately 300 K. The following three phenomena determine the nature of behavior of a fuel drop inside the combustion chamber:

- The deceleration of the drop as a result of aerodynamic drag
- The heat transfer between the fuel drop and the surrounding air
- The mass transfer of fuel vapors away from the fuel drop

As the fuel is injected into the cylinder, heat transfer occurs between the fuel and hot air surrounding it. This results in an increase in fuel vapor pressure and the evaporation rate. As the rate of mass transfer of fuel vapor away from the drop increases, the fraction of the heat transferred to the drop surface which is available to increase further the drop temperature decreases. This results in a decrease in the drop velocity. Since the convective heat transfer coefficient is a strong function of velocity, the convective heat transfer decreases as the drop velocity decreases. With a decrease in the vapor temperature, there will be an increase in local vapor pressure. Finally it results in a

thermodynamic equilibrium [43]. Studies using phenomenological models and computational fluid dynamic models indicate that, almost 70%-95% of the fuel is vaporized at the start of combustion. 1ms after the fuel injection, almost 90% of the fuel is evaporated. However, in a typical medium speed DI diesel engine, only 10-35% of the fuel has reached the flammability limit. Hence it is proved by previous research that combustion in a DI engine is mixing limited, rather than evaporation limited [44]. The different models mentioned above uses coupled conservation equations for liquid droplets for effective study of the fuel vaporization rate within a diesel fuel spray.

3.4 Ignition Delay

3.4.1 Definition and Discussion

Ignition delay is defined as the time lag between the start of injection to start of combustion. It is usually measured in degrees of crank angle. The start of injection is identified as the time when the injector needle lifts off its seat. The start of combustion is determined from the change in slope of the heat release rate, determined from the pressure data. Whereas the start of combustion can be well determined from the pressure curve. Before the heat release process inside a diesel engine, both physical and chemical processes must take place. The physical process includes the atomization of fuel, vaporization of the atomized fuel droplets, and mixing of air and fuel. The chemical process includes the pre-combustion reactions of fuel, air, and residual gases that is present inside the combustion chamber that leads to auto ignition. Both these factors are determined by the engine design parameters, operating point and fuel characteristics.

Main factors affecting the atomization process are the density and viscosity of the fuel, density of the gas, and nozzle geometry. High cylinder pressure, high fuel injection pressure, small orifice, and optimum viscous fuel results in good atomization. Pressure and temperature inside the cylinder, volatility of fuel, size, velocity, and distribution of the fuel droplets determines its rate of vaporization. The rate of mixing of fuel is determined by the design of the combustion chamber and injector. Various types of cylinder and piston head designs are available to enable proper mixing of the fuel and air. This is done by creating swirl and turbulence inside the combustion chamber. The number and arrangement of injector sprays, the cone angle, extend of spray penetration and air flow determines the rate of air mixing inside the cylinder. The chemical part of the ignition delay is largely affected by the type and nature of fuel used, the in-cylinder temperature and pressure, and the distribution of fuel. The chemical part of the delay consists of cracking of higher HC molecules, oxidation reactions of the A/F mixture etc.

Cetane number is a measure of the ignition quality of the diesel fuel. It is defined as the percentage of normal-Cetane in a mixture of normal-Cetane and alpha-Methyl Naphthalene which has the same ignition delay as that of the test fuel when combustion is carried out under prescribed operating conditions. Hence Cetane number is the measure of the ignition delay. A low Cetane number indicates longer ignition delay. This can cause excessive premixed combustion that results in “diesel knock”.

3.4.2 Factors Affecting Ignition Delay

As mentioned in section 3.4.1, large number of factors affects the ignition delay. The ignition delay is affected by engine design parameters, operating points and the fuel

characteristics. Brief discussions about various factors that affect ignition delay are discussed below.

- Injection Timing: Too early or too late injection timings can result in an increase in ignition delay. Advanced injection timings results an increase in ignition delay. This is because the instantaneous temperature and pressure inside the cylinder is too low to enable auto ignition. Unconventionally late injection timings also increase the ignition delay. Hence the most favorable period of injection for conventional combustion is between these two.
- Load: As the load is increased, the ignition delay decreases [45]. This is partly because, with an increase in load, the in-cylinder temperature and wall temperature increases. This results in an increase in charge temperature at the time of injection which results in a shorter ignition delay.
- Rate, and Velocity of injection and drop size: All these factors are governed by the factors such as injector nozzle hole size, injection pressure, type and geometry of nozzle etc. Under normal operating conditions, as the injection pressure is increased, there will be a decrease in ignition delay because of better atomization of the fuel droplets. Smaller the size, better mixing of the air and fuel which results in a shorter ignition delay.
- Intake air temperature and pressure: The properties at the inlet also determine the ignition delay inside the combustion chamber. This is because; it alters the properties of the charge during the period of ignition delay. Higher the intake pressure and temperature, lesser will be the ignition delay. This is because; the

fuel droplets can reach the auto-ignition point quickly due to higher temperature and pressure. Other factor affecting the temperature and pressure is the compression ratio. Higher the compression ratio, lesser will be the ignition delay.

- Engine Speed: Load remaining a constant, with an increase in engine speed, there will be a decrease in ignition delay in time (ms). This is because as the engine speed increases, the peak temperature inside the cylinder increases [46].
- Swirl Rate: Swirl determines the rate of mixing of the air and fuel. Better swirl means better mixing of air and fuel thus reducing the ignition delay. This is because better swirl increases the turbulence inside the cylinder. This results in an increased heat transfer, thus lowering the temperature.
- Oxygen Concentration: The oxygen concentration of the charge into which the fuel is injected inside the cylinder greatly affects the ignition delay. The oxygen concentration can change if there is any recirculation of the exhaust gas into the combustion chamber to reduce the emissions. Decrease in oxygen concentration increases the ignition delay.

3.5 Conventional Combustion in DI Engines

Combustion in a conventional DI engines occurs in four stages. These stages are identified from heat release diagram for a DI engine. The four stages of combustion are as follows:

- Ignition delay: As explained in section 3.4, ignition delay can be defined as the time lag between the start of injection to start of combustion. It is usually

measured in degrees of crank angle. This can be identified as a change in slope in heat release diagram.

- Premixed or rapid combustion phase: A part of A/F mixture which has been properly mixed and is within the flammability limits during ignition delay period, burns rapidly for a few crank angle degrees. A high rate of heat release is usually observed during this phase.
- Mixing controlled combustion phase: After the premixed combustion phase is over, the next stage of combustion is the mixing controlled phase. This phase of combustion is controlled by the rate at which the mixture is available for burning. Even though there are several process occurring this time like atomization, vaporization, mixing of A/F mixture, and preflame chemical reactions, mixing of A/F mixture is extremely important. The peak heat release rate may or may not reach the level of premixed combustion phase. But the rate of heat release decreases as this stage progresses.
- Late combustion phase: This stage is characterized by the late combustion taking place inside the combustion chamber during the expansion stroke. A small amount of fuel might be present that didn't take part in any of the combustion process described earlier. Say some amount of fuel might be present in soot or some unburnt combustion products. Proper mixing of air and fuel later during the expansion stage might result in the combustion of these fuel during this stage. The amount of heat release is very less during this stage.

3.6 Drawbacks of Diesel Engine

Compared to a SI engine, there are some drawbacks of a diesel engine.

- Diesel engine is heavier than a spark ignition engine for similar power output. This is because of the higher compression ratio used in a diesel engine, thus requiring heavy materials for its construction. The lean operation of a diesel engine also decreases the power density.
- The starting of a conventional diesel engine is a bit tough when compared to its gasoline counterpart because of its large inertia and high compression force required.
- The main defect of a diesel engine is its emission characteristics. The emission problems with diesel engines are explained in section 3.7.

3.7 Pollution Caused by Diesel Engine

The operation of diesel engine results in the emission of various products such as NO_x, PM, CO and HC. Most of these products are harmful for the health and wellness of human beings. Stringent pollution norms call for the reduction in the emission of these harmful species. For this purpose, it is important to understand the soot-NO_x trade off.

3.7.1 Soot-NO_x Trade Off

There are three primary NO formation mechanisms: thermal NO formation, prompt NO formation and fuel NO formation. In a typical combustion system, the thermal NO formation dominates. Thermal NO formation is the result of dissociation of oxygen, nitrogen and hydroxyl radical which occurs at high temperature. Prompt NO is the result of interaction of HC fuel molecules with molecular nitrogen to ultimately

generate NO. Prompt NO formation occurs even before the attainment of high temperature. Fuel NO is the result of oxidation of the nitrogen in the fuel. Hence, it can be seen that NO formation is a strong function of temperature. Higher the temperature, higher is the NO formation.

The soot formation is a characteristic of HC diffusion flames. The net soot release is the difference between the soot formation and soot oxidation. The soot formation is a strong function of the A/F ratio as well as temperature, while the soot oxidation is a function of temperature (assuming a lean equivalence ratio). The soot formation and oxidation depends on the formation of precursor species PAH, particle oxidation, particle inception, and surface growth and agglomeration. Dec observed that the formation of PAH occurs within a reaction zone which supplies fragmented and radical species to a diffusion reaction zone. Thus a rich premixed mixture generates high levels of soot precursors thus increasing the soot formation.

Conventionally any attempt to reduce NO_x formation increases soot, and vice versa. This relationship is known as the diesel soot-NO_x trade off.

3.7.2 Defeating Soot-NO_x Trade Off

Two main methods have been developed to defeat this soot-NO_x trade off. One method is the after treatment of exhaust gas. The development of exhaust oxygen sensors, fuel injectors and closed loop electronic control modules encouraged the development and use of TWC. The TWC is a combination of platinum, palladium and rhodium that reduce and oxidize the exhaust mixtures NO, CO and HC. The TWC catalyst has an efficiency of more than 80%. Even thought the TWC catalyst

successfully reduces the emissions, the successful working of TWC requires the engine to operate consistently at an equivalence ratio that provides the best mixture of the exhaust species. The second method of defeating the soot-NO_x trade off is to prevent the formation of regulated species. This is achieved by proper mixing of fuel and lowering of flame temperature. This lead to the development of LTC. Two main methods have been developed to achieve the low temperature combustion. They are HCCI and PCI.

HCCI combustion combines two famous modes of combustion used in internal combustion (IC) engines: homogenous charge spark ignition (conventional gasoline engines) and heterogeneous charge compression ignition (conventional diesel engines). HCCI attempts to burn a perfectly homogenous mixture of air and fuel by auto ignition induced by compression. A nearly homogenous mixture reduces the locally rich zone. Coupled with dilution by addition of EGR, HCCI can reduce the soot and NO_x formation. Diesel fuel has poor volatility and high ignitability thus making it is difficult to vaporize the fuel. Once it is vaporized, it results in a rapid combustion, thus making it difficult to control. Manifold injection and early injection strategies have been proposed to generate HCCI combustion.

Both manifold injection and early injection strategies have their own limitations. The use of the former is limited due to low power density at low compression ratios. And the latter creates a very high HC and CO, often accompanied by with high smoke if wall wetting issues exist. A possible alternative is the injection of fuel more close to the TDC; say 25° BTDC, single injection strategy combined with a high level of EGR. The

ignition delay caused by the EGR results in proper mixing of the A/F mixture. This is followed in PCI combustion strategy.

3.7.3 Exhaust Gas Recirculation (EGR)

Exhaust gas recirculation (EGR) is used in most gasoline engines and diesel engines for NO_x reduction. EGR works by recirculating a part of exhaust back into the engine cylinder. In a diesel engine, addition of exhaust adds more incoming mass to the cylinder thus reducing the oxygen concentration. However in case of gasoline engines, a unit of A/F is replaced by a unit of EGR. Thus there won't be any change in the A/F ratio. As explained in section 3.4.2, a reduction in oxygen concentration inside the cylinder by EGR causes an increase in ignition delay. Increase in ignition delay reduces the peak temperature and pressure created inside the cylinder due to combustion. Also EGR introduces components such as carbon dioxide and water that have higher specific heats than oxygen and nitrogen at the pre-combustion temperatures. Thus the incoming EGR takes up a part of energy generated inside the engine thus delaying the combustion. Thus the reduced combustion temperature results in a reduction of NO formation.

The amount of EGR applied to an engine is usually expressed as percentage. It is defined as the ratio of recycled gases to the mass of engine intake. In the inlet air from the atmosphere, there is negligible amount of CO_2. But in the recirculated exhaust, there is a large amount of CO_2. So in most of the experimental methods, the EGR ratio is measured by comparing the CO_2 concentrations between the exhaust and the intake of the engine. i.e.

$$EGR(\%) = \frac{mass\ of\ \ EGR}{mass\ of\ \ fuel + mass\ of\ EGR + mass\ of\ \ air} \tag{16}$$

If hot exhaust is directly recirculated back into the cylinder of the engine, it is known as hot EGR, and if the EGR is cooled by using an inter cooler and then is applied to the engine, it is known as cool EGR. There are basically two types of EGR circulation methods: low pressure loop EGR and high pressure loop EGR [5].

Figure 3.3 indicates a low pressure loop EGR. Low pressure loop EGR is usually possible because there will be a positive differential pressure between the turbine outlet and compressor inlet. The presence of a throttling valve ensures sufficient driving pressure for the EGR flow. The exhaust gas from the engine is used to run a turbine to operate the compressor. Exhaust from the turbine is cooled using an EGR cooler, passed through a throttle valve and is mixed with the incoming fresh air. This air-exhaust mixture is then compressed using compressor. The compressed mixture is then cooled using an intercooler, which is then supplied to the engine. In general, low pressure loop EGR is not used.

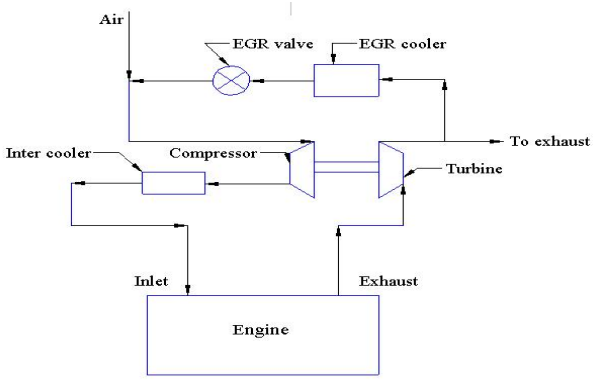

Fig. 3.3 Low pressure loop EGR.

Figure 3.4 indicates the schematic of a high pressure loop EGR. For the effective working of the high pressure EGR, the upstream pressure of the turbine should be greater than the boost pressure. A method to increase the boost pressure is by the use of VGT. The turbocharger provides more control on the EGR rate and also on the boost pressures at various speeds and loads. The EGR flow occurs when there is a favorable pressure difference between the exhaust and intake manifold. The VGT present in the exhaust tends to increase the pressure in the exhaust manifold. This is accomplished by the vanes inside the VGT. The vanes alter the exhaust gas flow across the turbine blades thus providing a resistance of flow. This resistance of flow increases the pressure in the exhaust manifold.

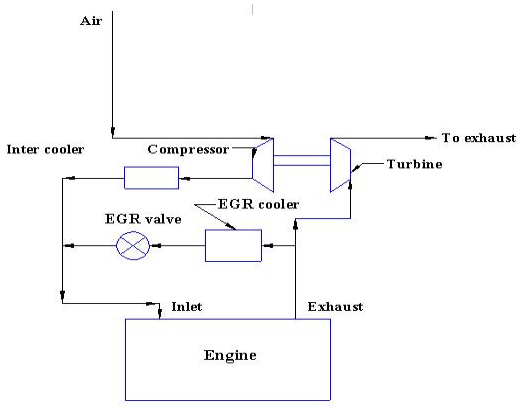

Fig. 3.4 High pressure loop EGR.

The EGR flow components should be resistance to high temperature and pressure. Usually the EGR ducts are made of flexible structures such as stainless steel bellows so as to absorb thermal expansion and to tolerate mechanical vibration.

4. RESULTS AND DISCUSSIONS

4.1 Pressure Characteristics

The data obtained from the data acquisition system of the test engine is fed into the UMHR software to obtain the heat release characteristics. The output from the UMHR program is used to study the variation of various parameters during the combustion process inside the cylinder of the engine. As the basis to this study, it is necessary to understand the variation of pressure with crank angle for different rates of EGR and injection timings. The in-cylinder pressure versus crank angle data over the compression and expansion strokes of the engine can be used to obtain much vital information on the progress of combustion. Figure 4.1 to figure 4.4 indicate the variation of pressure versus crank angle for a constant EGR at various injection timings for cylinder 1. Close observation of the plot of pressure versus crank angle for a constant EGR at various injection timing reveals that the peak value of the pressure decreases as the injection timing is retarded. The peak pressure was observed for an injection timing of 18° BTDC. A “double humping” is observed in the case of injection timing of 9° BTDC. The first “hump” observed was the peak pressure created during the compression stroke and the second “hump” was the pressure rise as a result of the main combustion during the expansion stroke. The peak pressure shifts towards the TDC with early injection timing as a result of the fact that the combustion takes place due to earlier injection. Table 4.1 indicates the start of combustion for each of the conditions under study. Start of combustion is defined as the location when 10% of burn has occurred.

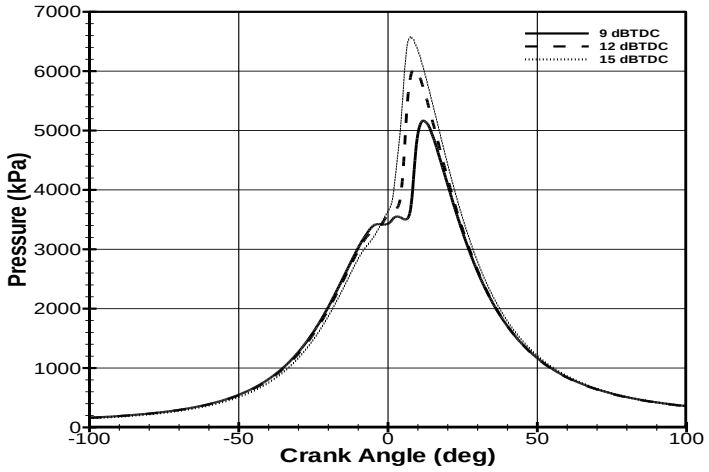

Fig. 4.1 Pressure versus crank angle for lean PCI combustion at EGR= 39% for three injection timings for cylinder 1.

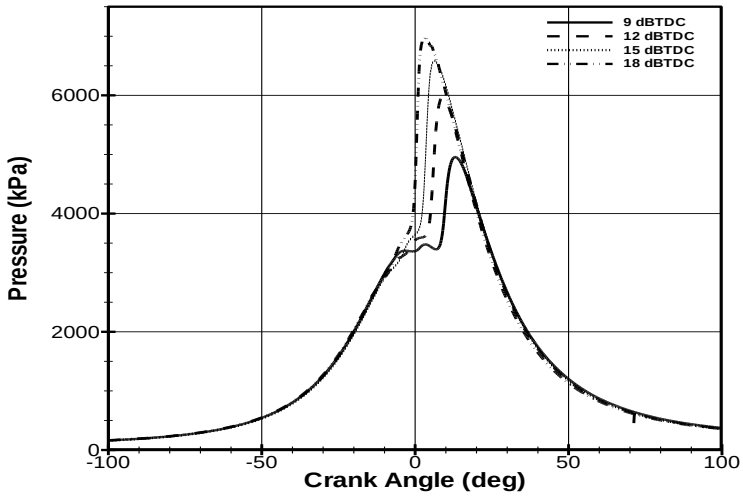

Fig. 4.2 Pressure versus crank angle for lean PCI combustion at EGR= 40% for four injection timings for cylinder 1.

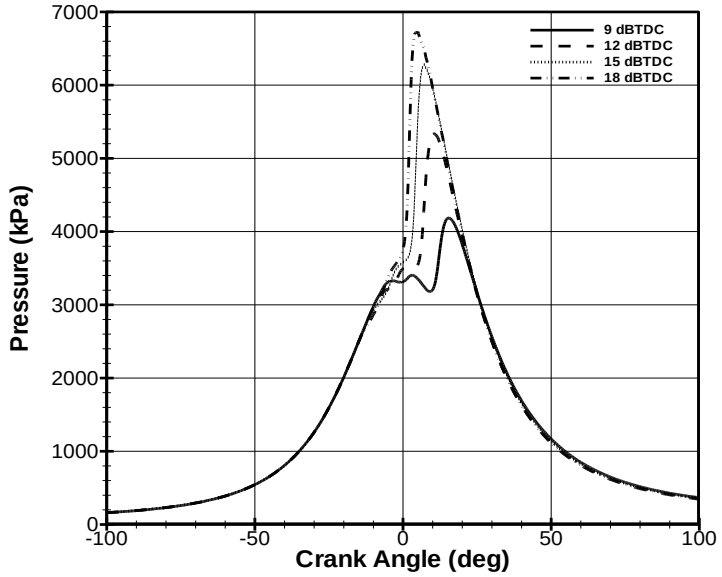

Fig. 4.3 Pressure versus crank angle for lean PCI combustion at EGR= 41% for four injection timings for cylinder 1.

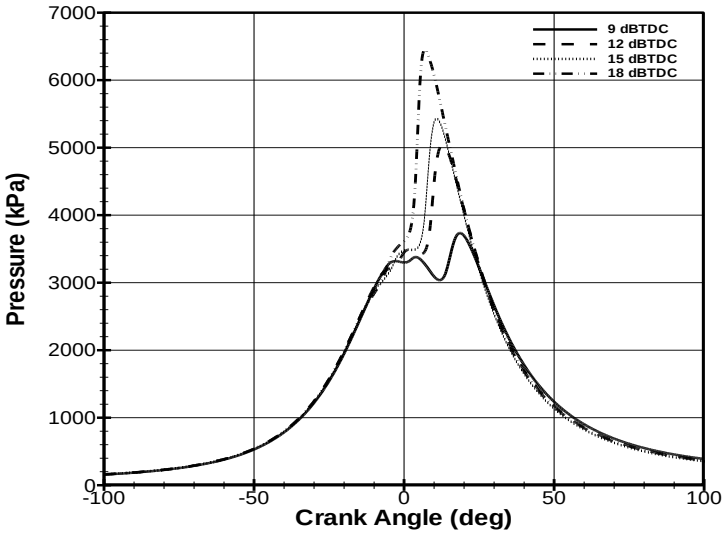

Fig. 4.4 Pressure versus crank angle for lean PCI combustion at EGR= 42% for four injection timings for cylinder 1.

Table 4.1 Start of combustion (°BTDC) for different combinations of injection timings and EGR

	Injection Timing 18° BTDC	Injection Timing 15° BTDC	Injection Timing 12° BTDC	Injection Timing 9° BTDC
EGR=39%	-	-1.25	-3.75	-7
EGR=40%	1	-1.5	-4.25	-7.75
EGR=41%	-0.5	-2.5	-5.5	-9.75
EGR=42%	-2.25	-5.25	-6.75	-11

The negative sign in table 4.1 indicates that the combustion is taking place after TDC. For example, the start of combustion for injection timing of 9° BTDC and EGR 39% is 7° after the top dead center, which is during the expansion stroke. So, it is evident from this table that as the injection is advanced, the start of combustion will also be advanced. As the injection timing is advanced, larger part of combustion takes place at higher temperatures and pressures due to early start of combustion. This result in a higher peak pressure observed above for advanced injection timing of 18° BTDC. But for late injection timings, most of the combustion takes place during the expansion stroke, resulting in lower reaction temperatures and pressures.

Figure 4.5 to figure 4.8 indicate the variation of pressure with crank angle for a fixed injection timing and varying EGR for cylinder 1. It is inferred from these plots that as the EGR increases, the peak pressure decreases. This result was also observed by Zheng, et al. [8].

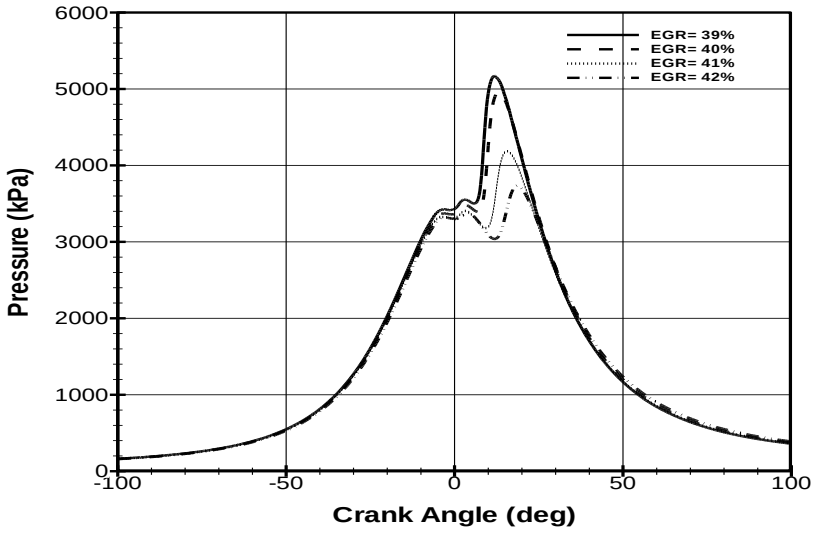

Fig. 4.5 Pressure versus crank angle for lean PCI combustion at four EGR rates for an injection timing of 9° BTDC for cylinder 1.

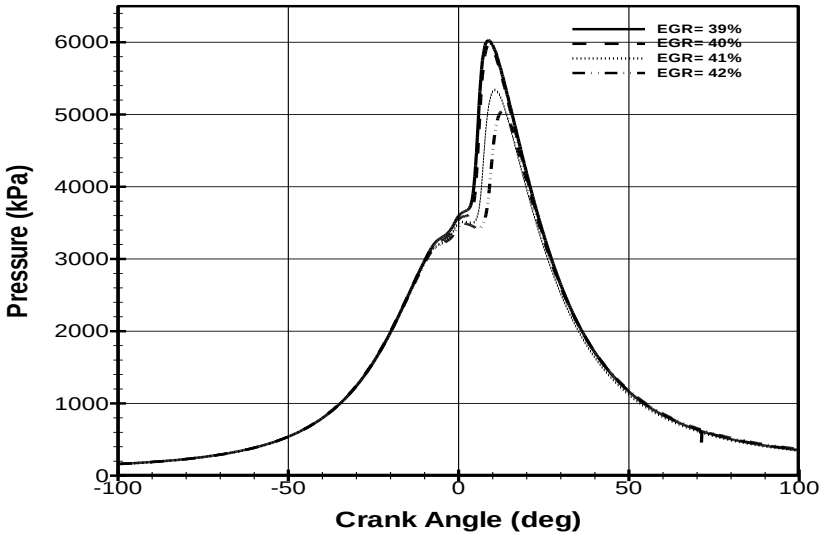

Fig. 4.6 Pressure versus crank angle for lean PCI combustion at four EGR rates for injection timing of 12° BTDC for cylinder 1.

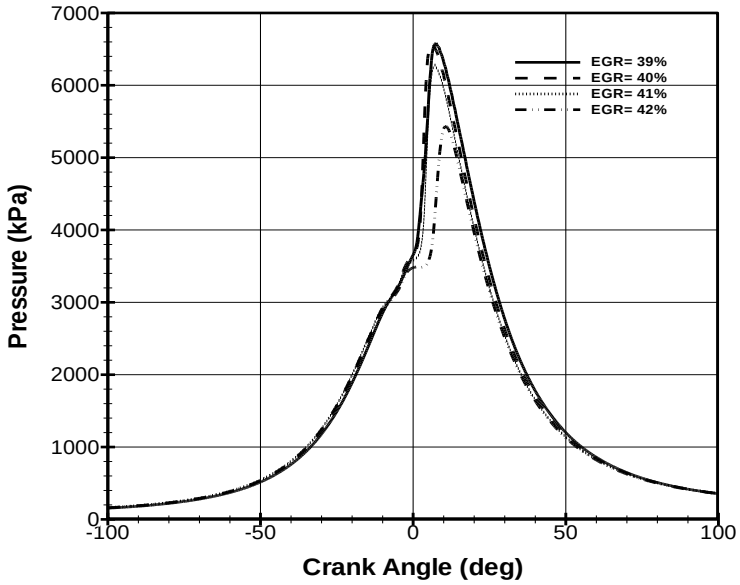

Fig. 4.7 Pressure versus crank angle for lean PCI combustion at four EGR rates for an injection timing of 15° BTDC for cylinder 1.

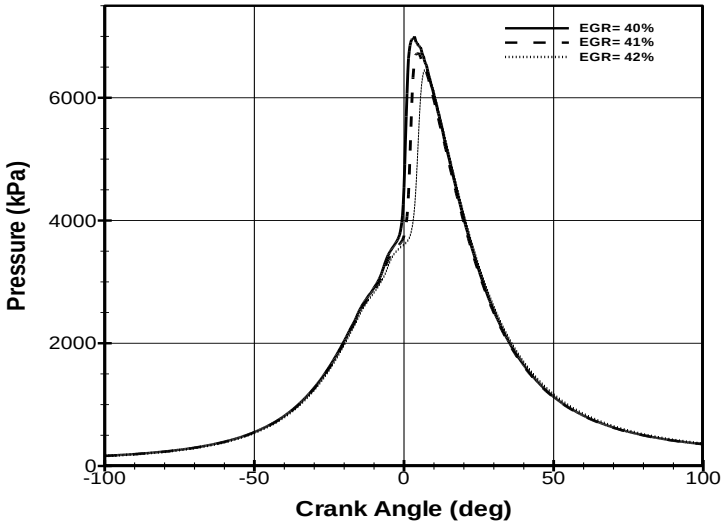

Fig. 4.8 Pressure versus crank angle for lean PCI combustion at three EGR rates for an injection timing of 18° BTDC for cylinder 1.

This decrease in the peak pressure might be due to the ignition delay and the decreased combustion temperature. Higher level of EGR increases the ignition delay due to the reduction in oxygen concentration thus affecting the A/F mixture composition in the cylinder. Table 4.2 indicates the ignition delay for various cases of study. Ignition delay is the time lag between the start of injection to start of combustion

Table 4.2 Ignition delay (degree) for different combinations of injection timings and EGR

	Injection Timing 9° BTDC	Injection Timing 12° BTDC	Injection Timing 15° BTDC	Injection Timing 18° BTDC
EGR=39%	16	15.75	16.25	-
EGR=40%	16.75	16.25	16.5	17
EGR=41%	18.75	17.5	17.5	18.5
EGR=42%	20	18.75	20.25	20.25

From the above table, for a fixed injection timing, as the EGR is increased (going down the table), the ignition delay increases. “Double Humping” phenomenon is observed for the plot of pressure versus crank angle for injection timing of 9° BTDC for all the EGR rates. The reason being the late combustion for 9° BTDC (table 4.1). The first “hump” is because of the peak pressure obtained during the premixed combustion during the compression stroke, and the second “hump” is the result of the main combustion taking place during the expansion stroke.

Pressure data inside the cylinder over the entire operating cycle can be used to calculate the work transfer from the gas to the piston. The cylinder pressure and its corresponding volume, for cylinder 1 can be plotted on a P-V diagram as shown in Figure 4.9 to figure 4.12. Figure 4.9 to figure 4.12 indicate the pressure versus volume for a constant EGR at different injection timings for cylinder 1. It can be seen that the peak pressure decreases with retarded injection timing. The indicated work per cycle is obtained by calculating the area bound by the P-V curve.

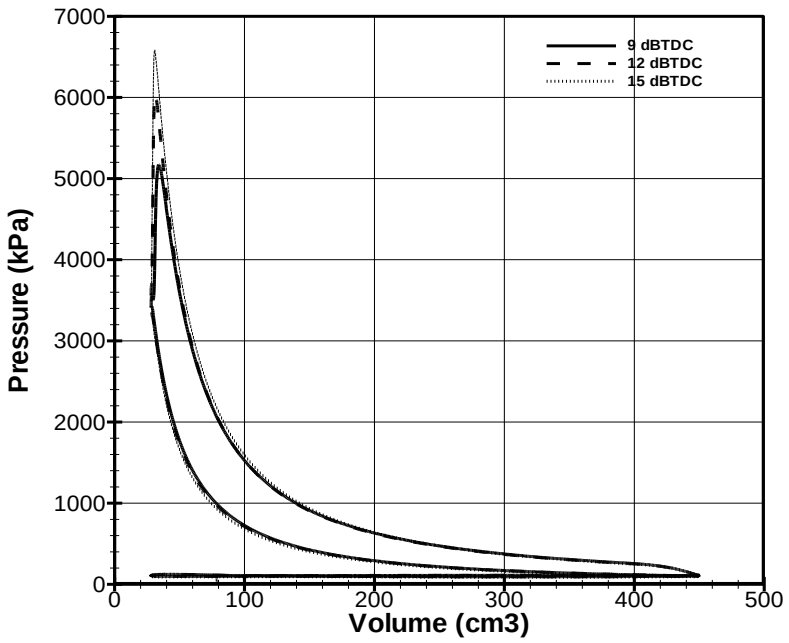

Fig. 4.9 Pressure versus volume for lean PCI combustion at EGR= 39% for three injection timings for cylinder 1.

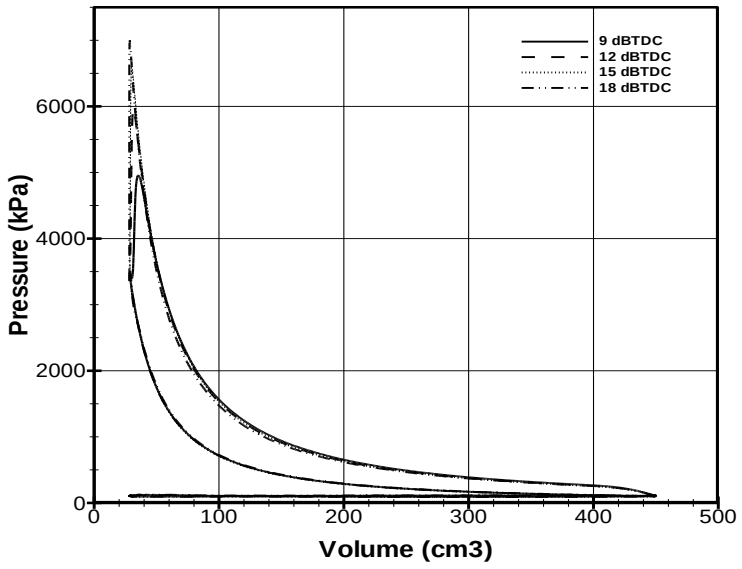

Fig. 4.10 Pressure versus volume for lean PCI combustion at EGR= 40% for four injection timings for cylinder 1.

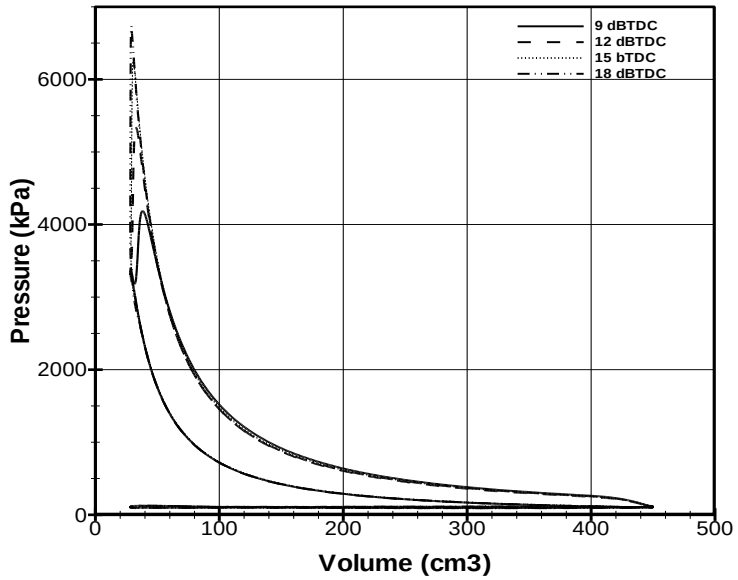

Fig. 4.11 Pressure versus volume for lean PCI combustion at EGR= 41% for four injection timings for cylinder 1.

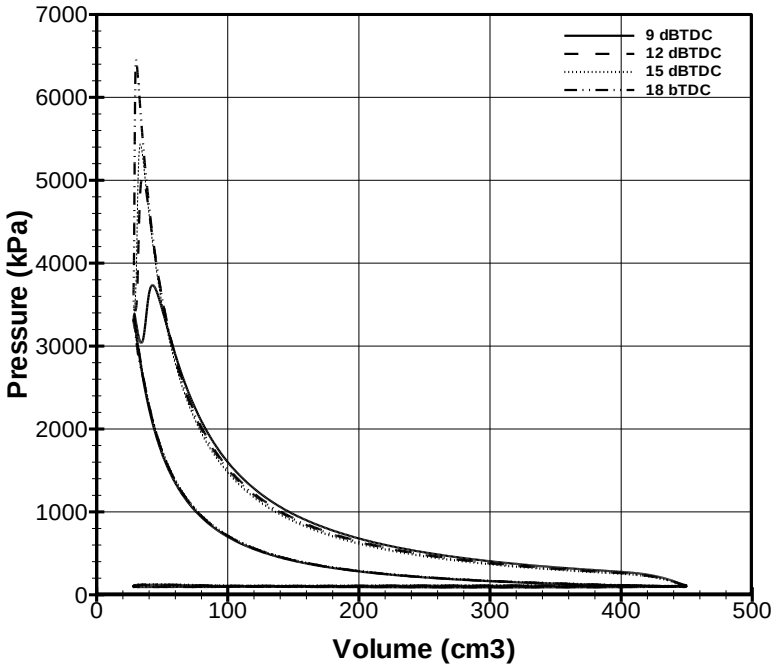

Fig. 4.12 Pressure versus volume for lean PCI combustion at EGR= 42% for four injection timings for cylinder 1.

Figure 4.13 to figure 4.16 indicate the variation of pressure with volume for a constant injection timing and varying EGR for cylinder 1. The decreasing pressure with EGR at constant injection timing can be observed. Hence, there is a decrease in gross indicated work as EGR is increased.

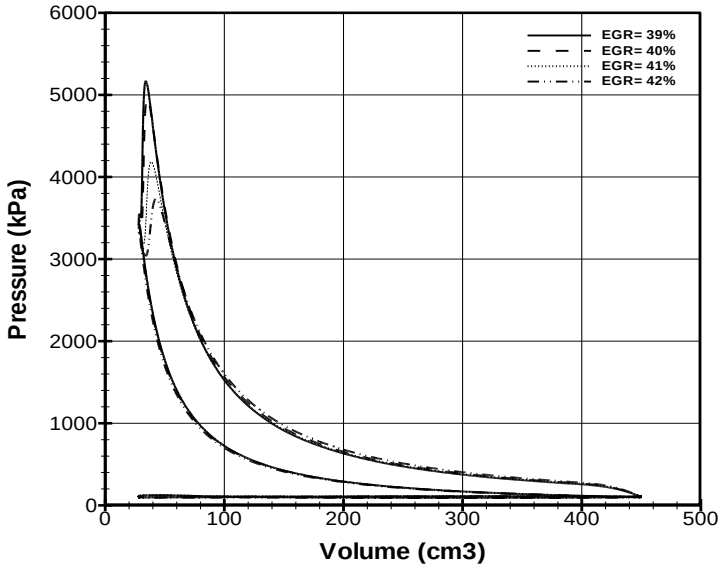

Fig. 4.13 Pressure versus volume for lean PCI combustion at an injection timing of 9° BTDC for four EGR rates for cylinder 1.

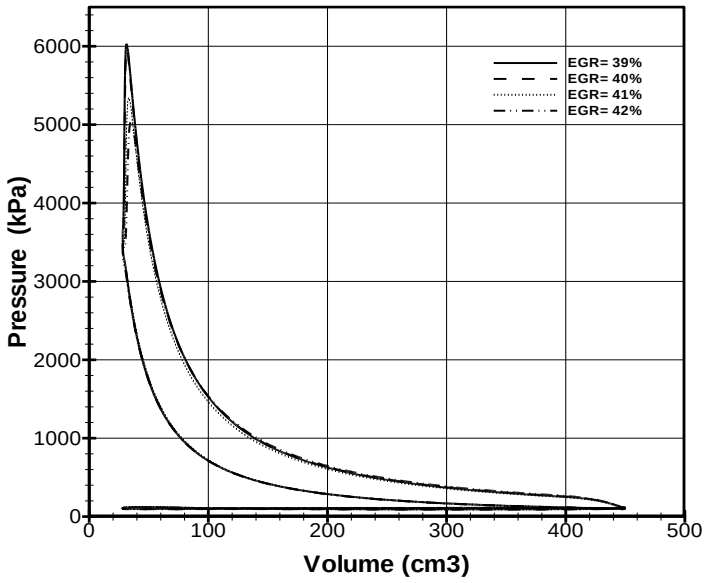

Fig. 4.14 Pressure versus volume for lean PCI combustion for an injection timing of 12° BTDC at four EGR rates for cylinder 1.

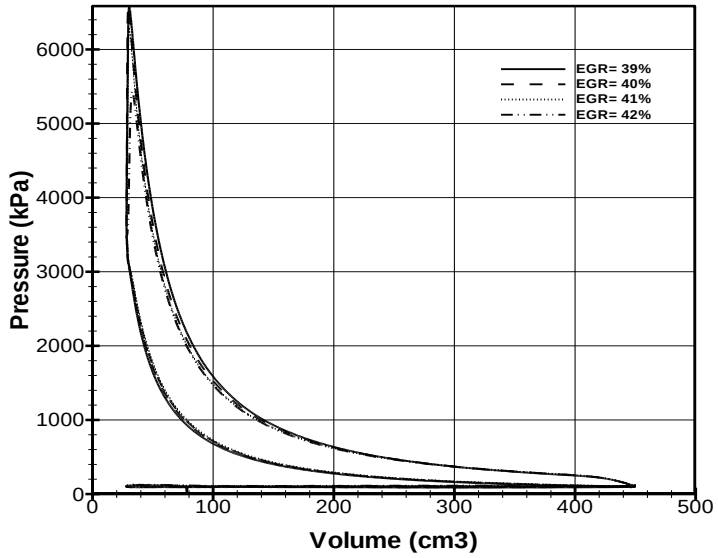

Fig. 4.15 Pressure versus volume for lean PCI combustion at an injection timing of 15° BTDC at four EGR rates for cylinder 1.

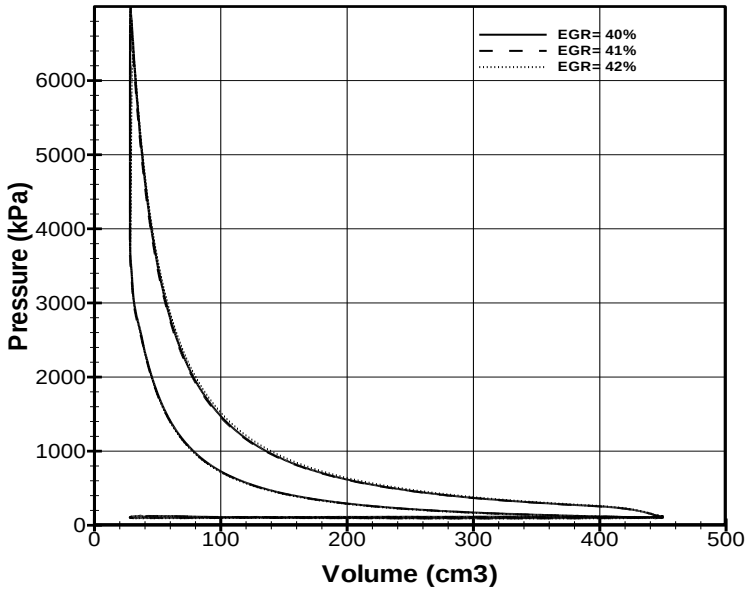

Fig. 4.16 Pressure versus volume for lean PCI combustion for an injection timing of 18°BTDC for three EGR rates for cylinder 1.

4.2 Rate of Heat Release Analysis

This section describes the method of computation of the rate of heat release. The rate of heat release is the sum of rate of work done, rate of change of internal energy and rate of heat transfer.

4.2.1 Rate of Work Done versus Crank Angle

The variation of rate of work with crank angle is calculated from the P-V diagram described in section 4.1. This data is useful in the calculation of total rate of heat release the total work done, $IMEP_{gross}$, $IMEP_{net}$, and PMEP. Figure 4.17 to figure 4.20 indicates the variation of work done with crank angle for a constant EGR and varying injection timing for cylinder 1.

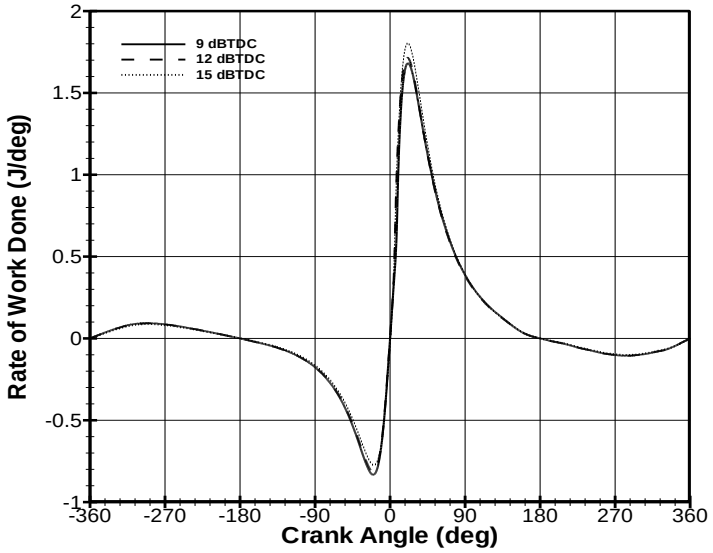

Fig. 4.17 Rate of work done versus crank angle for lean PCI combustion at EGR= 39% for three injection timings for cylinder 1.

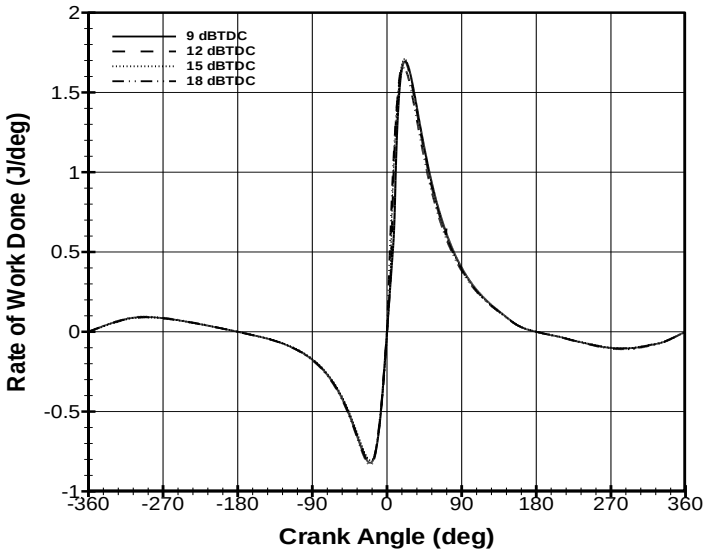

Fig. 4.18 Rate of work done versus crank angle for lean PCI combustion at EGR= 40% for four injection timings for cylinder 1.

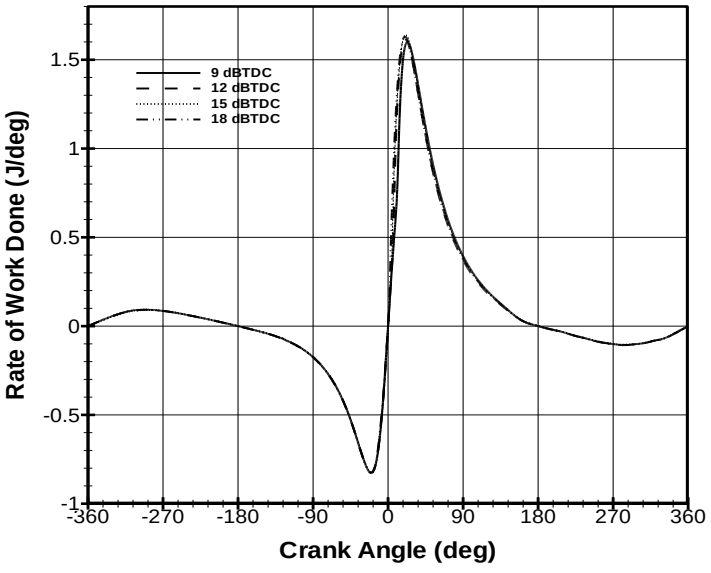

Fig. 4.19 Rate of work done versus crank angle for lean PCI combustion at EGR= 41% for four injection timings for cylinder 1.

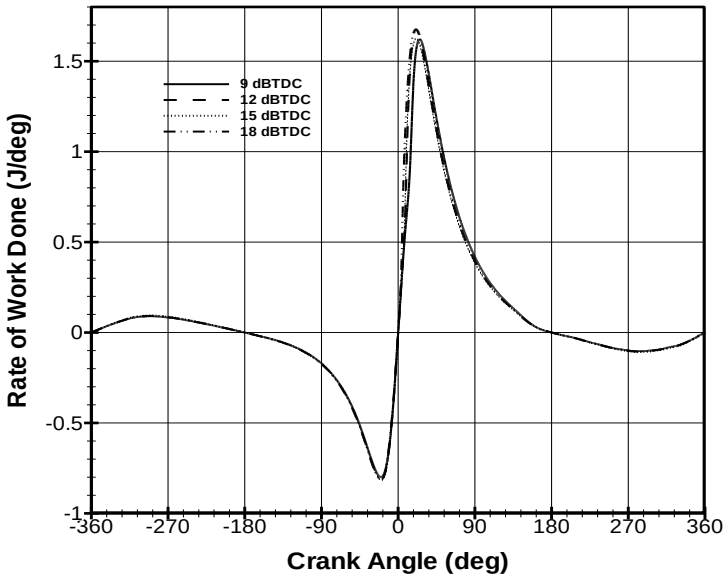

Fig. 4.20 Rate of work done versus crank angle for lean PCI combustion at EGR= 42% for four injection timings for cylinder 1.

For the plot of work done versus crank angle for EGR= 40%, it is observed that the maximum peak work done is for injection timing of 15° BTDC and the least peak work done is for injection timing of 18° BTDC. It's more of a tradeoff between increased heat transfer and combustion phasing. Too early of combustion increases heat transfer and takes incomplete advantage of full expansion stroke. In the plot of work done versus crank angle for EGR= 39%, the peak work done is obtained for injection timing of 15° BTDC, followed by 12° BTDC and 9° BTDC. This is because of the larger ignition delay for the injection timing of 15° BTDC. As the ignition delay increases, more fuel accumulates and burns simultaneously near the TDC thus releasing more heat

and hence work done. The negative work done in the above figures indicates the work done on the system during the compression stroke. Also it can be noted that there is an increase in work done per crank angle from 20° BTDC. This is because of the rapid increase in the change in volume. The work done is calculated as $\sum P\Delta V$. So a rapid change in the volume results in a rapid change in the work done. Figure 4.21 indicates the variation of change in volume with crank angle for cylinder 1.

Figure 4.22 to figure 4.25 indicate the variation of work done with crank angle for a constant injection timing and varying EGR for cylinder 1.

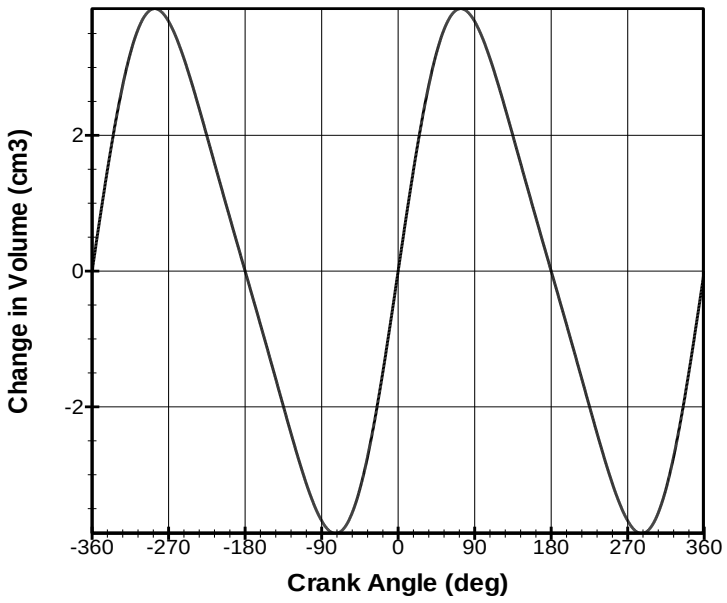

Fig. 4.21 Change in volume versus crank angle for cylinder 1.

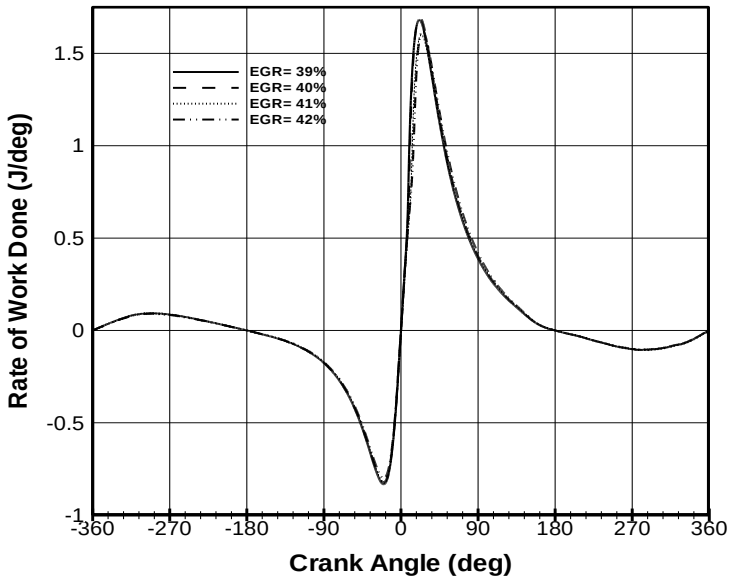

Fig. 4.22 Rate of work done versus crank angle for lean PCI combustion at an injection timing of 9° BTDC for four EGR rates for cylinder 1.

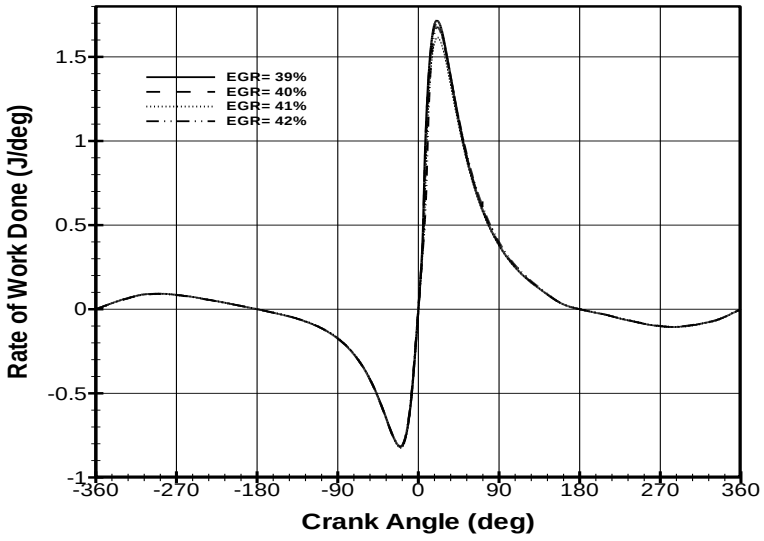

Fig. 4.23 Rate of work done versus crank angle for lean PCI combustion at an injection timing of 12° BTDC for four EGR rates for cylinder 1.

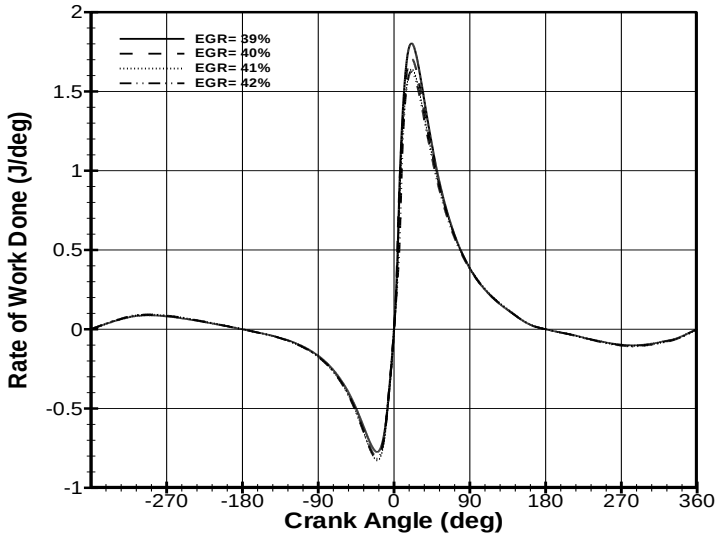

Fig. 4.24 Rate of work done versus crank angle for lean PCI combustion at an injection timing of 15° BTDC for four EGR rates for cylinder 1.

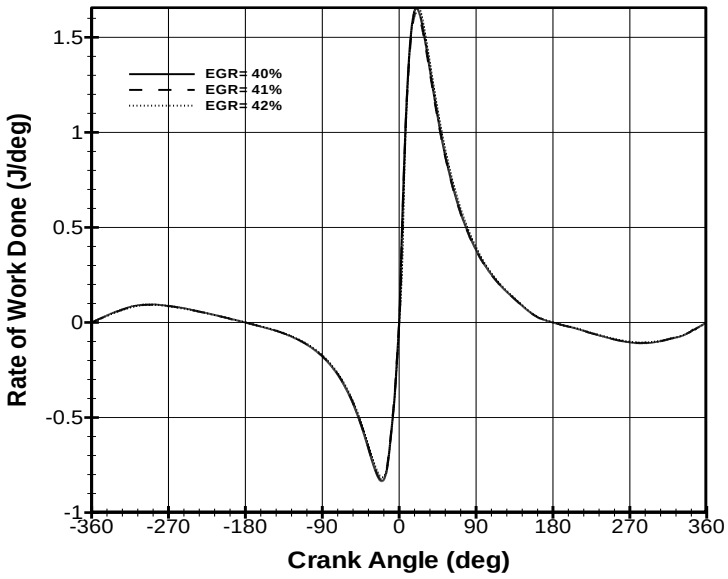

Fig. 4.25 Rate of work done versus crank angle for lean PCI combustion at an injection timing of 18° BTDC for three EGR rates for cylinder 1.

4.2.2 Rate of Change in Internal Energy versus Crank Angle

Determination of change in internal energy is of significant importance in the calculation of rate of heat release, total net heat release, and energy distribution. Figure 4.26 to Figure 4.29 indicates the variation of rate change in internal energy with crank angle at constant EGR for varying injection timings for cylinder 1. It indicates that the peak change in internal energy increases with an advance in injection timing. This is because of the high temperature and pressure created inside the cylinder as a result of early combustion. Figure 4.30 to Figure 4.33 indicates the variation of rate change in internal energy with crank angle at constant injection timings for varying EGR for cylinder 1. It can be inferred that, with injection timing held constant, the peak rate of change of internal energy decreases with increase in EGR. This might be due to the "cooling effect" provided by the EGR. As EGR increases, the in-cylinder mixture becomes leaner. This results in lower combustion temperature that results in a decrease of change in the internal energy.

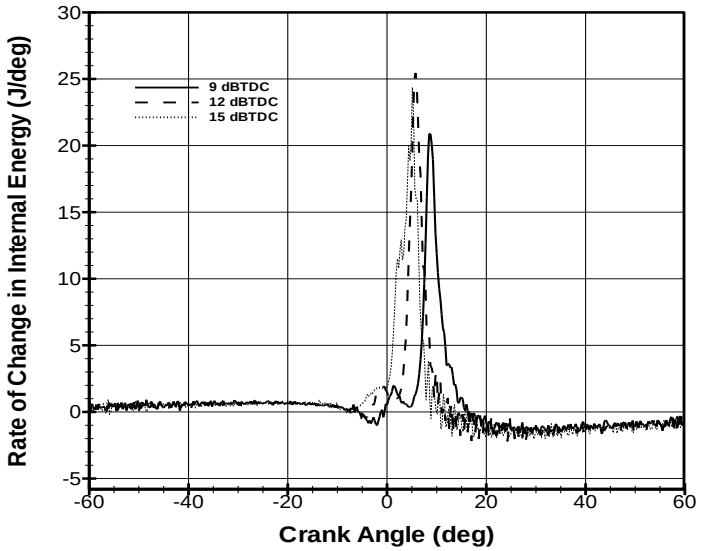

Fig. 4.26 Rate of change in internal energy versus crank angle for lean PCI combustion at EGR= 39% for three injection timings for cylinder 1.

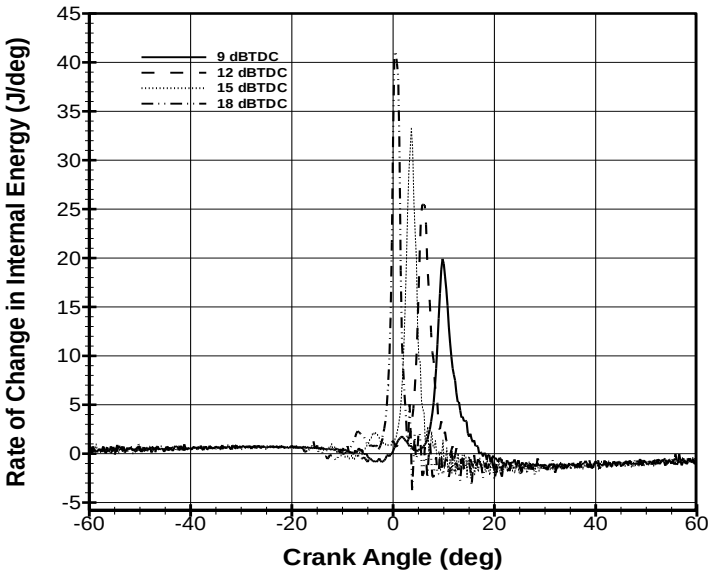

Fig. 4.27 Rate of change in internal energy versus crank angle for lean PCI combustion at EGR= 40% for four injection timings for cylinder 1.

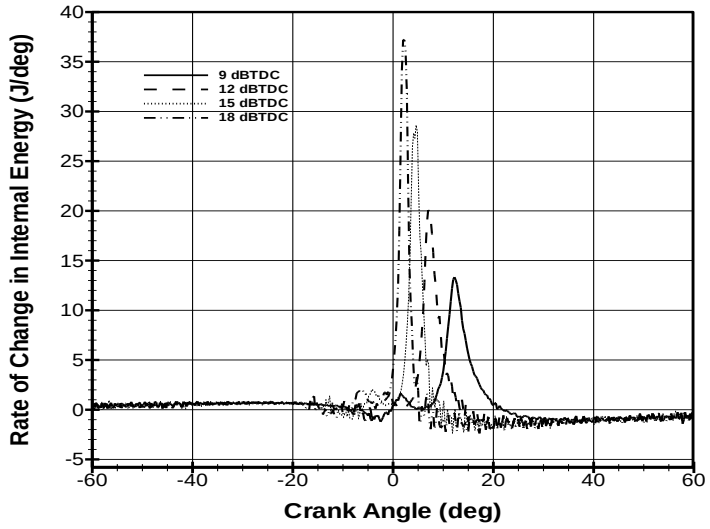

Fig. 4.28 Rate of change in internal energy versus crank angle for lean PCI combustion at EGR=41% for four injection timings for cylinder 1.

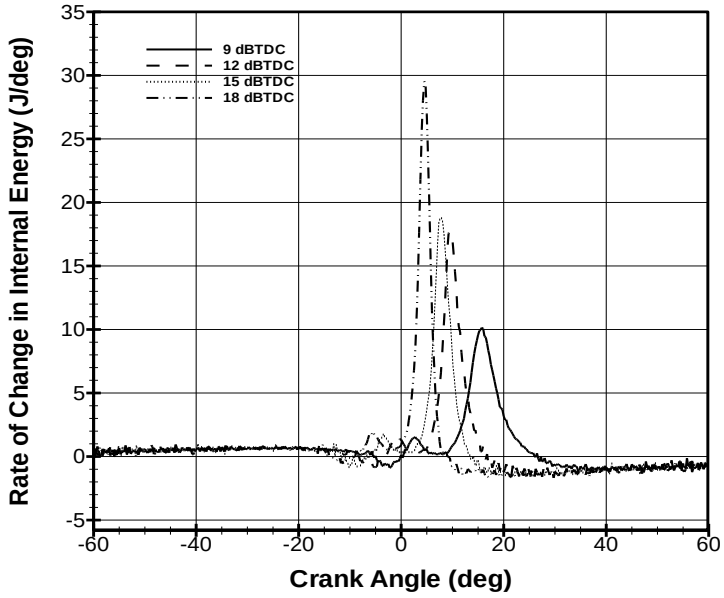

Fig. 4.29 Rate of change in internal energy versus crank angle for lean PCI combustion at EGR= 42% for four injection timings for cylinder 1.

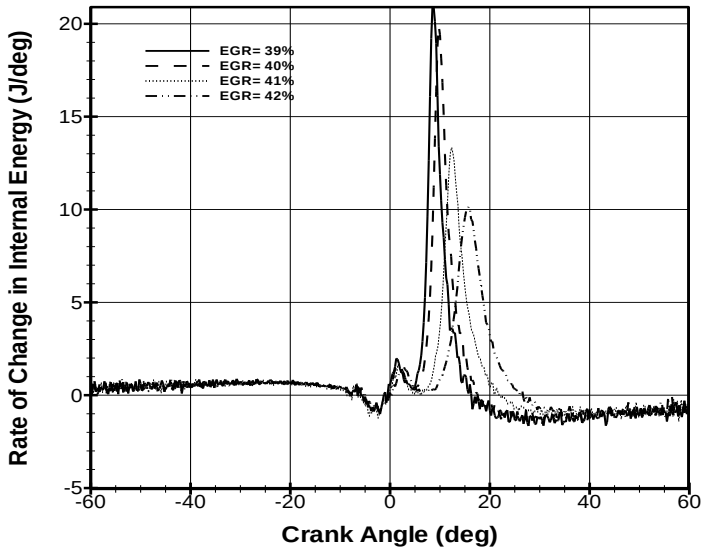

Fig. 4.30 Rate of change in internal energy versus crank angle for lean PCI combustion at an injection timing of 9° BTDC for four EGR rates for cylinder 1.

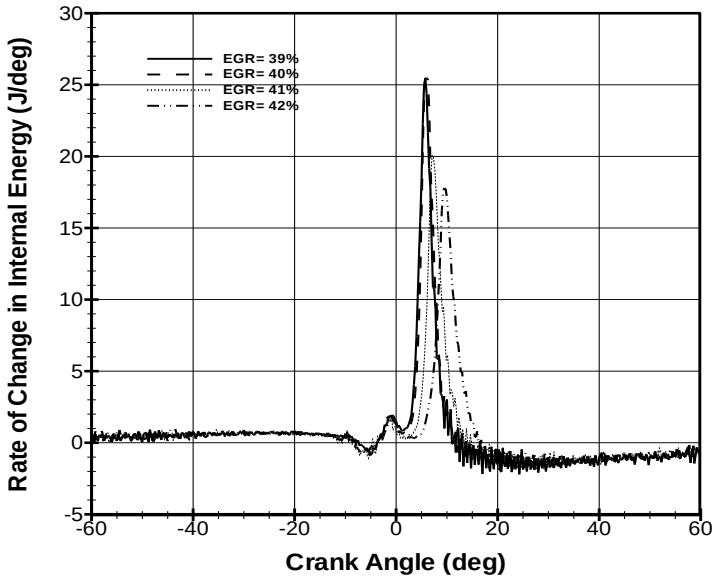

Fig. 4.31 Rate of change in internal energy versus crank angle for lean PCI combustion at an injection timing 12° BTDC for four EGR rates for cylinder 1.

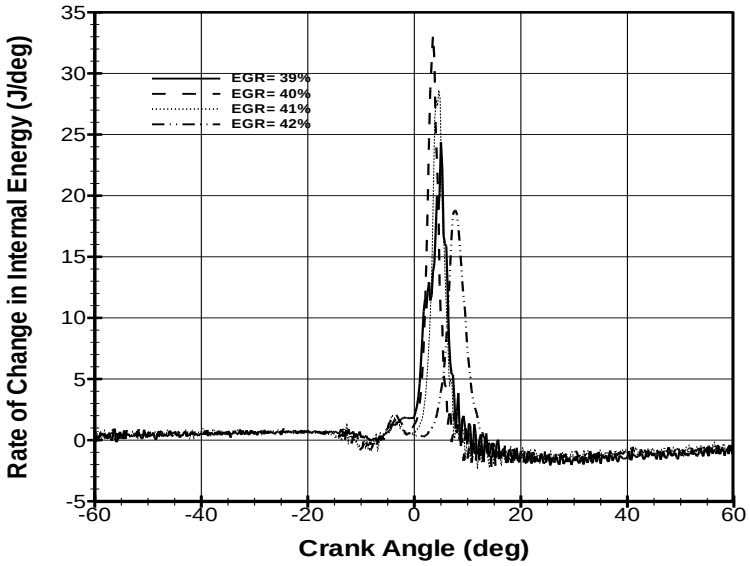

Fig. 4.32 Rate of change in internal energy versus crank angle for lean PCI combustion for an injection timing of 15° BTDC for four EGR rates for cylinder 1.

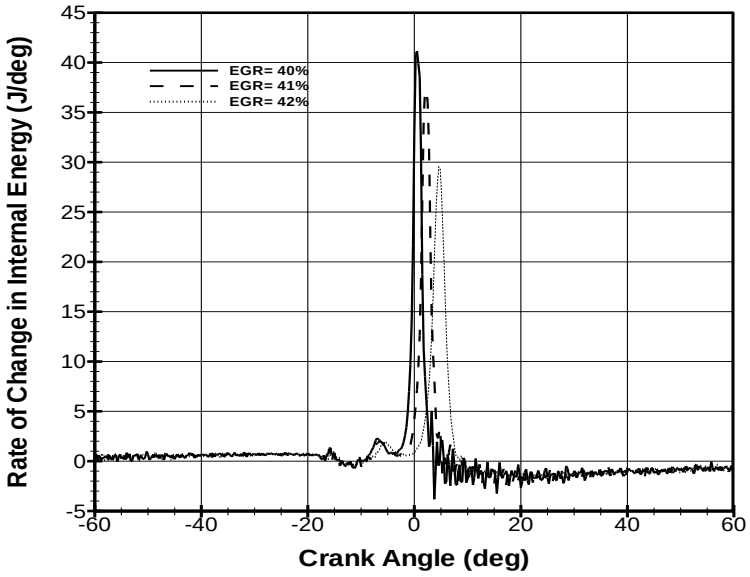

Fig. 4.33 Rate of change in internal energy versus crank angle for lean PCI combustion for an injection timing of 18° BTDC for three EGR rates for cylinder 1.

4.2.3 Net Accumulated Heat Transfer Energy versus Crank Angle

The variation of accumulated heat transfer energy with crank angle is used to calculate rate of heat release, total net heat released and energy distribution. Figure 4.34 to figure 4.37 indicate the net accumulated heat transfer energy as a function of crank angle for different injection timings at constant EGR for cylinder 1. It can be seen that, as the injection timing is retarded, the peak heat transfer decreases. For all the EGR rates, the highest heat transfer was observed for the injection timing of 18° BTDC. This is because of the decreasing peak temperature. Figure 4.38 to Figure 4.41 indicates the plot between the temperature with crank angle. The plot between peak temperatures with injection timing for cylinder 1 is shown in Figure 4.42. The variation of the accumulated heat transfer with crank angle can be explained from the temperature versus crank angle plots. The variation of the net heat transfer follow the same trend as that of the temperature. It is also evident that as the injection timing is retarded, the peak temperature inside the cylinder decreases. One reason for lower peak heat transfer can be the effect of radiation heat transfer. Higher the temperature inside the cylinder more will be the contribution of radiation heat transfer (equation 5). But as the injection timing is retarded, the temperature inside the cylinder decreases. So the effect of radiation heat transfer reduces. Also the slope of the heat transfer plot indicates the rate of heat transfer. The slope of 18° > 15° > 12° > 9°. This shows that the rate of heat transfer decreases as the injection timing is retarded. This is because of the early start of combustion for 18° BTDC. An early start of combustion means that the time available for the heat transfer is high. A negative heat transfer is observed around crank angle of

100° BTDC for all the plots. This is because, at crank angles where the negative heat transfers are observed, the temperature inside the cylinder is less than the assumed wall temperature (500° K). This makes an artificial effect on the heat transfer. The program stops calculating at exhaust valve opening.

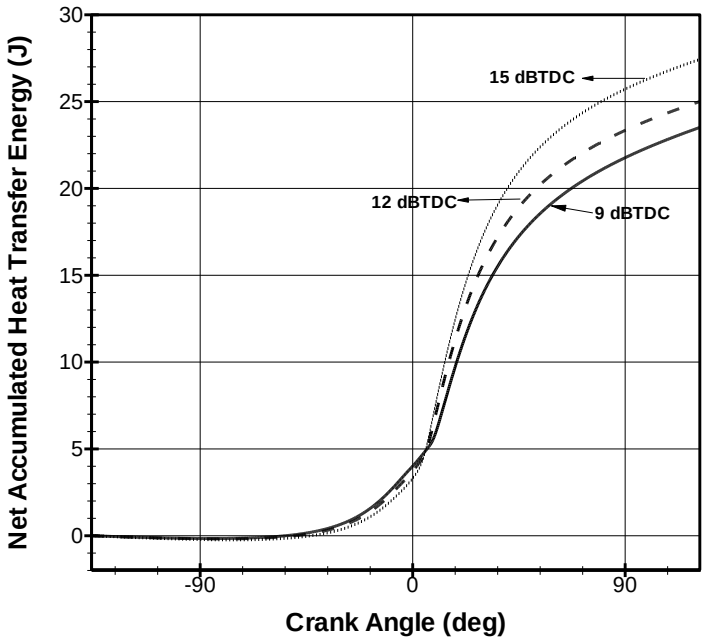

Fig. 4.34 Net accumulated heat transfer energy versus crank angle for lean PCI combustion at EGR= 39% for three injection timings for cylinder 1.

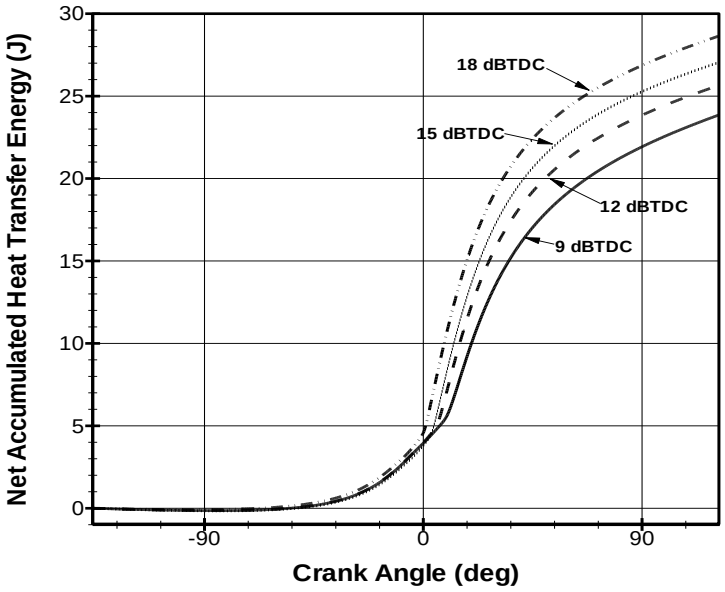

Fig. 4.35 Net accumulated heat transfer energy versus crank angle for lean PCI combustion at EGR= 40% for four injection timings for cylinder 1.

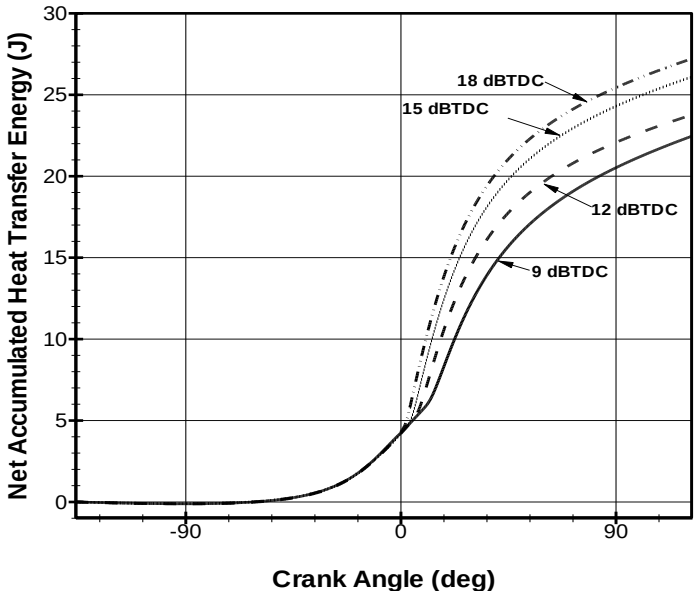

Fig. 4.36 Net accumulated heat transfer energy versus crank angle for lean PCI combustion at EGR= 41% for four injection timings for cylinder 1.

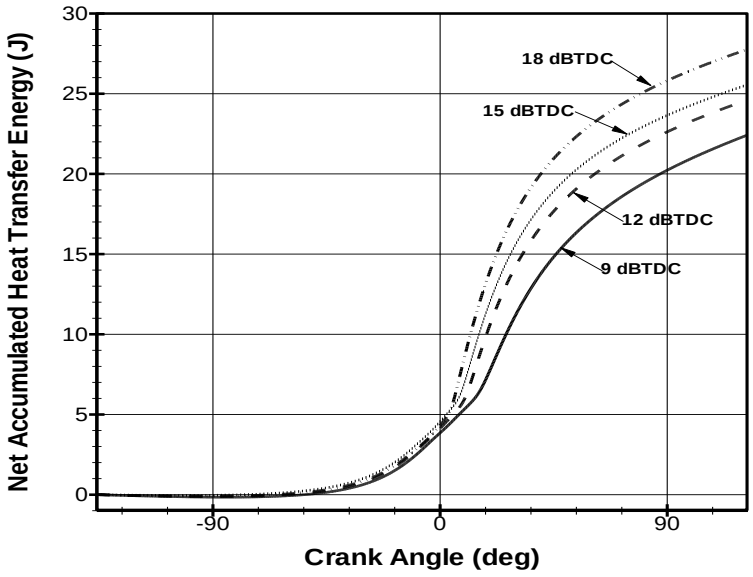

Fig. 4.37 Net accumulated heat transfer energy versus crank angle for lean PCI combustion at EGR= 42% for four injection timings for cylinder 1.

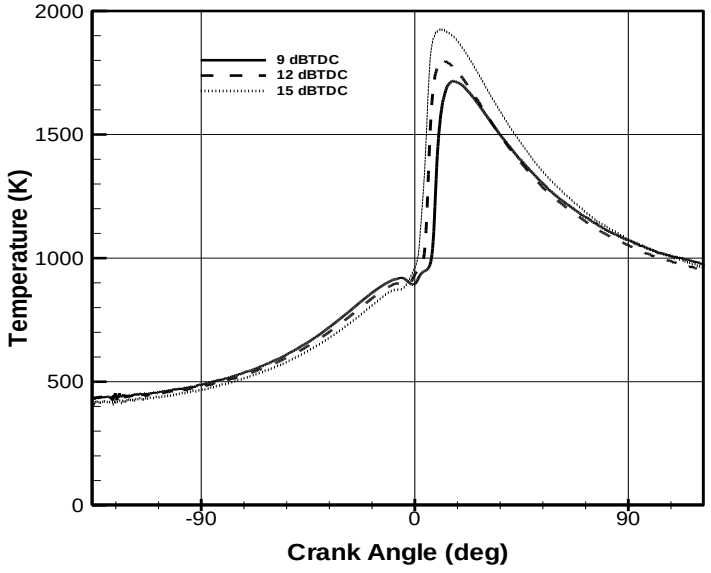

Fig. 4.38 Temperature versus crank angle for lean PCI combustion at EGR= 39% for three injection timings for cylinder 1.

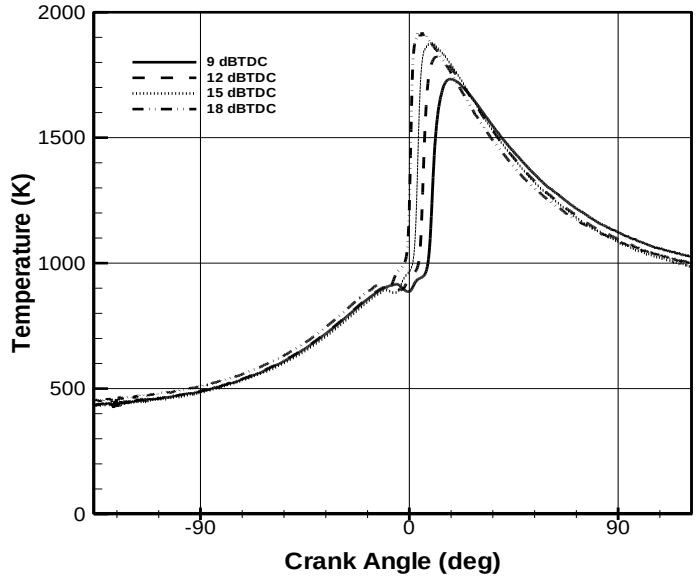

Fig. 4.39 Temperature versus crank angle for lean PCI combustion at EGR= 40% for four injection timings for cylinder 1.

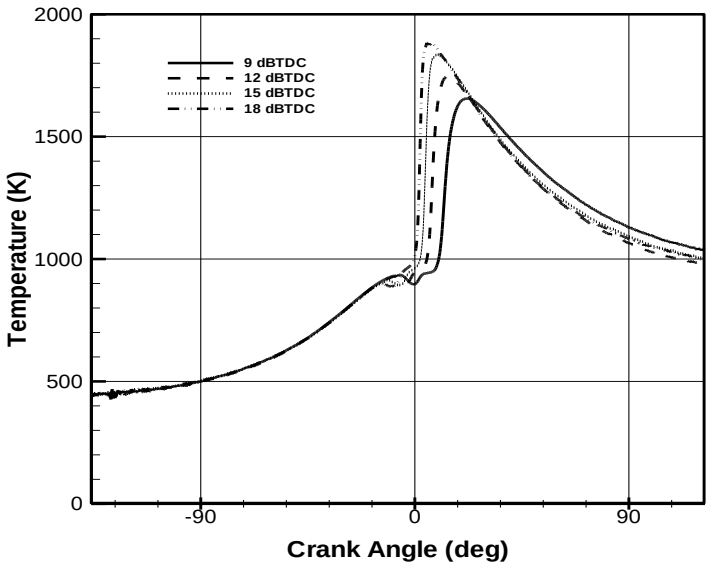

Fig. 4.40 Temperature versus crank angle for lean PCI combustion at EGR= 41% for four injection timings for cylinder 1.

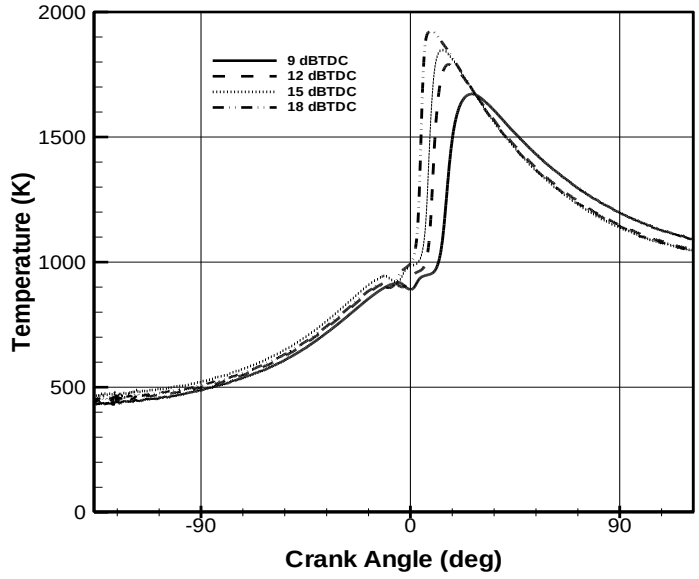

Fig. 4.41 Temperature versus crank angle for lean PCI combustion at EGR= 42% for four injection timings for cylinder 1.

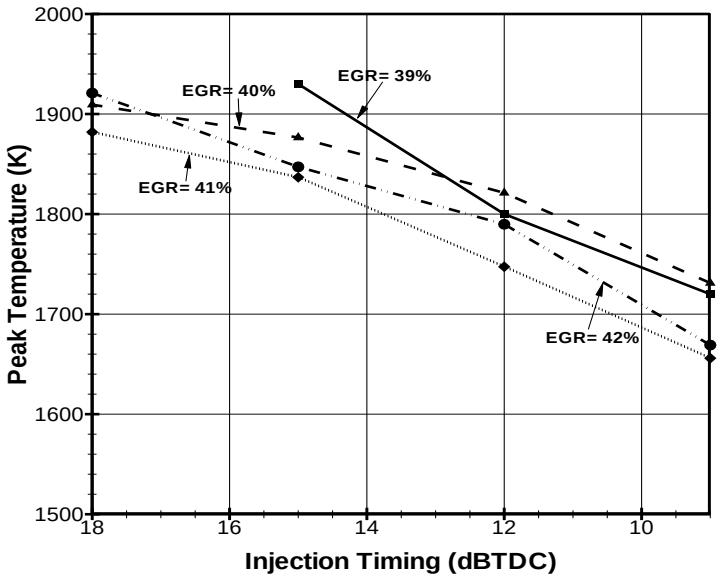

Fig. 4.42 Peak temperature versus injection timing for PCI combustion for four EGR rates for cylinder 1.

Figure 4.43 to figure 4.46 indicate the variation of net accumulated heat transfer energy with crank angle for different EGR at constant injection timings for cylinder 1. For injection timing of 9° BTDC, it is observed that the peak heat transfer is a function of peak temperature. The peak heat transfer is maximum for 40% EGR. Figure 4.47 to figure 4.50 shows the variation of temperature with crank angle. The variation of the net accumulated heat transfer energy with crank angle can be explained from the temperature versus crank angle plots. The variation of the accumulated heat transfer follow the same trend as that of the temperature. Figure 4.51 indicates the variation of peak temperature with EGR for cylinder 1. It is seen that for injection timing of 9° BTDC, the peak temperature is observed for EGR= 40%. Similarly the least peak heat transfer is for EGR= 41%. The lowest peak temperature is also observed for EGR=42%. For injection timing of 12° BTDC, the peak heat transfer reduces in the order 40%, 39%, 42% and 41%. This is the same trend observed for the peak temperatures also. For injection timing 15° BTDC, the same trend explained above follows with maximum peak heat transfer and peak temperature observed for EGR= 39%, followed by 40%, 41%, and 42%. The effect of radiation heat transfer can also be a reason for the trend observed above as radiation heat transfer is a function of temperature.

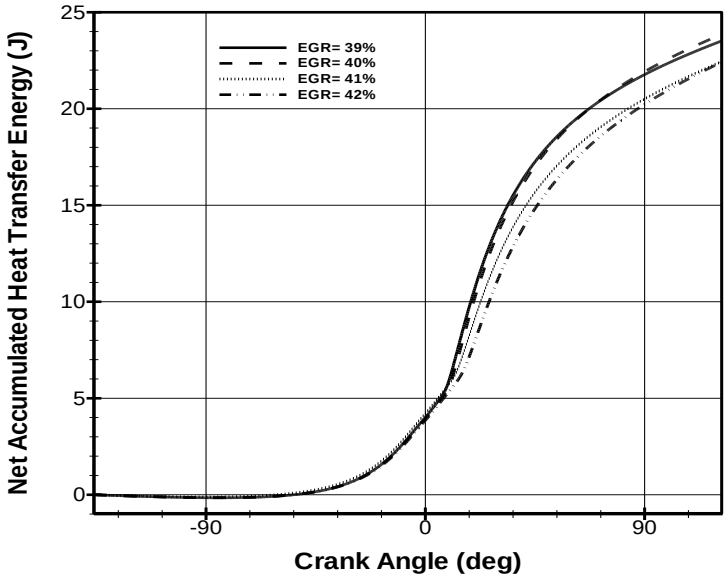

Fig. 4.43 Net accumulated heat transfer energy versus crank angle for lean PCI combustion at an injection timing of 9° BTDC for four EGR rates for cylinder 1.

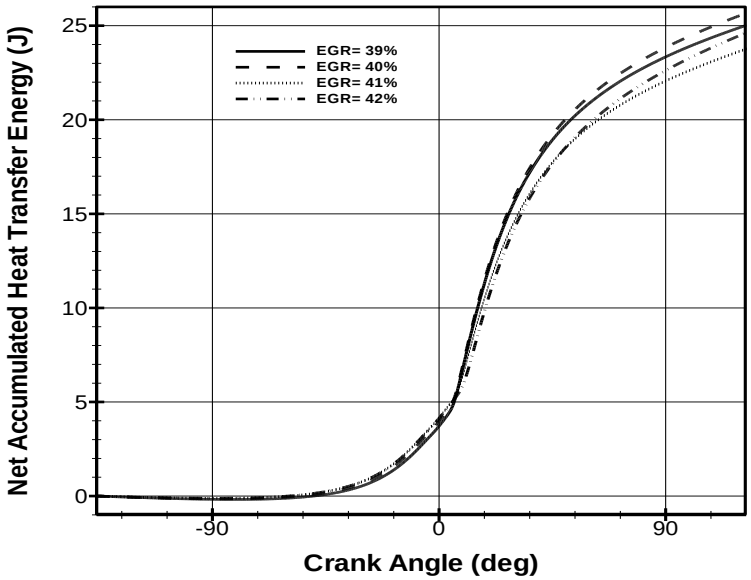

Fig. 4.44 Net accumulated heat transfer energy versus crank angle for lean PCI combustion at an injection timing of 12° BTDC for four EGR rates for cylinder 1.

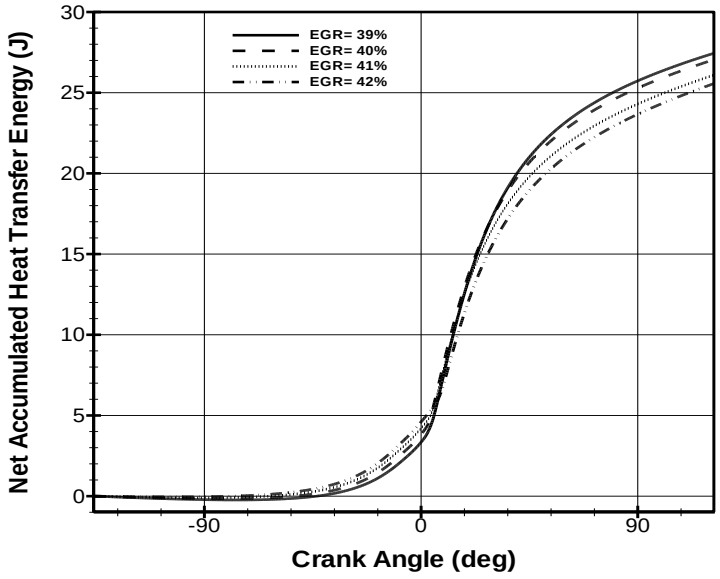

Fig. 4.45 Net accumulated heat transfer energy versus crank angle for lean PCI combustion at an injection timing of 15° BTDC for four EGR rates for cylinder 1.

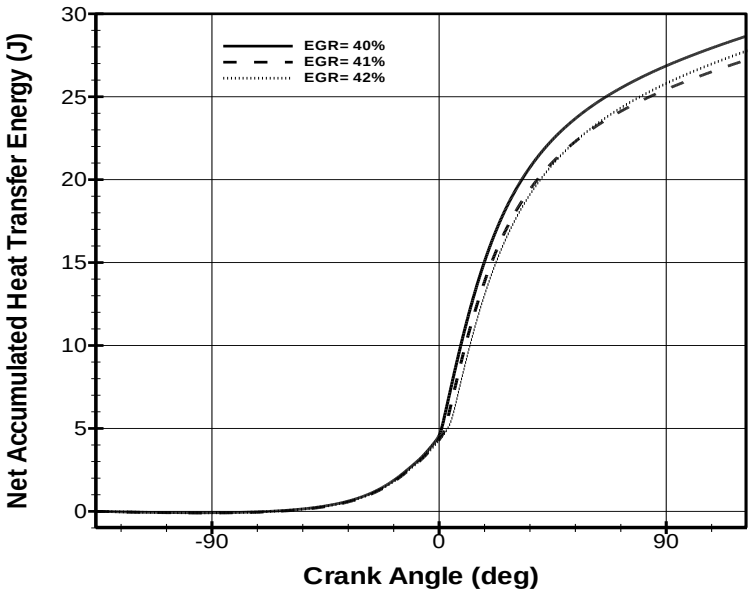

Fig. 4.46 Net accumulated heat transfer energy versus crank angle for lean PCI combustion at an injection timing of 18° BTDC for three EGR rates for cylinder 1.

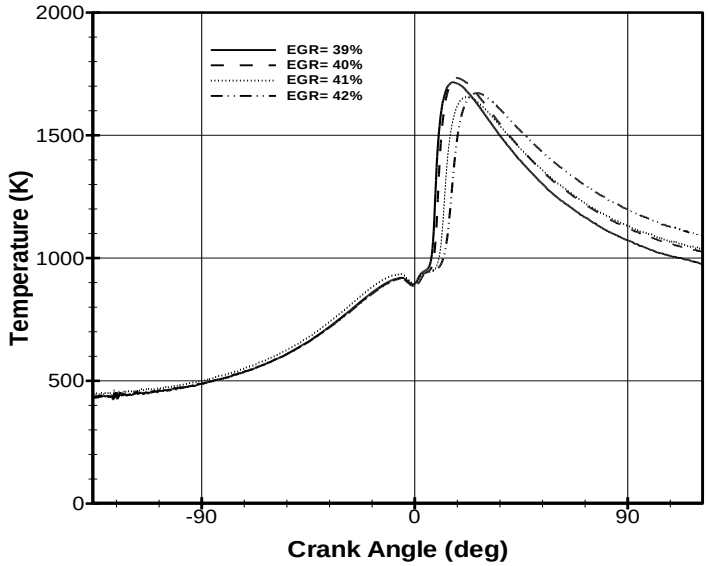

Fig. 4.47 Temperature versus crank angle for lean PCI combustion at an injection timing of 9° BTDC for four EGR rates for cylinder 1.

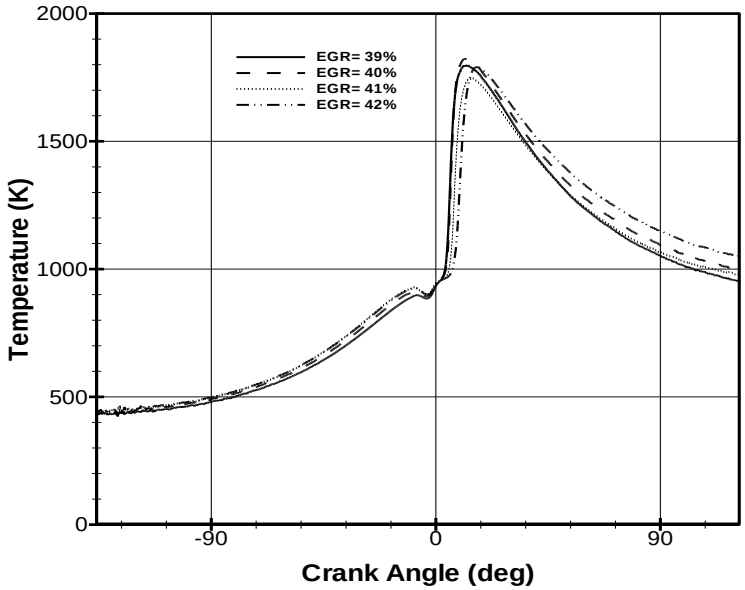

Fig. 4.48 Temperature versus crank angle for lean PCI combustion at an injection timing of 12° BTDC for four EGR rates for cylinder 1.

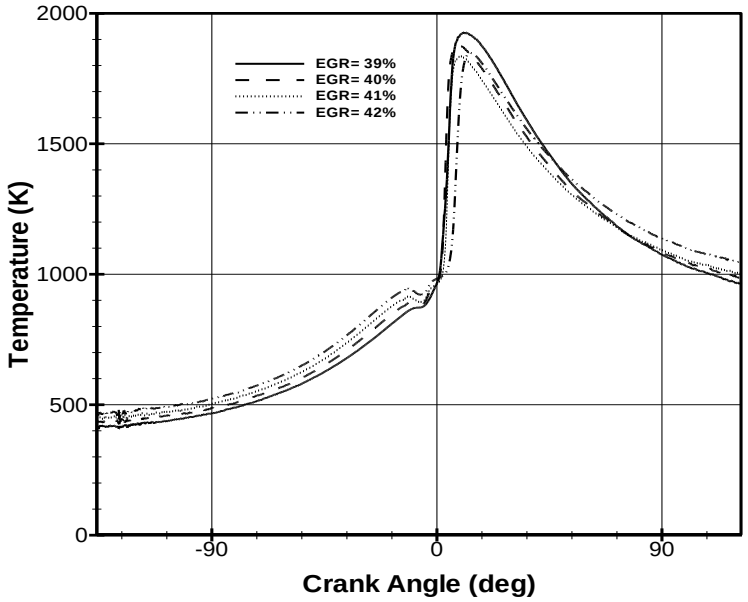

Fig. 4.49 Temperature versus crank angle for lean PCI combustion at an injection timing of 15° BTDC for four EGR rates for cylinder 1.

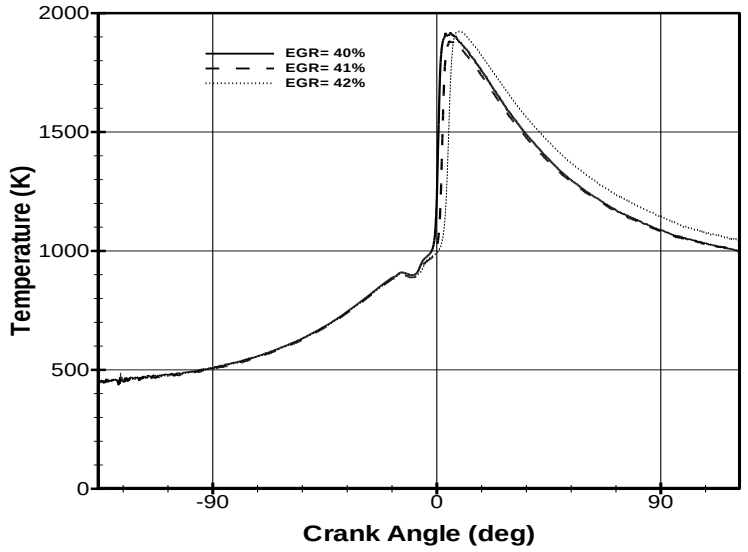

Fig. 4.50 Temperature versus crank angle for lean PCI combustion at an injection timing of 18° BTDC for three EGR rates for cylinder 1.

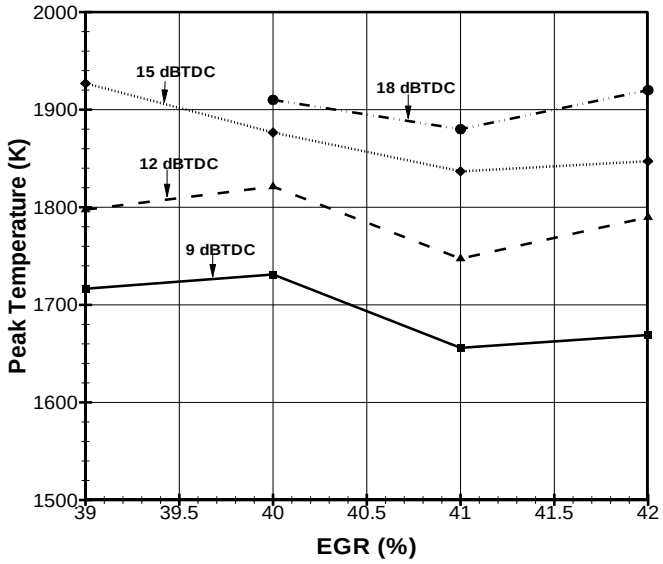

Fig. 4.51 Peak temperature versus EGR for lean PCI combustion for four injection timings for cylinder 1.

4.2.4 Net Accumulated Heat Release versus Crank Angle

The net accumulated heat release is the sum of rate of work done, rate of change in internal energy and the rate of heat transfer. So any change or trends observed in the accumulated heat release is attributed to the above three factors. The calculation of rate of heat release is important as it is required for the calculation of net indicated thermal efficiency and in the study of energy distribution. Figure 4.52 to Figure 4.55 indicates the variation of net accumulated heat release versus crank angle for a constant EGR at various injection timing for cylinder 1. A negative heat release is observed near the 0° BTDC crank angle for all the cases under study. This means that the heat is absorbed rather than released. This indicates the vaporization of fuel occurring inside the cylinder

during that time. For EGR= 39%, the peak heat released is observed for injection timing 15° BTDC, followed by 12° BTDC, and 9° BTDC. The change in internal energy for both 15° and 12° are almost the same. But the heat transfer for 15° is greater than 12°. This is the reason for the highest heat released in the case of 15° BTDC.

For EGR= 40%, the peak heat released is observed for 9° and 15° BTDC. For EGR= 41%, the peak heat released is observed for 18° BTDC. This is because of the high change in internal energy inside the cylinder and high heat transfer rate.

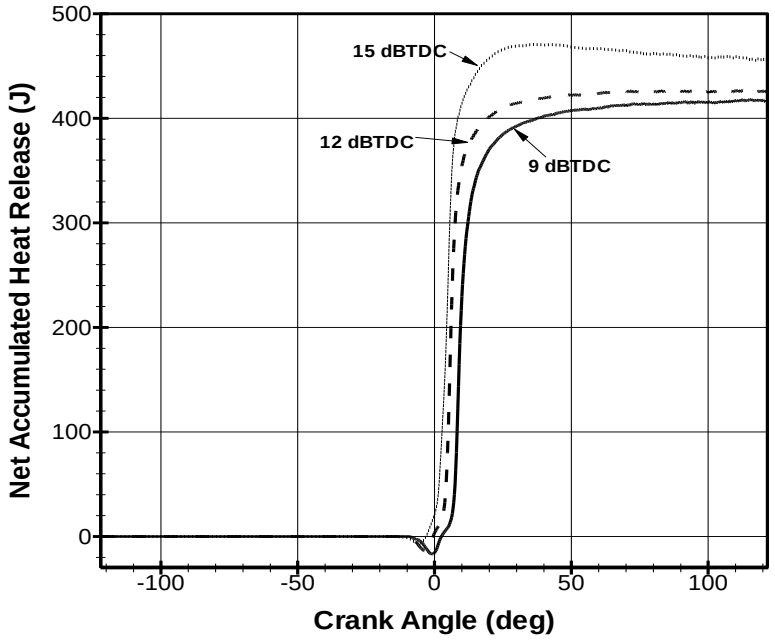

Fig. 4.44 Net accumulated heat release versus crank angle for lean PCI combustion at EGR= 39% for three injection timings for cylinder 1.

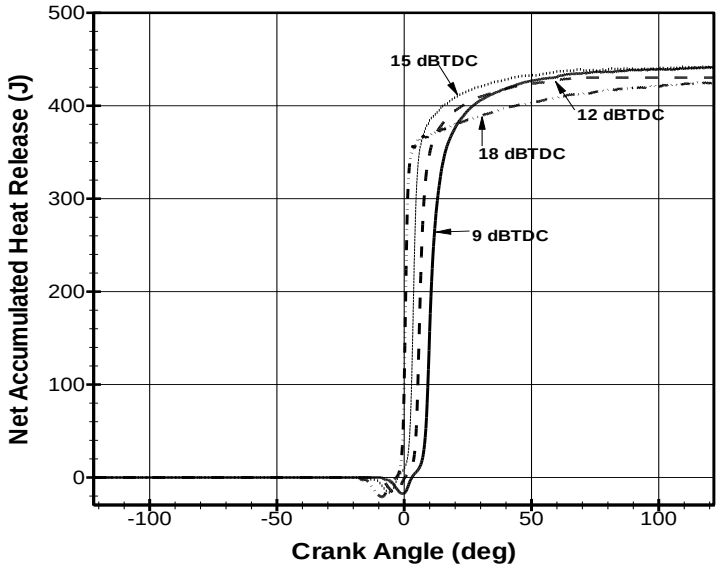

Fig. 4.53 Net accumulated heat release versus crank angle for lean PCI combustion at EGR= 40% for four injection timings for cylinder 1.

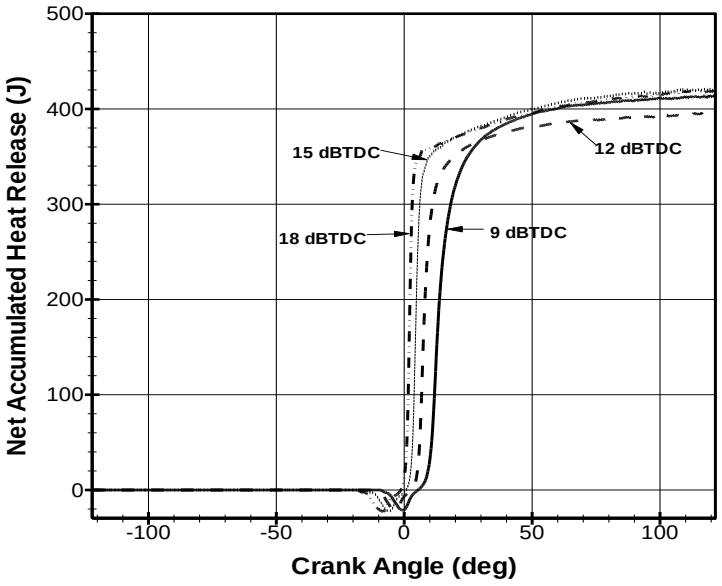

Fig. 4.54 Net accumulated heat release versus crank angle for lean PCI combustion at EGR= 41% for four injection timings for cylinder 1.

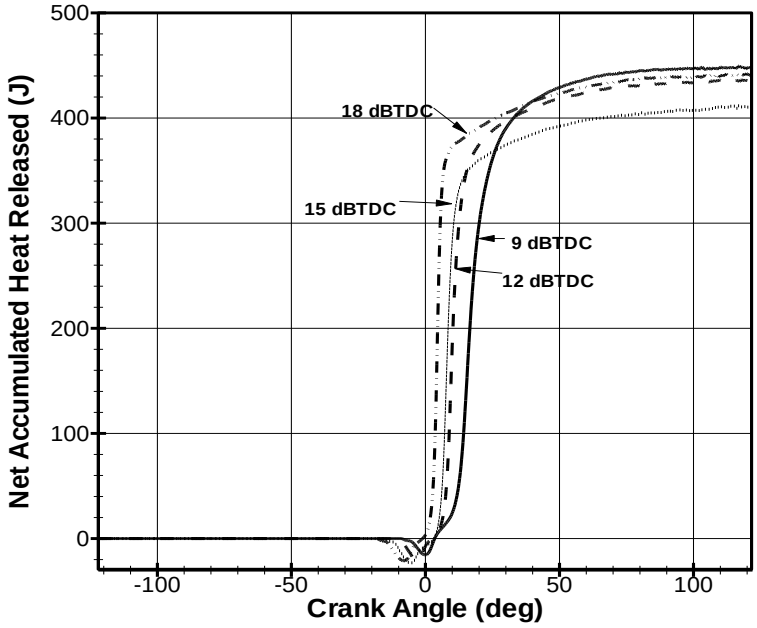

Fig. 4.55 Net accumulated heat release versus crank angle for lean PCI combustion at EGR= 42% for four injection timings for cylinder 1.

Figure 4.56 to Figure 4.59 indicates the variation of net accumulated heat release as a function of crank angle for varying EGR at constant injection timings for cylinder 1. The negative heat transfer near 0° BTDC crank angle is due to the fuel vaporization phenomenon described above. For injection timing of 9°, and 12° BTDC, the peak heat release is observed for EGR= 42%. For injection timing of 15° BTDC, the peak heat release is observed for EGR= 39%. This is due to the higher heat transfer rate and rate of work done. For injection timing of 18° BTDC, the peak heat release is observed for EGR= 42%.

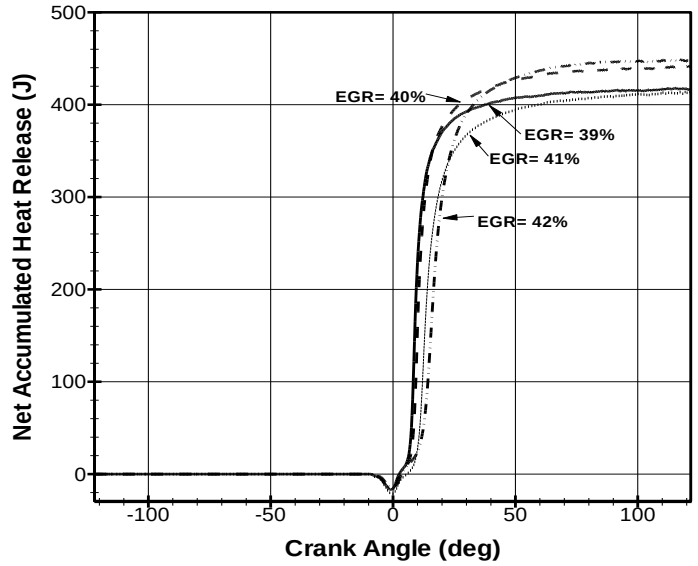

Fig. 4.56 Net accumulated heat release versus crank angle for lean PCI combustion at an injection timing of 9° BTDC for four EGR rates for cylinder 1.

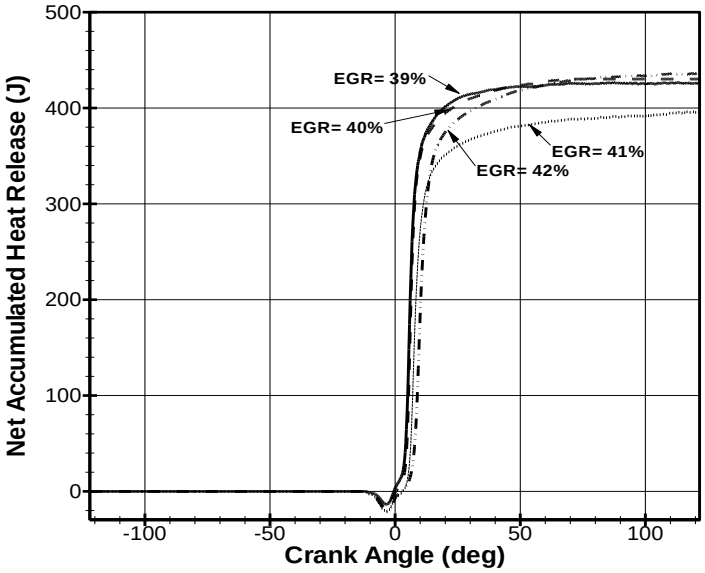

Fig. 4.57 Net accumulated heat release versus crank angle for lean PCI combustion at an injection timing of 12° BTDC for four EGR rates for cylinder 1.

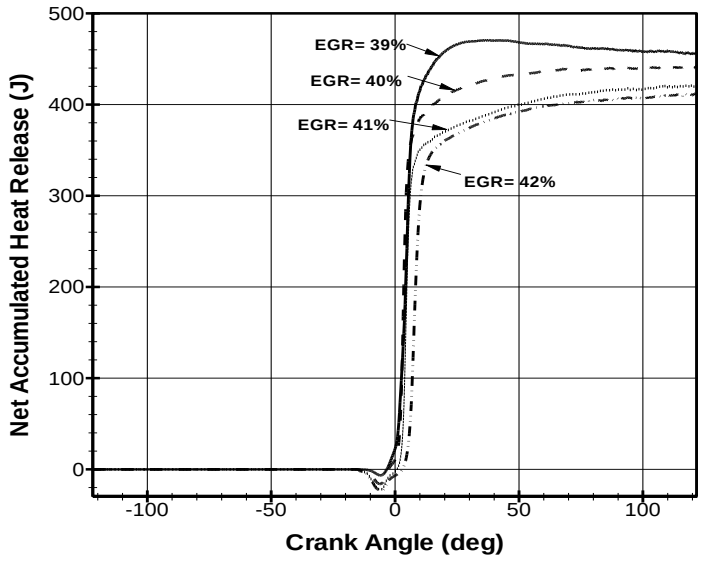

Fig. 4.58 Net accumulated heat release versus crank angle for lean PCI combustion at an injection timing of 15° BTDC for four EGR rates for cylinder 1.

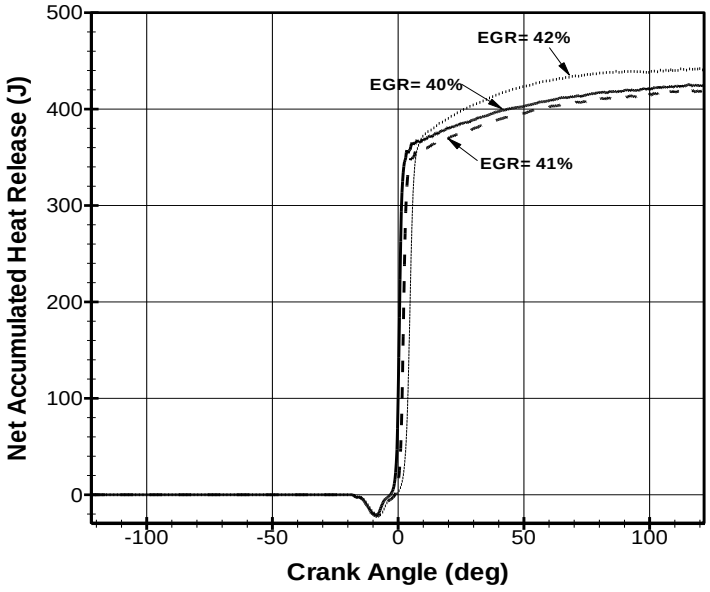

Fig. 4.59 Net accumulated heat release versus crank angle for lean PCI combustion at an injection timing of 18° BTDC for three EGR rates for cylinder 1.

4.3 Injection Timing Analysis

Till now the discussion was on the rate of work done, rate of change of internal energy, rate of heat transfer and rate of heat release. This section describes the variation of parameters such as total work done, total heat transfer, total change in internal energy, total net heat released, net indicated thermal efficiency, combustion efficiency and brake fuel conversion efficiency varies with injection timing.

4.3.1 Total Work Done versus Injection Timing

The total work done is obtained by summing the change of work done explained in section 4.2.1. A plot of work done as a function of injection timing is generated. Figure 4.60 indicates the variation of total work done with injection timing for cylinder 1. It is observed that for EGR= 40% and 41%, the total work done at 15° BTDC is greater than 18° BTDC even though maximum peak pressure is observed for injection timing of 18° BTDC. On close observation of pressure versus crank angle for EGR=40% and EGR= 41% (figure 4.2 and figure 4.3), it reveals that there is a rise in pressure due to premixed combustion inside the cylinder before the TDC. So some amount of energy is utilized in overcoming this rise in pressure inside the cylinder during the compression stroke. But for EGR= 42%, the total work done for injection timing 15° BTDC is less than 18° BTDC as no rise in pressure was observed in the pressure versus crank angle plot during the compression stroke (figure 4.7). EGR remaining a constant, it is observed that the work done decreases with retardation of injection timing from 15° BTDC for EGR rates 39%, 40% and 41%. One reason is the lower pressure and temperatures inside the cylinder with retardation of injection timing. Second reason being, as the injection

timing is retarded, the start of combustion gets delayed and major part of the combustion takes place during the expansion stroke. The exhaust valve opening point is fixed. Hence the time available for complete combustion reduces, thus reducing the total work output. The total work done for EGR= 42% and injection timing 15° BTDC shows a deviation from the usual pattern. This might be due to the uncertainties in this experiment.

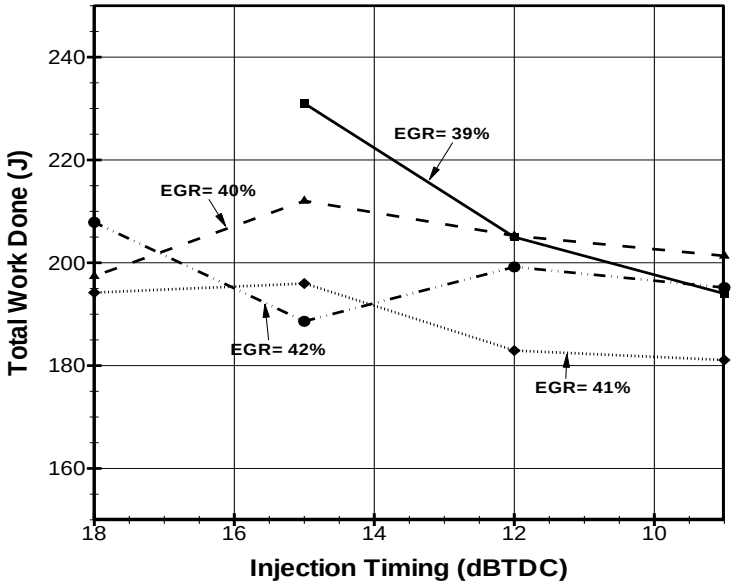

Fig. 4.60 Total work done versus injection timing for lean PCI combustion at four EGR rates for cylinder 1.

4.3.2 Total Change in Internal Energy versus Injection Timing

The total change in internal energy is obtained by the summation of the internal energy versus crank angle (section 4.2.2) for each case under study. The total change in internal energy has a direct effect on the total net heat released. Figure 4.61 indicates the

variation of total change in internal energy as a function of injection timing for cylinder 1.

For EGR= 39%, there is an increase in change in internal energy as the injection timing is retarded from 12° BTDC to 9° BTDC. The same trend is observed for EGR= 40%, for injection timing of 15° BTDC to 12° BTDC, EGR= 41% from 12° BTDC to 9° BTDC, and EGR= 42% from 15° BTDC to 9° BTDC. Change in internal energy is a strong function of temperature. Figure 4.62 indicates the variation of the turbine inlet temperature with injection timing at four EGR rates. It is evident that for all the cases discussed above, there is an increase in the temperature of the exhaust gas at the turbine inlet that contributes to a rise in the change in internal energy.

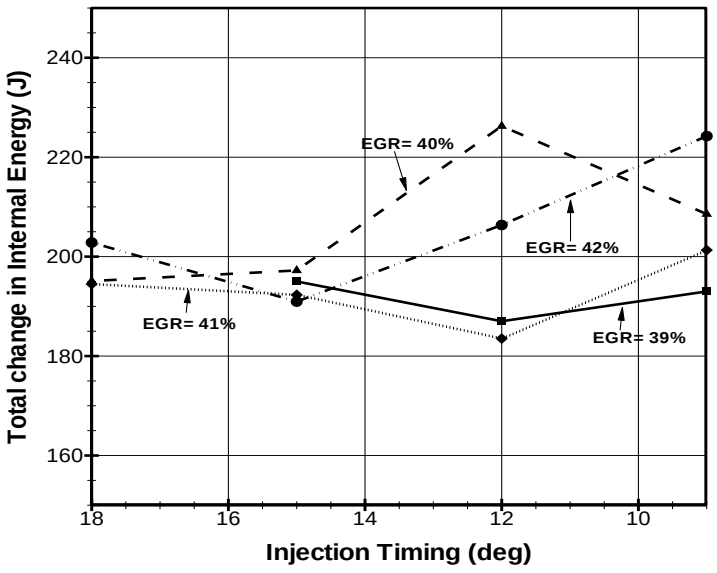

Fig. 4.61 Total change in internal energy versus injection timing for lean PCI combustion at four EGR rates for cylinder 1.

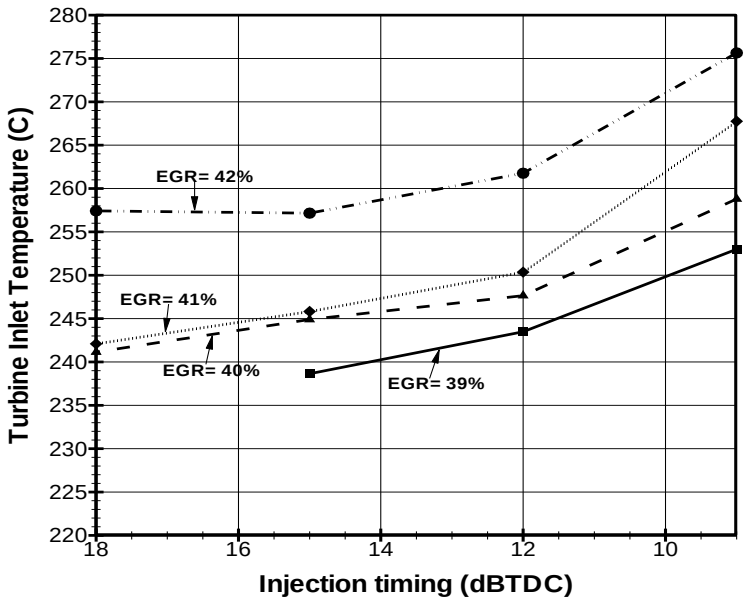

Fig. 4.62 Turbine inlet temperature versus injection timing for lean PCI combustion at four EGR rates.

4.3.3 Total Heat Transfer versus Injection Timing

The total heat transfer is calculated by the summation of the variation of net heat transfer with crank angle (section 4.2.3). The calculation of the total heat transfer is important for the analysis of the energy distribution. Figure 4.63 indicates the variation of the total heat transfer with injection timing for cylinder 1. It can be inferred that EGR remaining a constant, as injection timing is advanced, the heat transfer increases. This is because, with an advance in injection timing, there is an advance in the start of combustion also (table 4.1). Thus more time is available for the heat transfer process inside the cylinder of the engine. Another reason is the peak pressure and temperature

created within the cylinder of the engine as the injection timing is advanced. As the injection timing is advanced, the peak pressure increases (figure 4.1 to 4.3). Figure 4.42 indicates the variation of peak temperature with injection timing for cylinder 1. It shows that as the injection timing is advanced, the peak temperature increases. Another reason that can contribute to the decreasing heat transfer is the contribution of radiation heat transfer. The radiation heat transfer is a strong function of temperature. So as the temperature increases, the radiation heat transfer increases. The slope of each of these plots indicates the rate of heat transfer. On close observation it can noted that the trend of the increase in the heat transfer follows the trend in the increase in the peak temperature with advance in injection timing for most of the points.

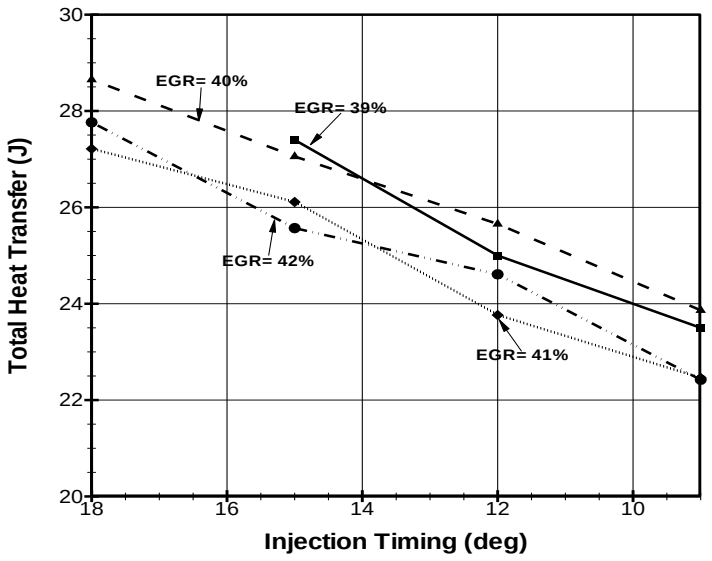

Fig. 4.63 Total heat transfer versus injection timing for lean PCI combustion at four EGR rates for cylinder 1.

4.3.4 Total Net Accumulated Heat Release versus Injection Timing

The total net heat release calculation is important for the analysis of energy distribution, and calculation of net indicated thermal efficiency. The total net heat released is the sum of the total work done (section 4.3.1), total change in internal energy (section 4.3.2) and total heat transfer (section 4.3.3). So the variation of all the above mentioned factors contributes to the change in the net heat released. Also the total net heat release can be calculated by adding the rate of heat release per crank angle revolution for the entire cycle (section 4.2.4). The total heat released is useful for the calculation of net indicated thermal efficiency (section 4.3.7) and in the analysis of energy distribution (section 4.3.5). Figure 4.64 indicates the variation of the total net heat release as a function of injection timing for cylinder 1.

For EGR= 39%, the total net heat released decreases with retardation of injection timing. This is because of the decrease in total heat transfer (figure 4.63) and the total work done (figure 4.60). The total change in the internal energy increases marginally. But this is not significant compared to the rate of decrease of the total heat transfer and total work done. For EGR= 40%, when the injection timing is retarded from 18° to 15° BTDC, the total net heat release increases. This is because of the increase in total work done. The rapid increase in the change in internal energy for EGR= 40% and variation of injection timing of from 15° BTDC to 12° BTDC, is the reason for the rise in total heat released during this period. The decrease in the total heat released for EGR= 42% as the injection timing is retarded from 18° to 15° is the result of the decreasing total work done, total change in internal energy and total heat transfer. The increase in the total net

heat released from 15° to 9° BTDC for EGR= 42% is the result of increase in the total change in internal energy.

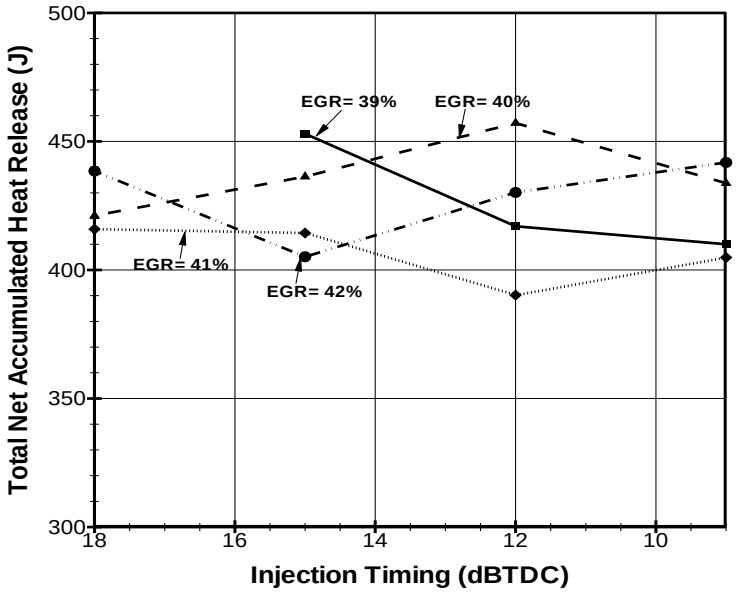

Fig. 4.64 Total net accumulated heat release versus injection timing for lean PCI combustion at four EGR rates for cylinder 1.

4.3.5 Energy Distribution

This section analyses the energy distribution inside the cylinder of the engine during the combustion process. That is, the relative contribution of total work done, total change in internal energy and total heat transfer, to the total heat released is analyzed. The prime motive here is to study how the contribution of the total heat transfer changes with injection timing for different EGR rates.

The energy distribution versus injection timing for a particular EGR rate for cylinder 1 is shown from figure 4.65 to figure 4.68. It can be inferred that, for constant EGR, with retarding injection timing, the contribution of total heat transfer to the total energy distribution decreases. The highest percentage change was observed for EGR=40%. There is a change of 1.4% in heat transfer as we retard the injection timing from 18° BTDC to 9° BTDC. The total work done also decreases as the injection timing is retarded. This is because of the thermodynamic state of the exhaust gas from the engine. Figure 4.62 indicates the variation of turbine inlet temperature with injection timing for various EGR rates. It indicates that as the injection timing is retarded, for a constant EGR rate, the exhaust temperature increases. This is because, the time available for full utilization of the energy released is less because of late combustion. That is there is an increase in the internal energy inside the cylinder which causes a decrease in the heat transfer and work done. Hence a large fraction of the energy is lost out the exhaust.

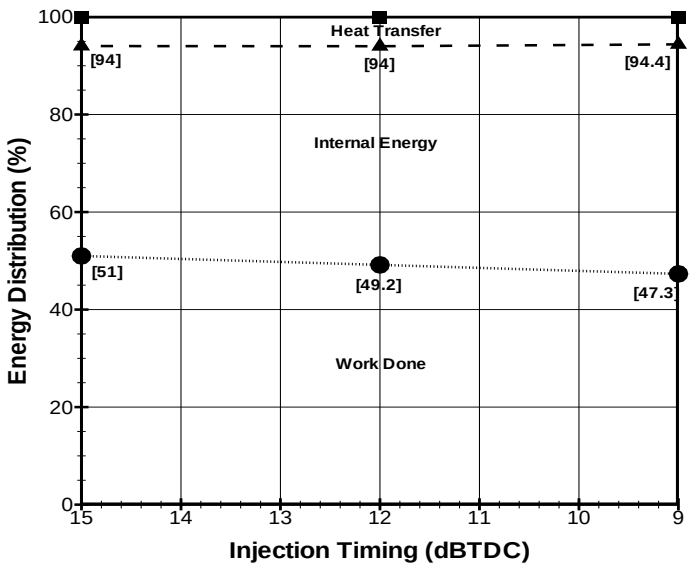

Fig. 4.65 Energy distribution versus injection timing for lean PCI combustion at EGR= 39% for cylinder 1.

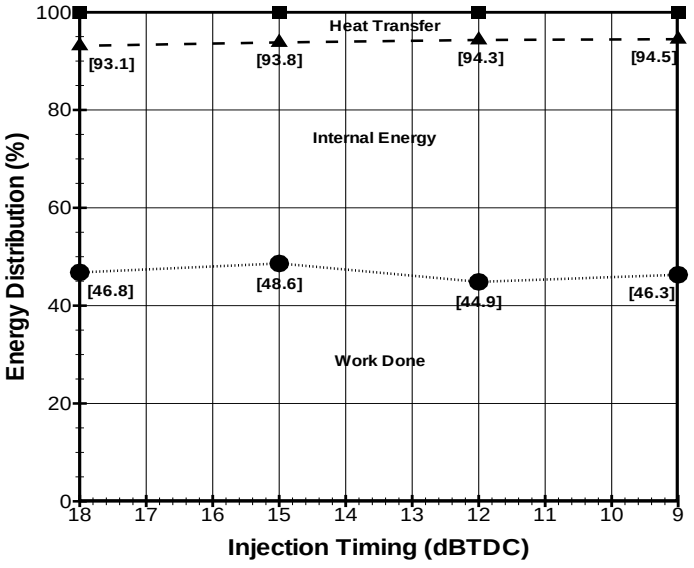

Fig. 4.66 Energy distribution versus injection timing for lean PCI combustion at EGR= 40% for cylinder 1.

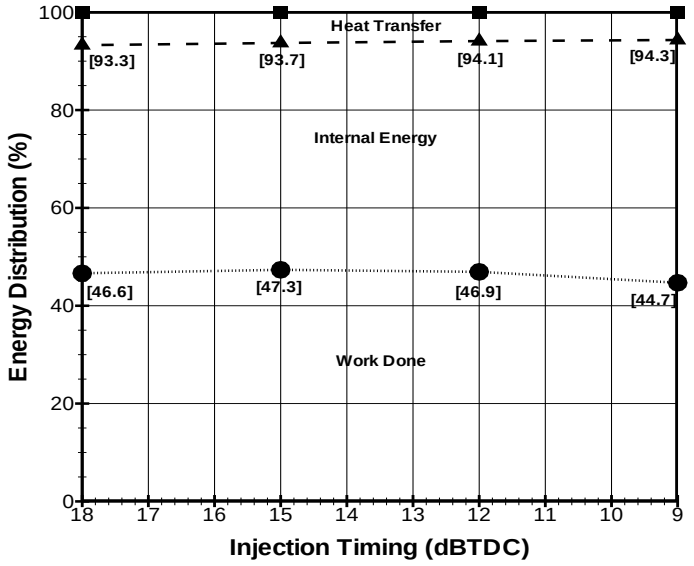

Fig. 4.67 Energy distribution versus injection timing for lean PCI combustion at EGR= 41% for cylinder 1.

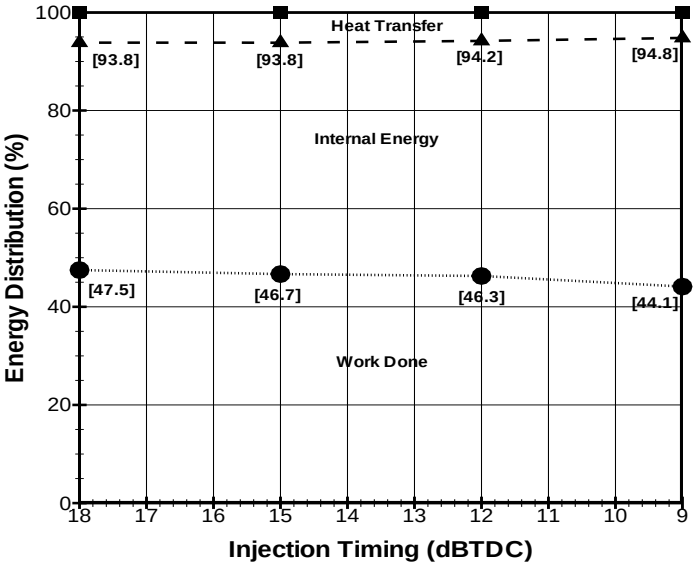

Fig. 4.68 Energy distribution versus injection timing for lean PCI combustion at EGR= 42% for cylinder 1.

4.3.6 Mean Effective Pressure Analysis with Varying Injection Timing

This section analyses the variation of various mean effective pressures with change in injection timing.

4.3.6.1 BMEP versus Injection Timing

Figure 4.69 indicates the variation of BMEP with injection timing. BMEP is actually a function of the total work output available at the crankshaft. It can be observed that for EGR= 42%, the BMEP decreases when the injection timing is retarded from 18° BTDC to 9° BTDC. For EGR= 41%, there is a slight increase in the BMEP when the timing is retarded. There is an observed increase in the BMEP for EGR= 39% when the injection timing is changed from 15° BTDC to 12° BTDC. From 12° BTDC to 9° BTDC, there is a decrease in BMEP. The variation of BMEP with injection timing for EGR= 40% shows a zig-zag variation with injection timing. What is the reason for all the above mentioned trends?

4.3.6.2 Average $IMEP_{net}$, FMEP versus Injection Timing

From equation 12,

$$BMEP = IMEP_{net} - FMEP \tag{17}$$

Hence, any trend changes observed in $IMEP_{net}$ or FMEP should reflect in the plot of BMEP. Figure 4.70 indicates the variation of average $IMEP_{net}$ with injection timing, and figure 4.71 indicates the variation of FMEP with injection timing. Net IMEP is the total work delivered to the piston over the entire cycle of the engine per unit displaced volume.

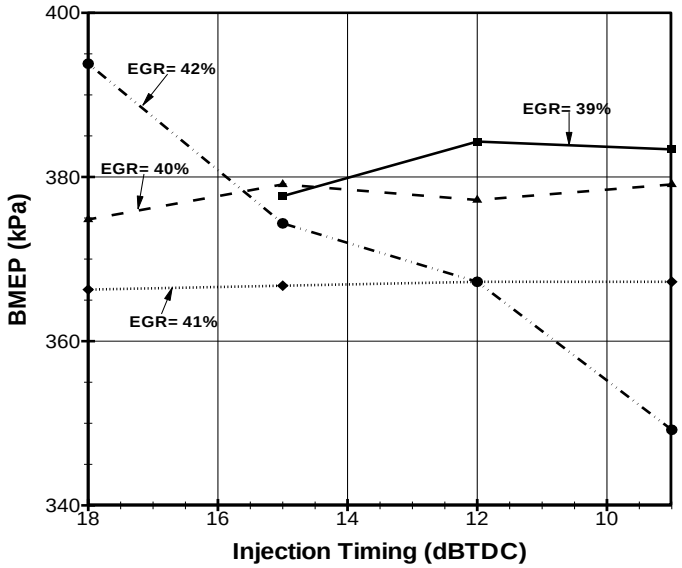

Fig. 4.69 BMEP versus injection timing for lean PCI combustion for four EGR rates.

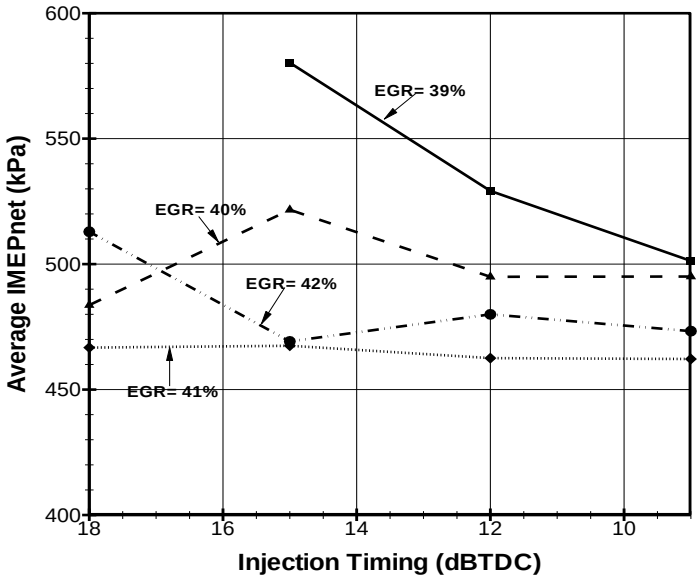

Fig. 4.70 Average $IMEP_{net}$ versus injection timing for lean PCI combustion for four EGR rates.

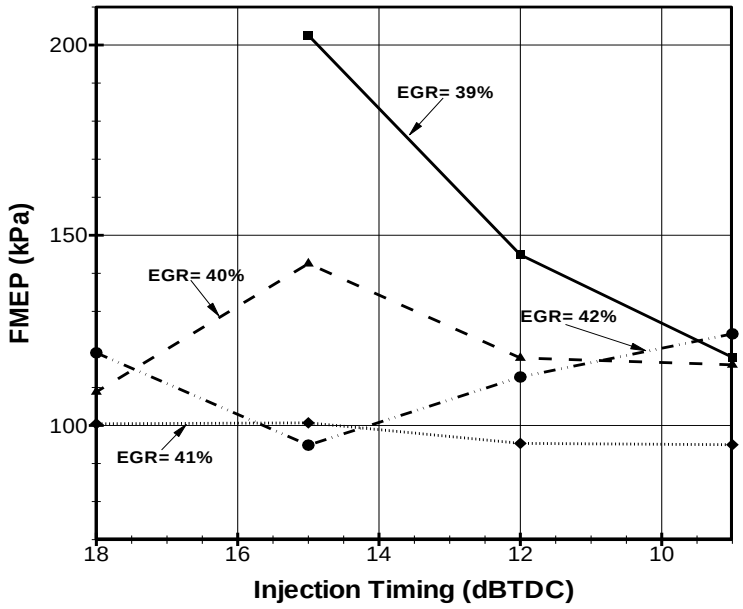

Fig. 4.71 FMEP versus injection timing for lean PCI combustion for four EGR rates.

For EGR= 39%, when injection timing is retarded from 15° BTDC to 9° BTDC, the FMEP decreases. While the average net IMEP increases from 15° to 12° BTDC and decreases from 12° to 9° BTDC. The observed increase in BMEP when injection timing from 15° to 12° is because of the decrease in FMEP. There is a net decrease in the average net IMEP from 12° to 9° BTDC, which results in a net decrease in the BMEP. The average net IMEP is almost a constant, for EGR= 41% when the injection timing is retarded from 18° BTDC to 9° BTDC. However there is a decrease in FMEP by almost 5 kPa, which is reflected in an increase in BMEP by 5 kPa when the injection timing is retarded from 18° to 9° BTDC. For EGR= 40%, both average net IMEP and FMEP

shows a zig-zag variation when injection timing is retarded from 18° to 9° BTDC. Average net IMEP increases approximately by 35 kPa, and the FMEP increases by 30 kPa from 18° to 15°. This accounts for increase in BMEP roughly by 5 kPa from 18° to 15°. When the injection timing is retarded from 12° to 9° BTDC, the average net IMEP remains a constant. But a decrease in FMEP is observed during this period, which accounts for the decrease in BMEP from 12° to 9° BTDC.

4.3.6.3 Average $IMEP_{gross}$, Average PMEP versus Injection Timing

Average net IMEP is the difference between the average gross IMEP and average PMEP. Figure 4.72 indicates the variation of average $IMEP_{gross}$ with injection timing and figure 4.73 indicates the variation of average PMEP with injection timing. The calculation of gross IMEP is described in section 2.3.4.1. It can be seen that the magnitude of PMEP is much smaller when compared to the gross IMEP. Hence the contribution of PMEP to net IMEP is less. The plot of net IMEP with injection timing follows the same trend as that of gross IMEP. The gross IMEP is basically the combustion work. The decrease in the gross IMEP observed for EGR= 39% and EGR= 41% is because of the decrease in the combustion efficiency, which will be explained in section 4.3.7. For EGR= 40%, the average gross IMEP for 15° BTDC is greater than 18° BTDC. This is more of a tradeoff between increased heat transfer and combustion phasing.

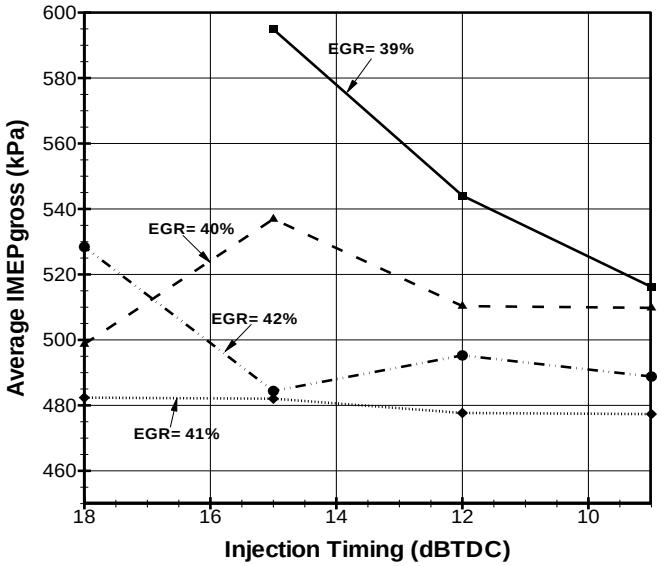

Fig. 4.72 Average $IMEP_{gross}$ versus injection timing for lean PCI combustion for four EGR rates.

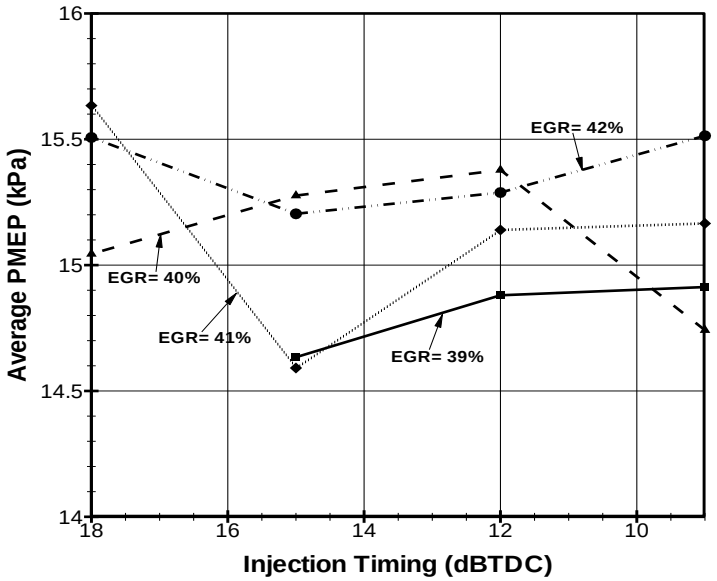

Fig 4.73 Average PMEP versus injection timing for lean PCI combustion for four EGR rates.

4.3.7 Combustion Efficiency versus Injection Timing

As a real consequence, a fraction of fuel's chemical energy is not released inside the cylinder of the engine during the combustion process. A part of it will be expelled through the exhaust in the form of incomplete combustion products. Figure 4.74 indicates the variation of combustion efficiency with injection timing. It can be inferred that with retardation of injection timing, the combustion efficiency decreases. More unburnt products in the exhaust imply lesser combustion efficiency. Combustion efficiency is a strong function of temperature. The peak temperature increases with advancing injection timing (figure 4.42). An increase in temperature decreases the products of incomplete combustion. As the fuel injection is retarded, the ignition delay increases. This increase in ignition delay results in a highly premixed, and low temperature combustion resulting in lesser unburnt products. Point corresponding to the condition EGR= 42% and injection timing of 12° BTDC is out of place in the plot. This might be due to the experimental uncertainties.

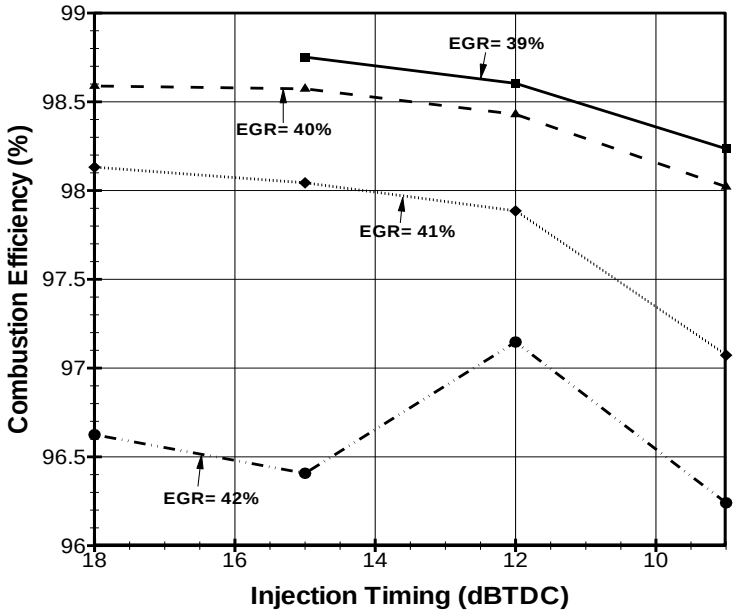

Fig. 4.74 Combustion efficiency with injection timing for lean PCI combustion at four EGR rates.

4.3.8 Brake Fuel Conversion Efficiency versus Injection Timing

Figure 4.75 indicates the variation of brake fuel conversion efficiency with injection timing for the engine. A decrease in the brake fuel conversion efficiency with injection timing is the expected trend. It is observed that this trend is valid only for EGR= 42%. This is because of the decrease in BMEP with retardation of injection timing (figure 4.69). For EGR= 39%, the change of efficiency when the injection timing is retarded from 15° to 9° BTDC is only 0.45%. The increase in the brake fuel conversion efficiency for EGR= 41% when the injection timing is retarded from 12° to 9° BTDC is because of the increase in total net heat release (figure 4.64). The zig-zag

variation of the brake fuel conversion efficiency follows the same trend as that of the total net heat release.

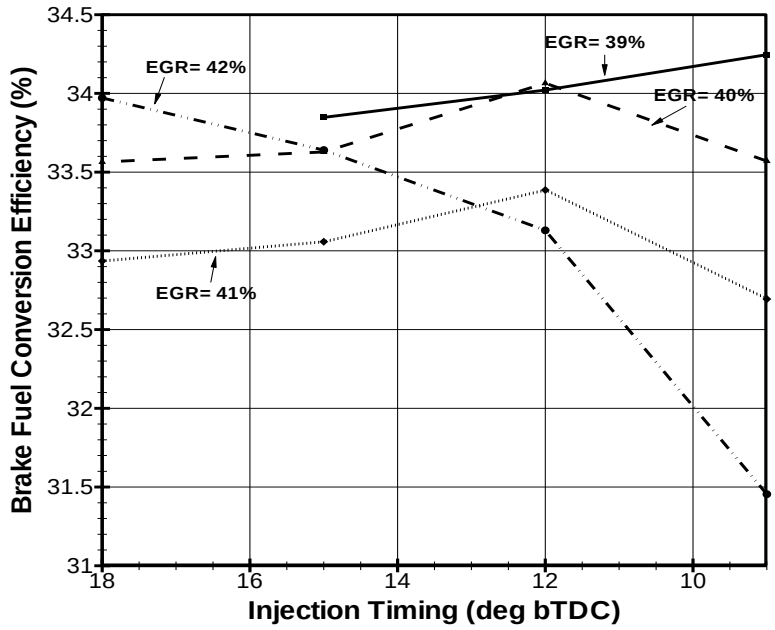

Fig 4.75 Brake fuel conversion efficiency versus injection timing for lean PCI combustion for four EGR rates.

4.4 EGR Analysis

A successful study was conducted for the variation of total work done, total change in internal energy, total heat transfer, net indicated thermal efficiency, combustion efficiency and brake fuel conversion efficiency with injection timing. This section deals with the study of the variation of the same parameter with change in EGR.

4.4.1 Total Work Done versus EGR

Figure 4.76 indicates how the total work done changes with EGR for cylinder 1 at four injection timings. The total work done is obtained by adding the work done per crank angle revolution (described in section 4.2.1) for the entire cycle.

For an injection timing of 9° BTDC, the total work done increases from EGR= 39% to EGR= 40%. The work done is a function of temperature and pressure. Even though there is a reduction of peak pressure when EGR is changed to 40% (figure 4.5), there is an increase in peak temperature (figure 4.51) which contributes to the rise increase in total work done. For injection timing of 15° BTDC, the total work done decreases with EGR. This is because of the fall in peak pressure (figure 4.7) and peak temperature (figure 4.51). At injection timing of 12° BTDC, the total work done almost remains a constant when EGR is changed from 39% to 40%. This is due to the negligible change in peak temperature and pressure. But the total work done shows a zigzag variation when the EGR is changed from 40% to 42%. This might be due to the zigzag variation in the peak temperature. The trend of total work done with variation in EGR for injection timing of 18° BTDC follows the trend of the peak temperature. It can be inferred from the above discussion that the total work done is a strong function of temperature. These variations in the total work done with EGR might affect the variation of mean effective pressures with EGR. This will be discussed in section 4.4.6.

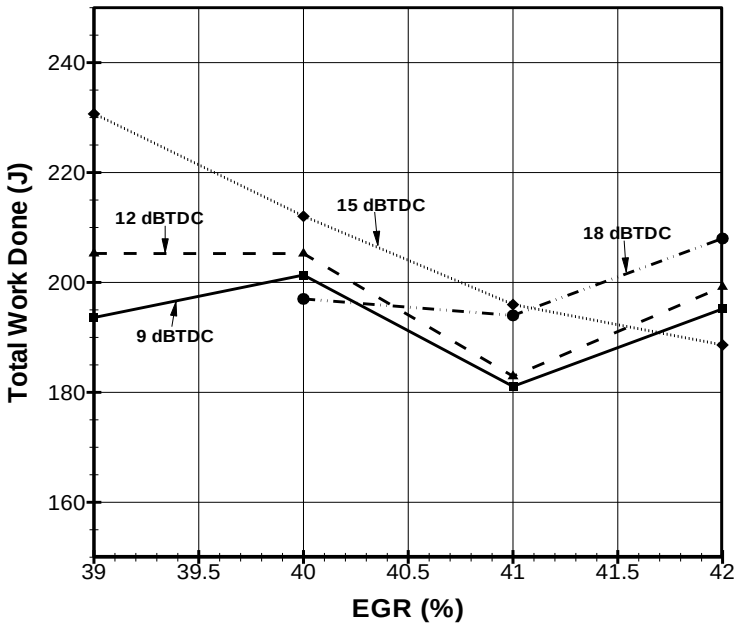

Fig. 4.76 Total work done versus EGR for lean PCI combustion at four injection timings for cylinder 1.

4.4.2 Total Change in Internal Energy versus EGR

Figure 4.77 indicates a total change in internal energy with EGR for cylinder 1 at four injection timings. The total change in internal energy is needed for the calculation of the total net heat release (section 4.4.4).

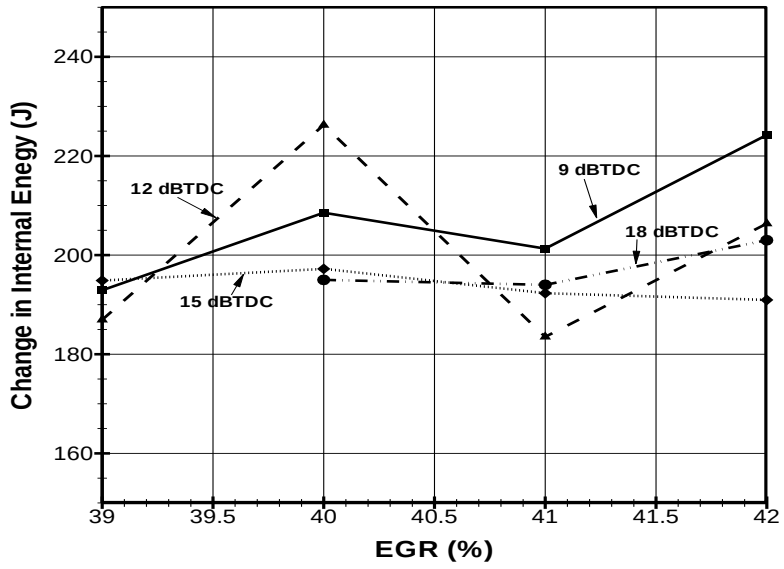

Fig. 4.77 Total change in internal energy versus EGR for lean PCI combustion at four injection timings for cylinder 1.

4.4.3 Total Heat Transfer versus EGR

The total heat transfer is significant in the calculation of the net heat release and in the analysis of the energy distribution. Figure 4.78 indicates the variation of the total heat transfer with EGR for cylinder 1 at four injection timings. The total heat transfer decrease with an increase in EGR. The total heat transfer is a function of temperature. The trend followed by each case under study is similar to the trend followed by the peak temperature for that case (figure 4.51). The increase in EGR reduces the peak temperature by increasing the ignition delay thus resulting in a lower heat transfer. Also the effect of radiation heat transfer reduces with an increase in EGR because of the lowering of the peak temperature.

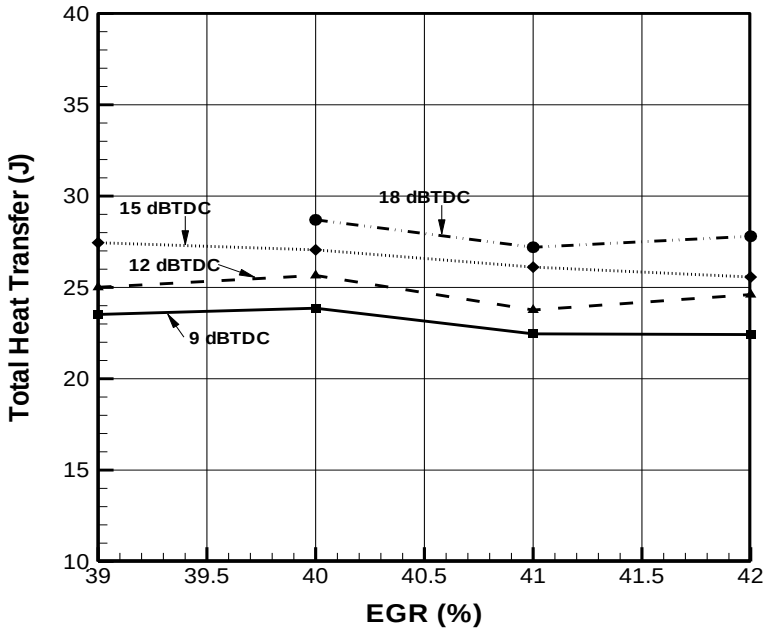

Fig. 4.78 Total heat transfer versus EGR for lean PCI combustion at four injection timings for cylinder 1.

4.4.4 Total Net Accumulated Heat Release versus EGR

The total net heat release is calculated by summing up the total work done, total change in internal energy, and total heat transfer or adding up the total heat release per crank angle basis for the entire cycle (section 4.2.4). So any change in the plot of total net heat released can be attributed to change in any of the three factors mentioned above. The total net heat release is used in the calculation of net indicated thermal efficiency (section 4.4.7) and in the analysis of energy distribution (section 4.4.5). Figure 4.79 indicates the variation of the total net heat release with EGR for cylinder 1 at four injection timings.

For injection timing of 15° BTDC, the total net heat release decreases with increase in EGR. This is due to the decrease in the total work done, total change in internal energy and total heat transfer. For injection timing of 9° BTDC, there is an increase in the total net heat release when EGR is changed from 39% to 40%. This is because of the increase in total work and total internal energy. The heat transfer almost remains a constant here. A zigzag variation is observed in the net heat release curve for 9° injection timing when the EGR is changed from 40% to 42%. This change is due to the zigzag variation in the total work done and total internal energy. The decrease in heat transfer during this period is negated by the increase in the total work and total change in internal energy.

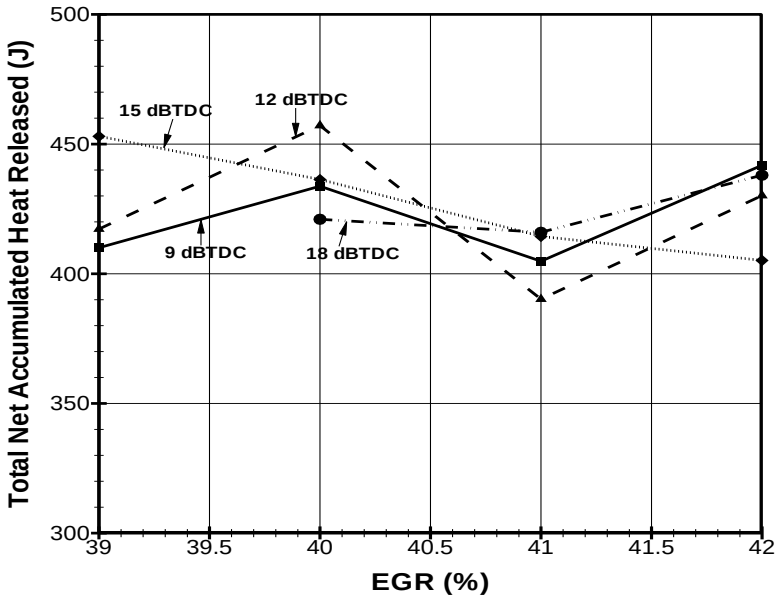

Fig. 4.79 Total net accumulated heat release versus EGR for lean PCI combustion at four injection timings for cylinder 1.

A zigzag variation in the total net heat release is observed for injection timings 12° BTDC and 18° BTDC also. The same zigzag trend is observed for the total work done, total change in internal energy and total heat transfer for each of these cases.

4.4.5 Energy Distribution

The energy distribution indicates how much of the total net heat released gets converted to total work done, total change in internal energy and total heat transfer. Prime motive here is to study how the contribution of total heat transfer changes as the EGR is changed. The energy distribution with EGR is plotted in figures 4.80 to 4.83. A definite trend for the contribution of heat transfer to the total energy distribution could not be inferred.

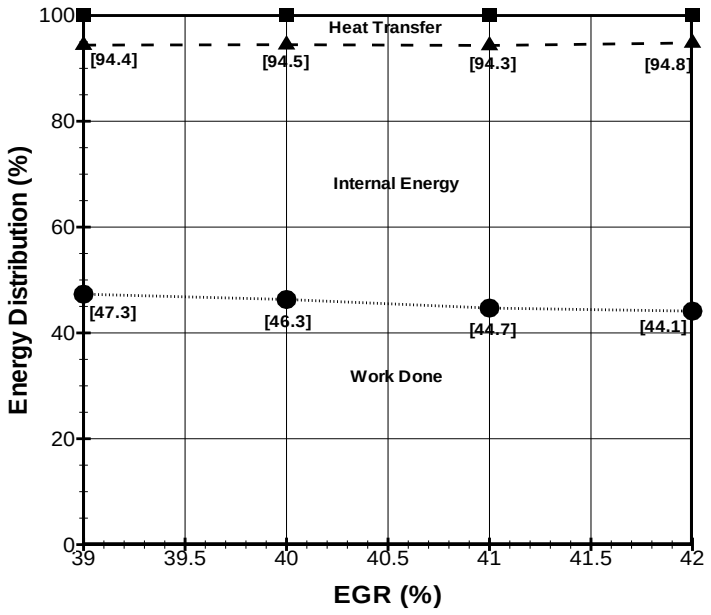

Fig. 4.80 Energy distribution versus EGR for lean PCI combustion at an injection timing of 9° BTDC for cylinder 1.

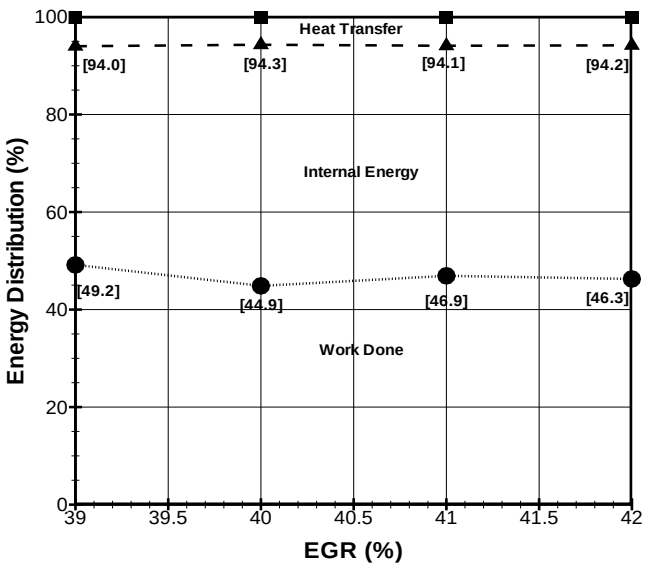

Fig. 4.81 Energy distribution versus EGR for lean PCI combustion at an injection timing of 12° BTDC for cylinder 1.

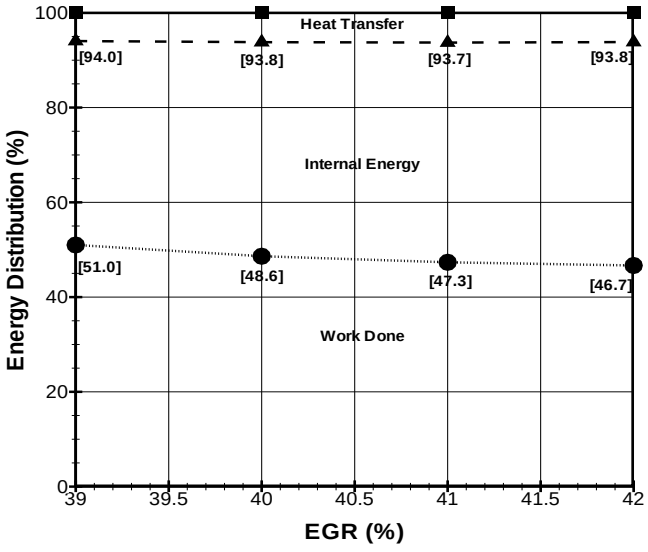

Fig. 4.82 Energy distribution versus EGR for lean PCI combustion at an injection timing of 15° BTDC for cylinder 1.

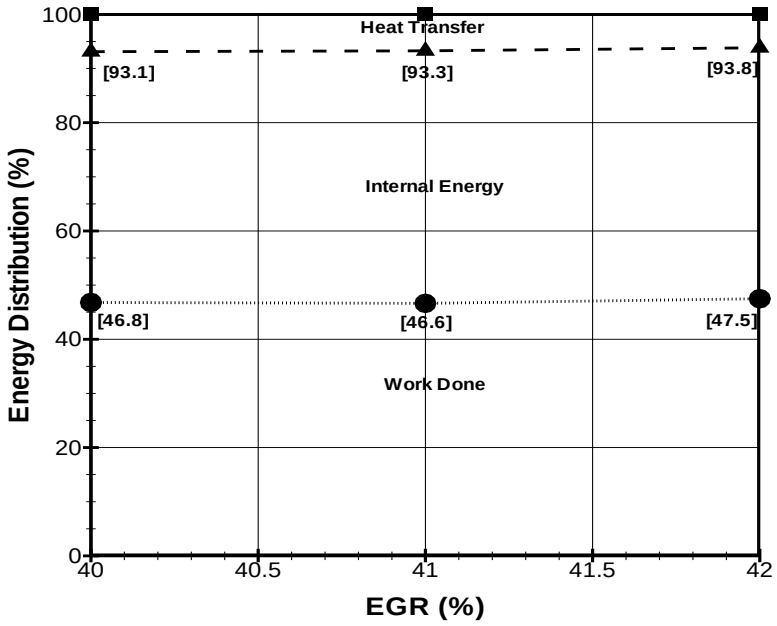

Fig. 4.83 Energy distribution versus EGR for lean PCI combustion at an injection timing of 18° BTDC for cylinder 1.

4.4.6 Mean Effective Pressure Analysis with Varying EGR rates

Section 4.3.6 threw light on the mean effective pressure analysis with variation in injection timing. This section analyses the variation of various mean effective pressures with change in EGR rates.

4.4.6.1 BMEP versus EGR

Figure 4.84 indicates the variation of BMEP with EGR. It can be inferred that for most of the cases, there is a decrease in BMEP with an increase in EGR. This might be due to the cooling effect provided by the EGR. For injection timing of 9° BTDC and 12° BTDC, there is a decrease in the BMEP when EGR is increased from 39% to 42%. 15°

BTDC injection timing shows a zig-zag variation in the BMEP with EGR. BMEP for injection timing of 18° BTDC decreases for EGR variation from 40% to 41% and increases for EGR variation from 41% to 42%. As explained in section 4.3.6, the variation of BMEP can be explained using the plots of average net IMEP and FMEP which will be explained in subsequent section.

4.4.6.2 Average $IMEP_{net}$, FMEP versus EGR

Figure 4.85 indicates the variation of average net IMEP with EGR and figure 4.86 indicates the variation of FMEP with EGR. Net IMEP is calculated using the work done data. The increase in the BMEP for injection timing of 15° BTDC when EGR is varied from 41% to 42% is because of a decrease in FMEP and an increase in average net IMEP. The constant BMEP for injection timing 12° BTDC from EGR= 41% to 42% is because, the effect of increase of average net IMEP is cancelled by an equal increase in FMEP. The average net IMEP decreases by almost 40 kPa when the EGR is increased from 39% to 41%. There is an observed 25 kPa decrease in the FMEP during this time. This is the reason why the BMEP plot described above shows a net decrease of around 15 kPa when the EGR is increased from 39% to 41%. A further increase in EGR to 42% results in a decrease in BMEP because the rate of decrease of average net IMEP is greater.

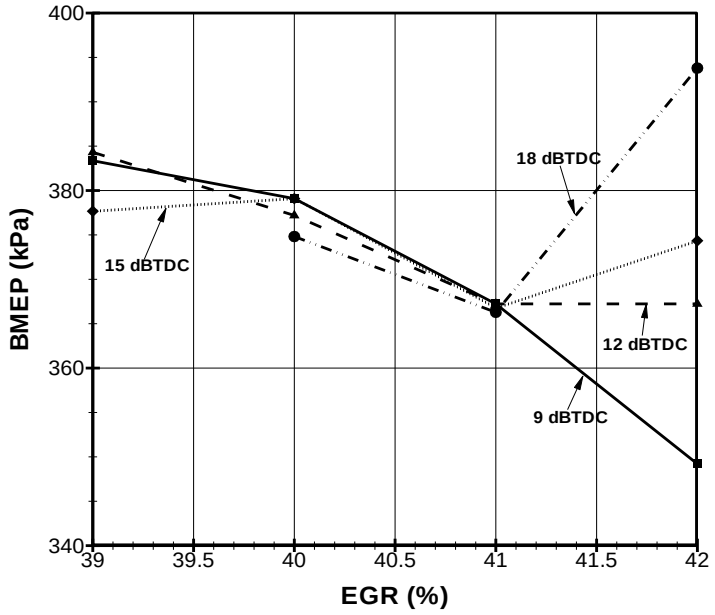

Fig. 4.84 BMEP versus EGR for lean PCI combustion for four injection timings.

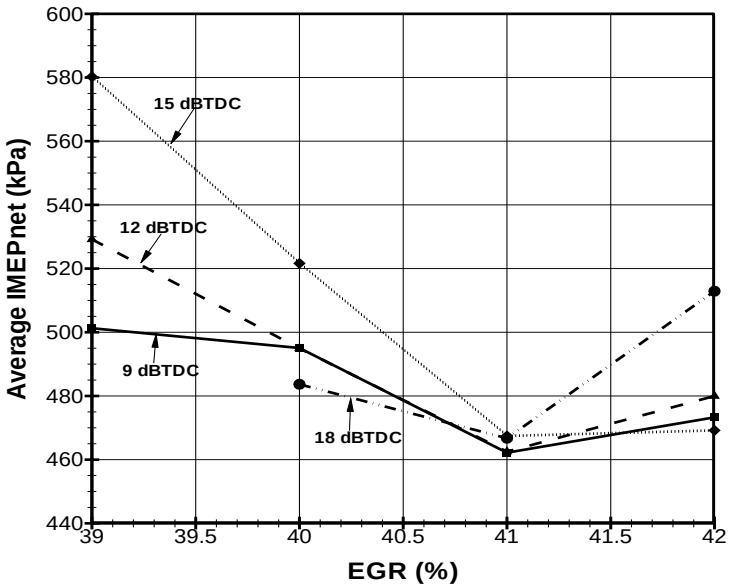

Fig. 4.85 Average $IMEP_{net}$ versus EGR for lean PCI combustion for four injection timings.

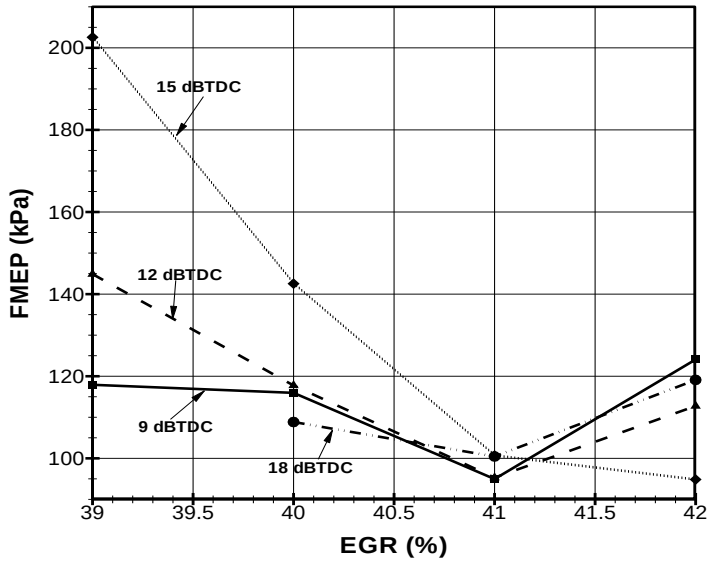

Fig. 4.86 FMEP versus EGR for lean PCI combustion for four injection timings.

4.4.6.3 Average $IMEP_{gross}$, Average PMEP versus EGR

Gross IMEP is calculated using the work done data. Average net IMEP is the difference between the average gross IMEP and average PMEP. The calculation of gross IMEP is described in section 2.3.4.1. Figure 4.87 indicates the variation of average $IMEP_{gross}$ with EGR and figure 4.88 indicates the variation of average PMEP with EGR. In most of the cases it is observed that average PMEP increases with EGR. This is because in a compression ignition engine, by increasing EGR, more mass is added into the inlet. This means, higher work is to be done to push the excess mass into the inlet. This means that there is an increase in average PMEP. As mentioned before, the value of average PMEP is much smaller when compared to average net IMEP. It is also observed that the trend of the average net IMEP follows the same trend as average gross IMEP.

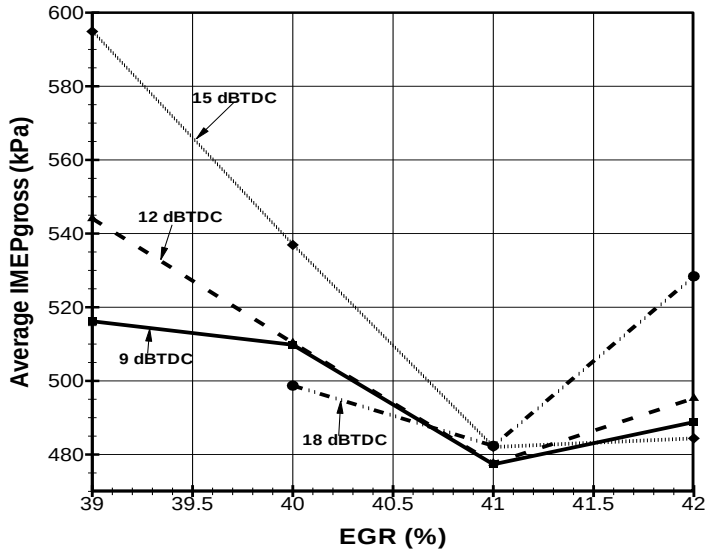

Fig. 4.87 Average $IMEP_{gross}$ versus EGR for lean PCI combustion for four injection timings.

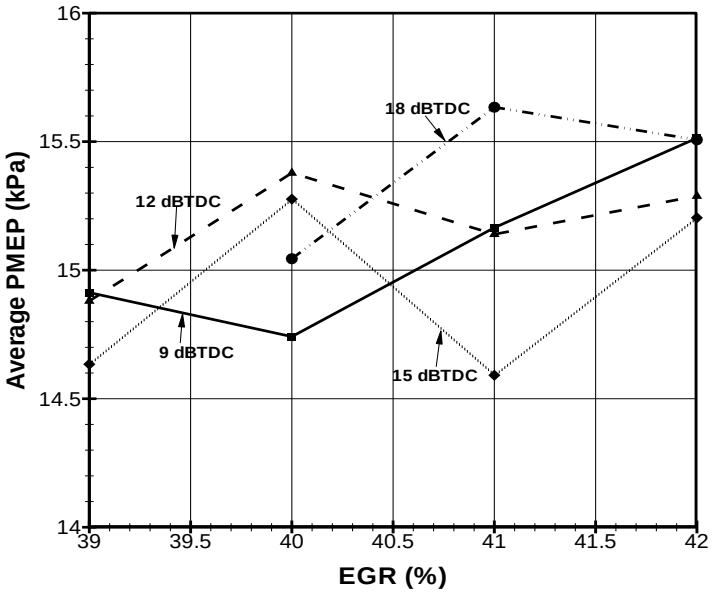

Fig. 4.88 Average PMEP versus EGR for lean PCI combustion for four injection timings.

The decrease in average gross IMEP is because of the decrease in combustion efficiency which will be explained in section 4.4.7. The average gross IMEP is basically the combustion work.

4.4.7 Combustion Efficiency versus EGR

Figure 4.89 shows the variation of combustion efficiency with EGR. Combustion efficiency is a part of brake fuel conversion efficiency. It can be inferred that the combustion efficiency decreases with increase in EGR. Combustion efficiency is 100%, if all the chemical energy of the fuel is converted to heat. Higher the amount of unburnt mixture in the exhaust system, lesser will be the combustion efficiency. In a combustion system, particles like HC and CO are formed due to incomplete combustion. So a high percentage of HC and CO in the exhaust indicates lower combustion efficiency. The main reasons are over lean A/F ratio reactions or over rich A/F ration reactions. When the mixture is over lean, then the excess oxygen surrounds the diffusion flame sheath and lowers the mixture's equivalence ratio below the lean flammability limit. In the case of over rich A/F ratio reactions, incomplete combustion occurs. As the EGR is increased, the mixture becomes leaner. This results in a higher production of HC and CO. Another factor affecting the formation of CO is the ignition delay. As EGR increases, the ignition delay lengthens (table 4.2) that creates a chance of lean A/F reactions. Another reason for the production of incomplete combustion products is A/F ratio. Decreasing A/F ratio increases the products of incomplete combustion. Figure 4.90 indicates the variation of the A/F ratio with change in EGR. It can be seen that the A/F ratio decreases with increase in EGR that causes the combustion efficiency to decrease.

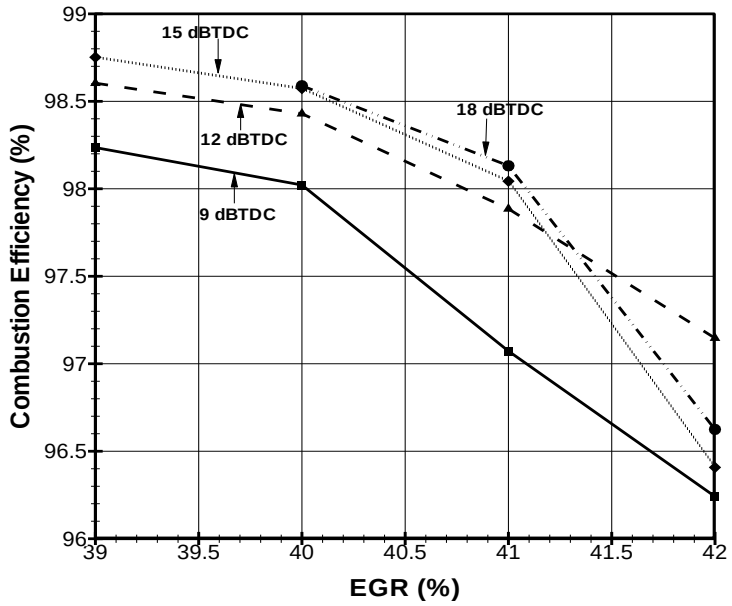

Fig. 4.89 Combustion efficiency versus EGR for lean PCI combustion at four injection timings.

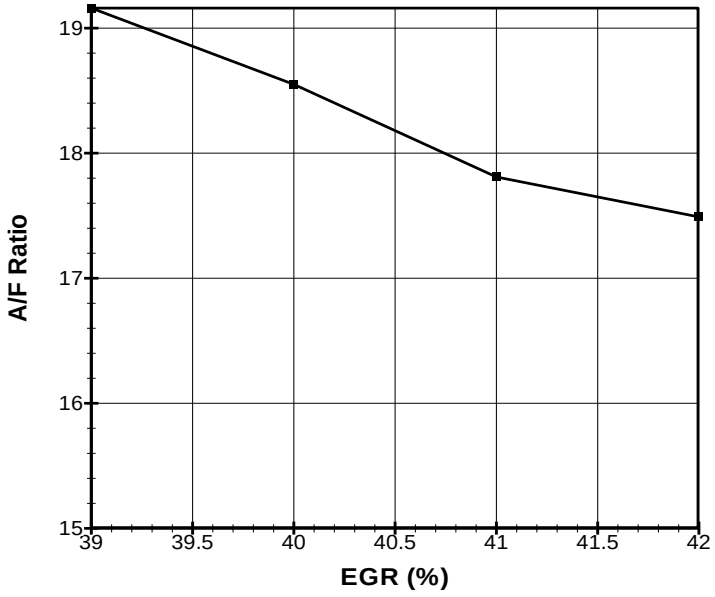

Fig. 4.90 A/F ratio versus EGR for lean PCI combustion.

4.4.8 Brake Fuel Conversion Efficiency versus EGR

The calculation of brake fuel conversion efficiency is explained in section 2.4.4.7. The variation in brake fuel conversion efficiency with EGR is studied for four injection timings of 9°, 12°, 15°, and 18° BTDC (figure 4.91).

Close observation of the plot of brake fuel conversion efficiency with EGR, for injection timing 9° and 12° indicates that the fuel conversion efficiency decreases with an increase in EGR. But for injection timings of 15° and 18° BTDC, an increase in brake fuel conversion efficiency was observed from EGR= 41% to EGR= 42%.

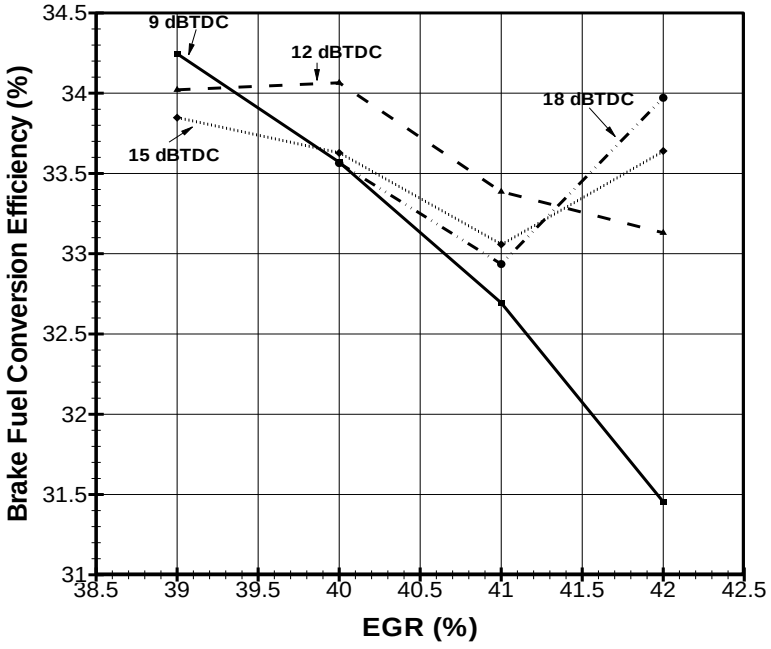

Fig. 4.91 Brake fuel conversion efficiency versus EGR for lean PCI combustion for cylinder 1 for four injection timings.

Brake fuel conversion efficiency is a reflection of BMEP. The trend that is followed by the brake fuel conversion efficiency with EGR follows the same trend of BMEP. The brake fuel conversion efficiency for injection timing of 12° BTDC decreases when EGR is increased from EGR= 41% to 42%. However BMEP remains a constant during this period of time. So this variation in the brake fuel conversion efficiency is due to the increase in the total net heat release (figure 4.79).

5. SUMMARY AND CONCLUSIONS

5.1 Summary

The study of PCI combustion led to the assessment that, using this technology, there can be significant and simultaneous reduction in NO_x and PM emissions with a slight loss of fuel conversion efficiency. This led to the analysis of variation of brake fuel conversion efficiency and energy transfer with EGR and injection timing. It is found that the brake fuel conversion efficiency decreases with an increase in EGR. The decrease in the brake fuel conversion efficiency with EGR is because of the decrease in the BMEP (net work output). Decrease in BMEP is because of the increase in FMEP, increase in pumping work and also decrease in the combustion temperatures and pressures. The decrease in peak pressure with increasing EGR is the result of an increase in the ignition delay due to the depletion of oxygen in the cylinder mixture. Lesser level of oxygen results in progressively delayed combustion pressure rise inside the cylinder. Moreover, it is shown that injection timing remaining constant, as the EGR is increased, the pressure moves away from the top dead center. A definite trend is not obtained for the contribution of heat transfer to the total energy distribution. However the total heat transfer decreases with increase in EGR because of decreasing combustion temperature. The decreased combustion temperature also results in lower radiation heat transfer. The decrease in the combustion efficiency is because of the increased formation of unburnt products due to increased ignition delay caused by the application of EGR and decreasing air-fuel (A/F) ratio.

The brake fuel conversion efficiency decreases with retardation of injection timing. The decrease in the brake fuel conversion efficiency is because of the decrease in combustion efficiency and reduced work output. One reason is the lower combustion pressure and temperature. Second reason being the delayed start of combustion, and major part of the combustion takes place in the expansion stroke. Hence the time available for the complete combustion reduces. EGR remaining constant, the peak value of the pressure decreases and it shifts towards the TDC with early injection timing. This is due to the early combustion as a result of the advanced injection timing. With retarding injection timing, the peak heat transfer, the total heat transfer, and the contribution of heat transfer to the total energy distribution decreases. The reduced total heat transfer might be due to the decrease in the combustion temperature inside the cylinder. The decreased combustion temperature also results in lower radiation heat transfer. The decrease in the contribution of the heat transfer to the total energy distribution is because of an increase in the internal energy inside the cylinder.

5.2 Conclusions

In conclusion, the objective of this research study have been satisfied in the successful analysis of the variation of brake fuel conversion efficiency and heat transfer with EGR and injection timing. The conclusions of this research study are listed below.

- The brake fuel conversion efficiency decreases with an increase in EGR and with retardation of injection timing.
- The total heat transfer decreases with increase in EGR and with retardation of injection timing.

- The contribution of the heat transfer to the total energy distribution decreases with retardation of injection timing, but a definite trend for the contribution of the heat transfer to the total energy distribution with EGR could not be established.

REFERENCES

[1] Heywood, J. B., 1988, *Internal Combustion Engine Fundamentals*, McGraw-Hill, New York.

[2] Jacobs, T., 2005, "Simultaneous Reduction of Nitric Oxide and Particulate Matter Emissions from a Light-Duty Diesel Engine Using Combustion Development and Diesel Oxidation Catalyst," Doctoral Dissertation, University of Michigan, Ann Arbor.

[3] Jacobs, T., Assanis, D., and Filipi, Z., 2003, "The Impact of Exhaust Gas Recirculation on Performance and Emissions of a Heavy-Duty Diesel Engine," *paper presented at SAE 2003 World Congress*, Detroit, MI, SAE Paper No. 2003-01-1068.

[4] Kumar, R., and Zheng, M., 2008, "Fuel Efficiency Improvements of Low Temperature Combustion Diesel Engines," *paper presented at SAE 2008 World Congress and Exhibition,* Detroit, MI, SAE Paper No. 2008-01-0841.

[5] Zheng, M., Reader, G., and Hawley, J., 2004, "Diesel Engine Exhaust Gas Recirculation-a review on Advanced and Novel Concepts," Energy Conversion and Management, Paper No. 2004-883-900.

[6] Jacobs, T. J., Bohac, S. V., and Assanis, D. N., 2005, "Lean and Rich Premixed Compression Ignition Combustion in a Light-Duty Diesel Engine," *paper presented at SAE 2005 World Congress & Exhibition,* Detroit, MI, SAE Paper No. 2005-01-0166.

[7] Ladommatos, N., Abdelhalim, S., Zhao, H., and Hu, Z., 1996, "The Dilution, Chemical, and Thermal Effects of Exhaust Gas Recirculation on Diesel Engine Emissions – Part 1: Effect of Reducing Inlet Charge Oxygen," SAE Paper No. 961165.

[8] Abd-Alla, G., 2001, "Using Exhaust Gas Recirculation in Internal Combustion Engines: A Review," Energy Conservation and Management, Paper No. 2002-1027-1042.

[9] Takeda, Y., and Keiichi, N., 1996. "Emission Characteristics of Premixed Lean Diesel Combustion with Extremely Early Staged Fuel Injection," SAE Paper No. 961163.

[10] Akagawa, H., Miyamoto, T., Harada, A., Sasaki, S., Shimazaki, N., and Hashizume, T., 1999, "Approaches to Solve the Problems of the Premixed Lean Diesel Combustion," *paper presented at the SAE 1999 International Congress & Exposition*, Detroit, MI, SAE Paper No. 1999-01-0183.

[11] Akihama, K., Takatori, Y., Inagaki, K., Sasaki, S., and Dean, A., 2001, "Mechanism of Smokeless Rich Diesel Combustion by Reducing Temperature," *paper presented at SAE 2001 World Congress*, Detroit, MI, SAE Paper No. 2001-01-0655.

[12] Kimura, S., Aoki, O., Kitahara, Y., and Aiyoshizawa, E., 2001, "Ultra-Clean Combustion Technology Combining a Low-Temperature and Premixed Combustion Concept for Meeting Future Emission Standards," *paper presented at SAE 2001 World Congress*, Detroit, MI, SAE Paper No. 2001-01-0200.

[13] Shimazaki, N., Tsurushima, T., and Nishimura, T., 2003, "Dual Mode Combustion Concept with Premixed Diesel Combustion by Direct Injection Near Top Dead Center," *paper presented at SAE 2003 World Congress & Exhibition*, Detroit, MI, SAE Paper No. 2003-01-0742.

[14] Yokota, H., Kudo, Y., Nakajima, H., Kakegawa, T., and Suzuki, T., 1997, "A New Concept for Low Emission Diesel Combustion," *paper presented at International Congress & Exposition 1997*, Detroit, MI, SAE Paper No. 970891.

[15] Iwabuchi, Y., Kawal, K., Shoji, T., and Takeda, Y., 1999, "Trail of New Concept Diesel Combustion System-Premixed Compression-Ignited Combustion," *paper presented at International Congress and Exposition,* Detroit, MI, SAE Paper No. 1999-01-0185.

[16] Ogawa, H., Kimura, S., Koike, M., and Enomoto, Y., 2000, "A Study of Heat Rejection and Combustion Characteristics of a Low Temperature and Premixed Combustion Concept Based on Measurement of Instantaneous Heat Flux in a Direct Injection Diesel Engine," *paper presented at SAE 2000 International Fuels & Lubricants Meeting & Exposition,* Baltimore, MD, SAE Paper No. 2000-01-2792.

[17] Tsurushima, T., Harada, A., Iwashiro, Y., Enomoto, Y., Asaumi, Y., and Aoyagi, Y., "Thermodynamic Characteristics of Premixed Compression Ignition Combustions," *paper presented at SAE 2001 International Spring Fuels & Lubricants Meeting,* Orlando, Fl, SAE Paper No. 2001-01-1891.

[18] Lechner, G. A., Jacobs, T. J., Chryssakis, C. A., Assanis, D. N., and Siewert, R. M., 2005, "Evaluation of a Narrow Spray Cone Angle, Advanced Injection Strategy to Achieve Partially Premixed Compression Ignition Combustion in a Diesel Engine," *paper presented at SAE 2005 World Congress and Exhibition,* Detroit, MI, SAE Paper No. 2005-01-0167.

[19] Zheng, M., Tan, Y., Mulenga, M., and Wang, M., 2007, "Thermal Efficiency Analysis of Diesel Low Temperature Combustion Cycles," *paper presented at SAE 2007 Powertrain & Fluid Systems Conference and Exhibition,* Rosemont, Il, SAE Paper No. 2007-01-4019.

[20] Turns, S., 1996, *An Introduction to Combustion*, McGraw-Hill, New York.

[21] Dec, J., 1997, "A Conceptual Model of DI Diesel Combustion Based on Laser-Sheet Imaging," *paper presented at SAE 1997 International Congress and Exposition,* Detroit, MI, SAE Paper No. 970873.

[22] Crabtree, D., Xia, Z., Varde, K., 1995, "An Investigation of Emission Control in a Small Spark Ignition Engine," *paper presented at SAE 1995 International Off-Highway & Powerplant Congress & Exposition,* Milwaukee, WI, SAE Paper No. 952079.

[23] Zhao, F., Asmus, T., Assanis, D., Dec, J., Eng, J., and Najt, P., 2003, *Homogeneous Charge Compression Ignition (HCCI) Engines,* Society of Automotive Engineers. Warrendale, Pennsylvania.

[24] Epping, K., Aceves, S., Bechtold, R., Dec, J., 2002, "The Potential of HCCI Combustion for High Efficiency and Low Emissions," *paper presented at SAE 2002 Future Car Congress,* Hyatt Crystal City, VA, SAE Paper No. 2002-01-1923.

[25] Gray III, A., and Ryan III, T., 1997, "Homogeneous Charge Compression Ignition (HCCI) of Diesel Fuel," *paper presented at International Spring Fuels and Lubricants Meeting & Exposition,* Dearborn, MI, SAE Paper No. 971676.

[26] Yanagihara, H., Sato, Y., and Mizuta, J., 1997, "A Study of DI Diesel Combustion under Uniform Higher-Dispersed Mixture Formation," *Society of Automotive Engineers of Japan Review Volume 18,* pp. 247-254.

[27] Pieroont, D. A., Montgomery, D. T., and Reitz, R. D., 1995, "Reducing Particulate and NO_x Using Multiple Injections and EGR in a D. I. Diesel," SAE Paper No. 950217.

[28] Alriksson, M., and Denbratt, I., 2006, "Low Temperature Combustion in a Heavy Duty Diesel Engine Using High Levels of EGR," *paper presented at SAE 2006 World Congress & Exhibition,* Detroit, MI, SAE Paper No. 2006-01-0075.

[29] Depcik, C., Jacobs, T., Hagena, J., and Assanis, D., 2007, "Instructional Use of a Single-Zone, Premixed Charge, Spark-Ignition Engine Heat Release Simulation," The International Journal of Mechanical Engineering Education, **135**, pp. 1-31.

[30] Lechner, G., 2003, "Feasibility and Limitations of Diesel Combustion in Multi-Cylinder Engines," Doctoral Dissertation, University of Michigan, Ann Arbor.

[31] ASTM., 2002, American Society for Testing and Materials International. Standard Test Method for Heat of Combustion of Liquid Hydrocarbon Fuels by Bomb Calorimeter. Standard Designation D 240-02.

[32] ASTM., 2004 American Society of Testing and Materials International. Standard Test Method for Distillation of Petroleum Products at Atmospheric Pressure. Standard Designation D 86-04b.

[33] Brunt, M. F. J., and Platts, K. C., 1999, "Calculation of Heat Release in Direct Injection Diesel Engines," *paper presented at 1999 International Congress and Exposition,* Detroit, MI, SAE Paper No. 1999-01-0187.

[34] Brunt, M. F., Rai, H., and Emtage, A. L., 1998, "The Calculation of Heat Release Energy from Engine Cylinder Pressure Data," *paper presented at 1998 International Congress and Exposition,* Detroit, MI, SAE Paper No. 981052.

[35] Krieger, R. B., and Borman, G. L., 1966, "The Computation of Apparent Heat Release for Internal Combustion Engines," ASME Paper No. 66-WA/DGP-4.

[36] Hohenberg, G. F., 1979, "Advanced Approaches for Heat Transfer Calculations," SAE Paper No. 790825.

[37] Stivender, D. L., 1971, "Development of a Fuel-Based Mass Emission Measurement Procedure," SAE Paper No. 710604.

[38] Diesel, R., June 16 1897, "Diesel's Rational Heat Motor," *A lecture given at the general meeting of the Society at Cassell,* Translated from the *Zeitschrift des Vereines*

[39] McCuistian, R., September 01 2006, "Diesels: Fueling up for a common rail invasion: get ready for a new wave in light-duty truck diesels for the 21st century. (Tech Advisor)," Can be accessed at: *http://goliath.ecnext.com/coms2/gi_0199-6860544/Diesels-fueling-up-for-a.html,* Accessed on May 30th 2008.

[40] Keller, P.S., "Turbocharging the IC Engine," Can be accessed at *http://mailman.egr.msu.edu/erl/ME444/handouts/TB1.ppt.,* Accessed on May 30th 2008.

[41] Arndt, R., "Mercedes 260D," Can be accessed at *http://strangevehicles.greyfalcon.us/MERCEDES%20260D.htm,* Accessed on May 30th 2008.

[42] Reitz, R. D., and Bracco, F. V., 1979, "On the Dependence of Spray Angle and Other Spray Parameters on Nozzle Design and Operating Conditions," SAE Paper No. 790494.

[43] Borman, G. L., and Johnson, J. H., 1962, "Unsteady Vaporization Histories and Trajectories of Fuel Drops Injected into Swirling Air," SAE Paper No. 620271.

[44] Kuo, T., Yu, R. C., and Shahed, S. M., 1983, "A Numerical Study of the Transient Evaporating Spray Mixing Process in the Diesel Environment," SAE Paper No. 831735.

[45] Gulder, O. L., Glavincevski, B. and Burton, G. F., 1985, "Ignition Quality Rating Methods for Diesel Fuels- A Critical Appraisal," SAE Paper No. 852080.

[46] Lyn, W.T., and Valdmanis, E., 1968, "Effects of Physical Factors on Ignition Delay," SAE Paper No. 680102.

VITA

Name:	Rahul Radhakrishna Pillai
Address:	C-501, Samrajya Apts, Fatehgunj Vadodara, Gujarat, India-390002
Email Address:	rahul1011@gmail.com
Education:	B. Tech, Mechanical Engineering, Mar Athanasius College of Engineering, 2005 M.S., Mechanical Engineering, Texas A&M University, 2008